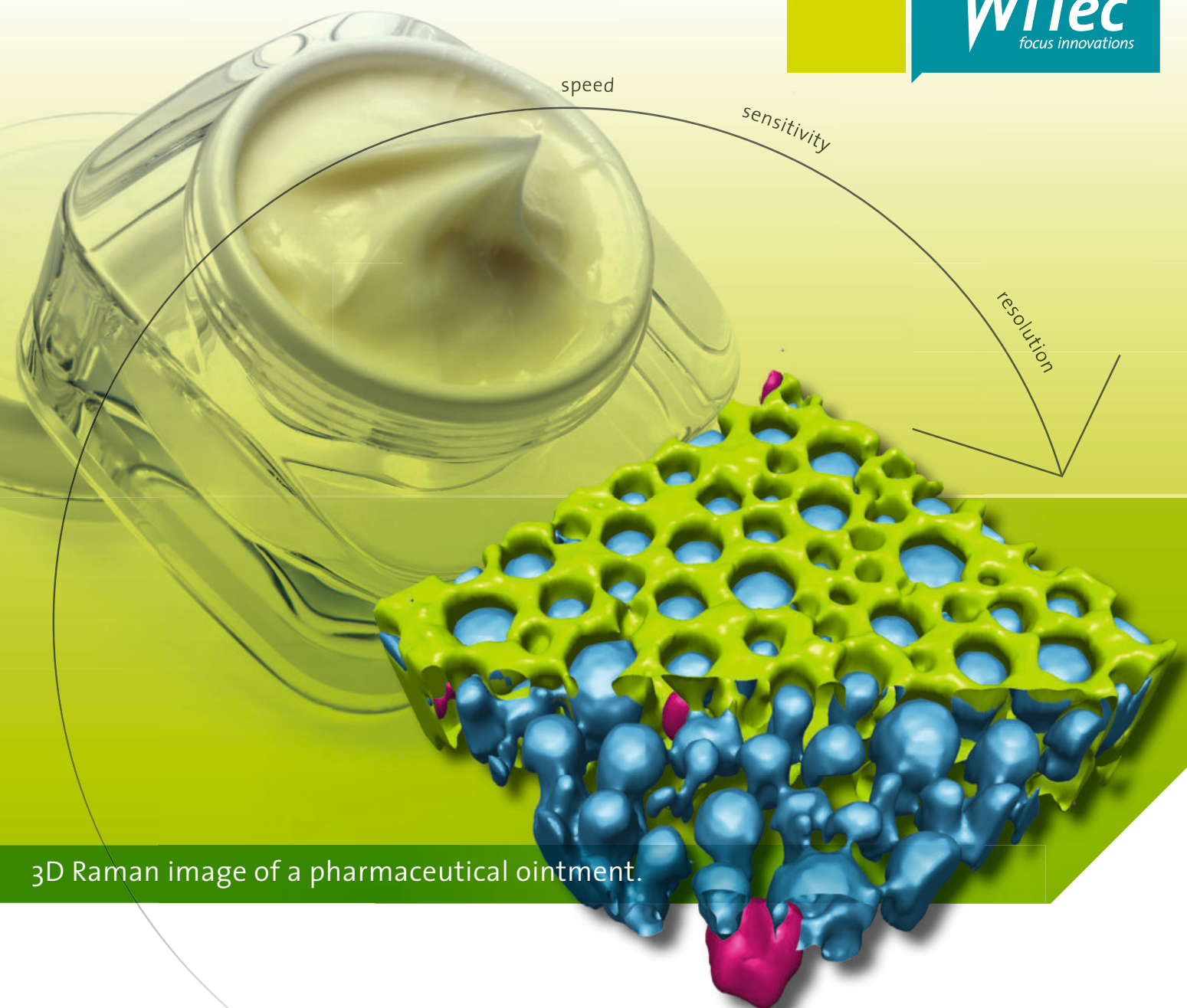


# 16th Confocal Raman Imaging Symposium

International Conference for  
Chemical Characterization & Imaging  
September 23-25, 2019  
Ulm, Germany





3D Raman image of a pharmaceutical ointment.

# 3D Raman Imaging

Turn ideas into **discoveries**

Let your discoveries lead the scientific future. Like no other system, WITec's confocal 3D Raman microscopes allow for cutting-edge chemical imaging and correlative microscopy with AFM, SNOM, SEM or Profilometry. Discuss your ideas with us at [info@witec.de](mailto:info@witec.de).



Raman · AFM · SNOM · RISE

[www.witec.de](http://www.witec.de)

## Welcome

*"Look deep into nature, and then you will understand everything better."*

*Albert Einstein*

With these sage words we welcome you to the 16<sup>th</sup> Confocal Raman Imaging Symposium in Ulm. 16 speakers will take you on a journey through the world of Raman microscopy developments and applications. You will take a deep look into how this technology can help you understand many things, if perhaps not everything, better. As in previous years, many fields of application will be represented, ranging from materials science to forensics to personalized medicine, in which Raman imaging plays an essential role.

Recently, the presence of microparticles in everyday products and in the environment has received a great deal of attention, not only from scientists but also from the wider public. Just in August, a group of researchers from the Alfred-Wegener-Institute in Bremerhaven (Germany) even detected plastic microparticles in remote polar regions, with particularly high concentrations in sea ice. As microplastics are thought to be hazardous to animals and humans, analyzing and quantifying them precisely is of great importance.

Raman spectroscopy is ideally suited to characterizing any sort of particle, so we developed the ParticleScout software package to automatically find, classify and identify microparticles using a confocal Raman microscope. This technology provides a superb solution to the challenges of microparticle analysis, which can be seen demonstrated vividly in our application note in the last section of this conference book – or on Wednesday, when we'll show ParticleScout in action at WITec headquarters.

We hope you'll enjoy the Symposium and your time in Ulm.



Olaf Hollricher, Joachim Koenen  
Managing Directors of WITec GmbH



**General Information**

**Invited Talks**

**Contributed Talks**

**Poster Abstracts**

**Application Note /  
White Paper**



SUBMIT UNTIL  
JANUARY 31

**WITec**  
focus innovations

# WITec Paper Award

The WITec PaperAward recognizes exceptional scientific publications in a peer-reviewed journal that include results and/or images acquired with a WITec microscope system. Scientists from all over the world are encouraged to submit their papers published (print or online) in the current year.

The use of a WITec microscope system should be clearly documented either in the „Materials and Methods“ section of the article or by other supporting documentation.

Each submitted paper is valid for one giveaway and any author of a paper can submit it.

A WITec jury will judge the submitted papers in terms of scientific relevance, data quality and the level of instrument feature utilization. The awards for the three best papers will be given to the first authors.

Once a year, a jury will appoint the winners of the annual award.

Entry deadline is January 31<sup>st</sup> of each year.

## How to contribute:

- 01 Send your paper (PDF format) to [papers@witec.de](mailto:papers@witec.de) and include your full contact information.
- 02 Receive a WITec thank-you gift for each new paper submitted.
- 03 Automatically participate in the WITec Paper Award competition. The first authors of the three best papers will receive a 500 € (GOLD), 300 € (SILVER) or 200 € (BRONZE) Amazon gift card.

Submit new scientific results acquired with a WITec microscope system to be placed in consideration for the WITec Paper Award. Each qualifying paper will automatically compete for the prize and WITec will send a small present to the person that submitted a paper.

## WITec Headquarters

WITec GmbH  
Lise-Meitner-Straße 6 . D-89081 Ulm . Germany  
Phone +49 (0) 731 140700 . Fax +49 (0) 731 14070200  
info@WITec.de . www.WITec.de





# General Information





# General Information

## Locations

### ***Conference Talks and Poster Sessions (23. - 24. September)***

Stadthaus Ulm, Münsterplatz 50, 89073 Ulm (directly southwest of the Ulm Minster)

### ***Conference Dinner (24. September, 7:00 p.m.)***

Restaurant "Ratskeller", Marktplatz 1, 89073 Ulm (ground floor of Town Hall)

### ***Equipment Demonstration (25. September)***

WITec Headquarters, Lise-Meitner-Str. 6, 89081 Ulm (parking spaces are available)

***See enclosed city map for details.***

## Bus Shuttle

WITec will provide a bus shuttle service on 25. September from the Ulm town center to WITec Headquarters and back.

Bus departure will be from the bus stop at the City Center / Tourist-Bus Parking Area at the corner of Neue Straße/ Glöcklerstraße (see enclosed city map).

Departure from town center to WITec: 8.30 a.m.

From WITec to the main station and town center: 3.30 p.m.

## Meals

Lunch and dinner on 24. September as well as lunch on 25. September will be provided by WITec.

## WLAN

WLAN connection for guests is available in the WITec Headquarters building.

WLAN name: Pegasus

WLAN password: Goldwing4all!

# Ulm & Neu-Ulm

## The Twin Cities on the Danube

### Middle ages meets modernity

Ulm's citizens are an audacious people; they commissioned star architect Richard Meier to design the dazzling white and geometric Stadthaus, located adjacent to the revered and ornate Ulm Minster. Modern buildings, including the Weishaupt museum and the glass-walled pyramidal central library, surround the medieval town hall.

Ulm is also home to a truly unique superstar, the Löwenmensch (lion-man). It was made in a cave near Ulm some 32,000 years ago from the tooth of a young mammoth. Löwenmensch is to date the oldest figurative art ever found.

Other famous residents of Ulm were Albert Einstein, born in the town, and resistance fighters Hans and Sophie Scholl, who were executed in 1943 in Munich.



Founded around 850 and long renowned as a free imperial city, Ulm has many sites of historical interest. The best known is the gothic Minster, the tallest church in the world. Begun in 1377, it was built for 20.000 people, then twice the population of the city. Building costs were paid completely by Ulm's citizens. Another nearby attraction is the historical town hall with its lavishly painted, early Renaissance facade. The ornamental astronomical clock was installed around 1520.

From here to the south-west extends the fishermen's and tanners' quarter with its half-timbered houses, which dates back to the Middle Ages. This district includes, at and over the river Blau, the Leaning House. Nearby is the Oath House. From 854 to the 14th century it was the King's Palace in Ulm, then it was used as a commercial center. Today it's the home of the local history museum. It plays a central role in an important Ulm tradition; every year on Schwörmontag, a public holiday in July, the Mayor of Ulm reaffirms the historical oath of the town's constitution.

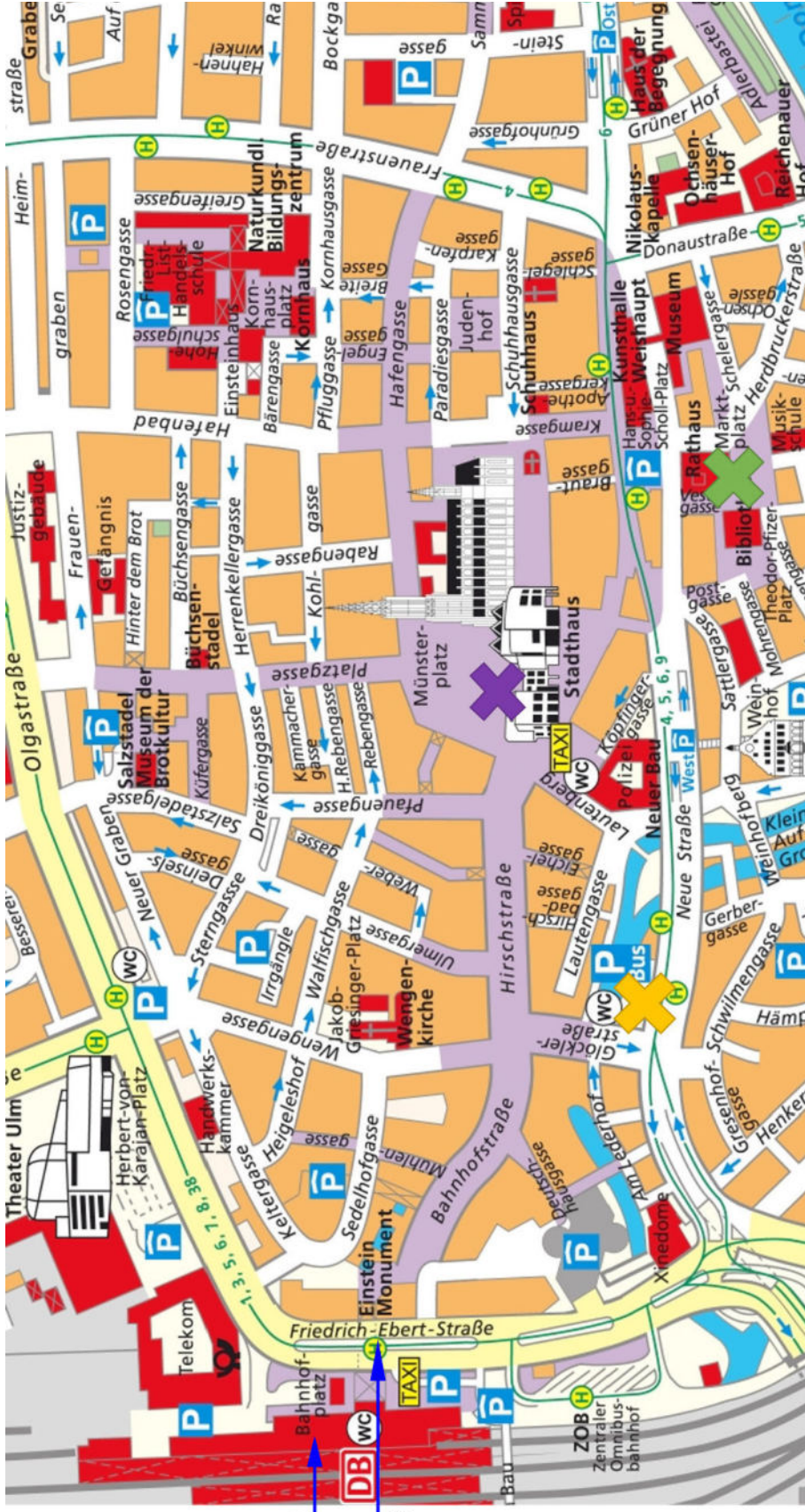


All images: Ulm/Neu-Ulm Touristik GmbH

Neu-Ulm and its Danube island were separated from Ulm in the aftermath of the Napoleonic Wars. Since then, Ulm has belonged to Baden-Württemberg, Neu-Ulm to Bavaria.



# City Map Ulm Symposium Locations 2019



Main Train Station  
Streetcar Line 2 to  
Science Park II

 Shuttle Bus from  
Ulm Town Center  
to WITec Headquarters

25. September, 8:30 a.m.

 Conference Location  
Stadthaus  
Münsterplatz 50

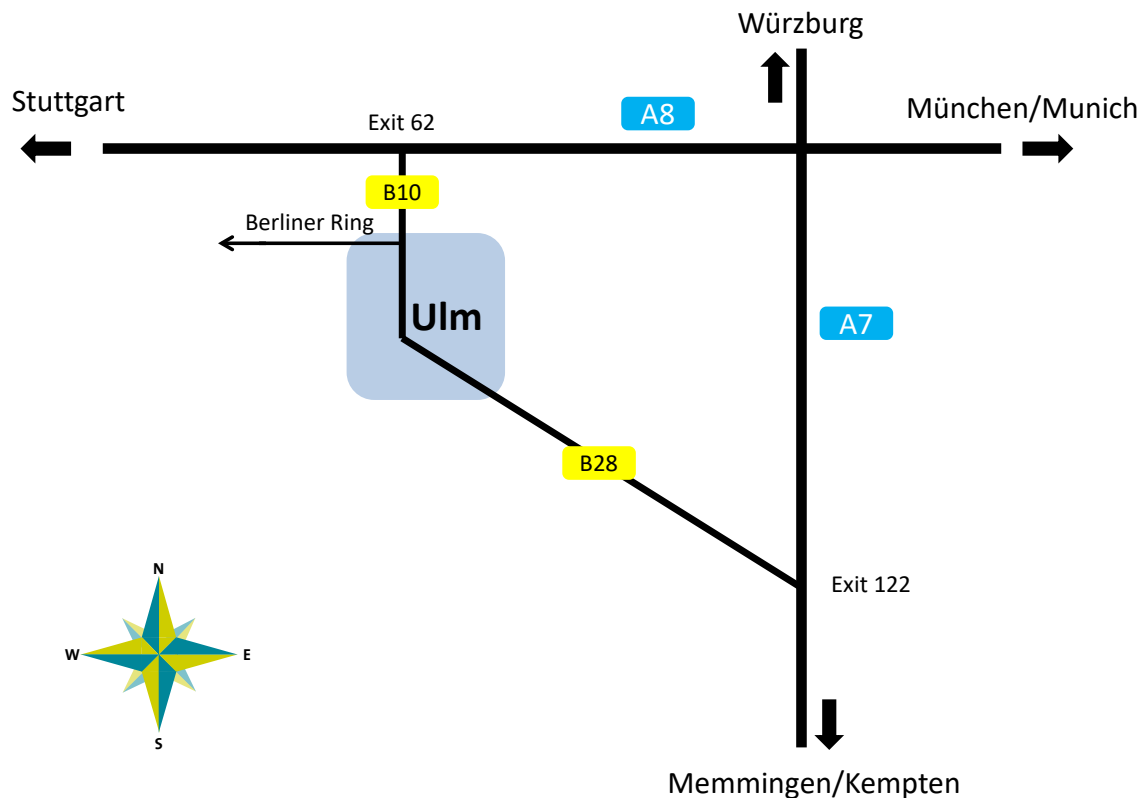
23. and 24. September

 Dinner at  
Restaurant Ratskeller  
Marktplatz 1

24. September, 7:00 p.m.



# Directions to WITec, Ulm



## Taxi Ulm Phone +49 (0)731 - 660 66

### By car

On motorway **A7 from the South** (Kempten/Memmingen):

At interchange Hittistetten take exit Ulm/Neu-Ulm/Senden (Exit 122). Drive past Neu-Ulm, continue along the B10 through Ulm, up the hill. Take exit Langenau/Wissenschaftsstadt/Kliniken/Eselsberg. Keep left - you are now on the Berliner Ring ...

On motorway **A7 from the North (Würzburg)**

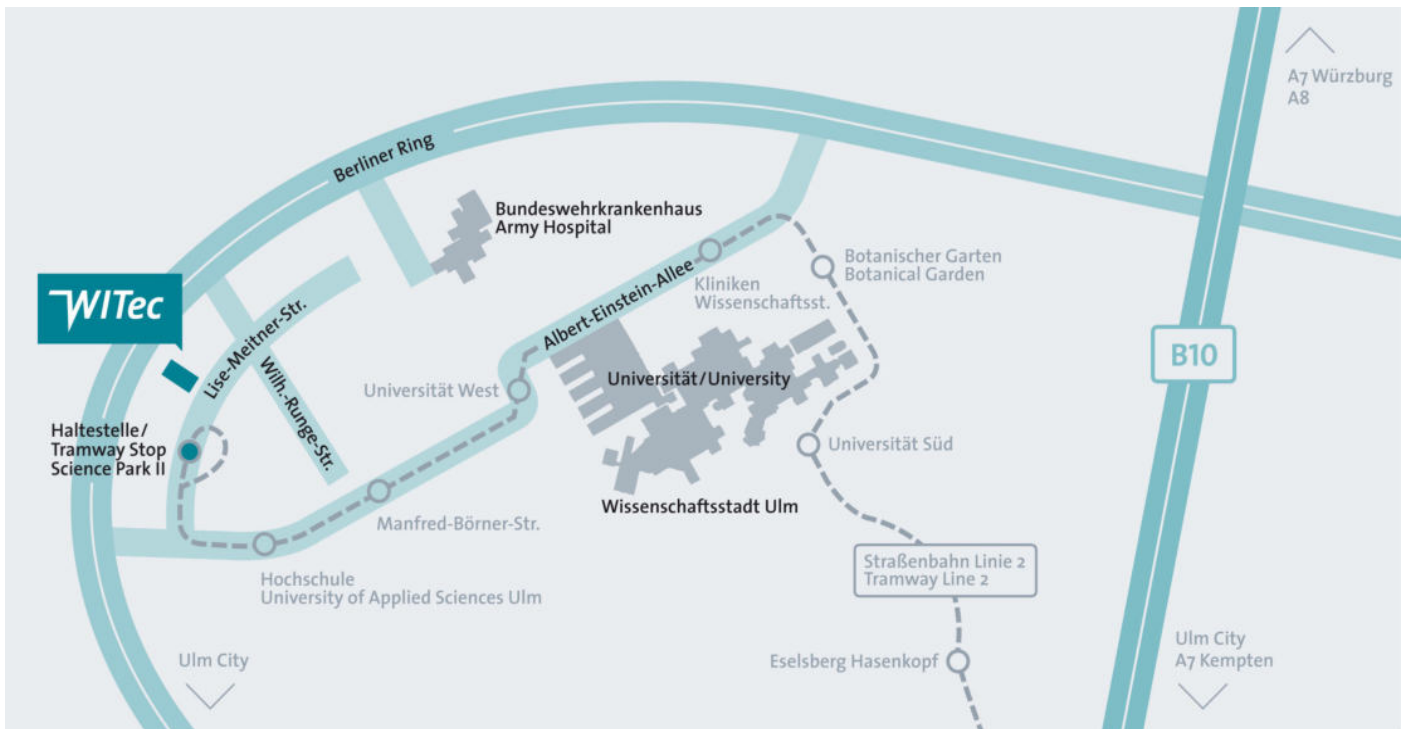
At interchange Ulm/Elchingen merge onto A8 towards Stuttgart. Take exit 62 Ulm-West onto the B10 towards Ulm/Friedrichshafen. After about 4 km take exit Blaustein/Wissenschaftsstadt to get onto the Berliner Ring ...

On motorway **A8 from East (München) and from West (Stuttgart)**

Take exit 62 Ulm-West onto the B10 towards Ulm/Friedrichshafen. After about 4 km take exit Blaustein/Wissenschaftsstadt to get onto the Berliner Ring ...

### ... continued

When you have reached the Berliner Ring, turn left at the second light onto Wilhelm-Runge-Straße / Science Park II. Then take the next exit to the right onto Lise-Meitner-Straße. After 200 meters you will have reached your destination, WITec Headquarters. Parking places are in front of the building.



## From airports by trains

### Frankfurt (280 km)

Take the train from the airport to Ulm Hbf (Ulm main station). Takes 2-2.5 hrs.

### Stuttgart (80 km)

Take the S-Bahn (local train) S3, platform 2, towards Backnang to Stuttgart Hbf. (main station). From there take a train to Ulm Hbf (Ulm main station). Takes 1.5 - 2 hrs.

### München / Munich (160 km)

Take the S-Bahn (local train) S8 to München-Pasing or the S-Bahn to München Hbf (main station). From there change to a train to Ulm Hbf. (main station). Takes 2-2.5 hrs.

### Memmingen (60 km)

Take the bus line 810 towards Memmingen Bahnhof / ZOB or line 982 towards Frundsbergstraße to Memmingen Bahnhof/ZOB. Then take a train to Ulm Hbf (main station).

### **There is extensive construction around of the Ulm train station, gh streetcar/tramway and taxis can be found there.**

From Ulm Hauptbahnhof (main station), take streetcar/tramway (Straßenbahn) Line 2 (Linie 2 in the direction of Science Park II) to the Science Park II stop. Get off at the final station (Science Park II) and walk uphill, along Lise-Meitner-Straße. After 150 meters you will find our building on your left hand side.



# Conference Program 2019

Monday, 23. September 2019		Stadthaus Ulm, Münsterplatz 50, Ulm
14:00 – 14:30		<i>Registration &amp; coffee</i>
14:30 – 14:45		Welcome
14:45 – 15:45	<b>Sebastian Schlücker</b>	The principles of Raman spectroscopy and its application in microscopy
15:45 – 16:00		<i>Coffee</i>
16:00 – 16:45	<b>Olaf Hollricher</b>	3D confocal Raman imaging: Instrumentation, resolution & configurations
16:45 – 17:30	<b>José F. Fernández</b>	Correlative Raman microscopy: Techniques and applications
17:30 – 19:30		<i>Poster session &amp; get-together with beer, wine and snacks</i>
19:30 – 20:30	<b>Charles Lyman</b>	Evening lecture: Innovations in microscopy

Tuesday, 24. September 2019		Stadthaus Ulm, Münsterplatz 50, Ulm
08:45 – 09:00		<i>Coffee</i>
	<b><i>Session I – Nanotechnology and Low-Dimensional Materials</i></b>	
09:00 – 09:30	<b>Yuan Huang</b>	Raman and photoluminescence studies of 2D materials under strain
09:30 – 10:00	<b>Holger Schmalz</b>	Raman imaging as a versatile tool for the characterization of multicomponent polymer particles/fibers and mesostructured systems
10:00 – 10:30	<b>Simon Thiele</b>	Serial section-based Raman tomography
10:30 – 11:00		<i>Coffee</i>
	<b><i>Session II – Geo Sciences</i></b>	
11:00 – 11:30	<b>Maria Sitnikova and Khulan Berkh</b>	Correlative Raman imaging and scanning electron microscopy (RISE): Mineralogical case studies
11:30 – 12:00	<b>Linda Prinsloo</b>	The role of Raman microscopy in pre-historic stone tool research
12:00 – 13:00		<i>Lunch &amp; poster session (continued)</i>
	<b><i>Session III – Life Sciences</i></b>	
13:00 – 13:30	<b>Katja Schenke-Layland</b>	Application of Raman microspectroscopy and imaging in personalized medicine approaches
13:30 – 14:00	<b>Peter Vikesland</b>	Surface-enhanced Rayleigh scattering: A novel means to improve SERS quantitation?
14:00 – 14:30		<i>Coffee</i>
	<b><i>Session IV – Applied Chemical Analyses</i></b>	
14:30 – 15:00	<b>Lars Meyer</b>	Raman microspectroscopy in industrial research: A medley of analytical applications
15:00 – 15:30	<b>Erik Emmons and Ashish Tripathi</b>	Raman chemical microscopy for rapid analysis of samples in chemical, biological and explosives defense
15:30 – 16:00		<i>Coffee</i>
	<b><i>Contributed Session – Oral Presentations</i></b>	
16:00 – 16:20	<b>Patrick Altmann</b>	Enabling cryogenic Raman spectroscopy
16:20 – 16:40	<b>Bastian Barton</b>	Raman imaging of additives in polymers: multivariate decomposition of 3D maps and super-resolution imaging
16:40 – 17:00	<b>Emil T. Bjerglund</b>	Detecting document fraud with Raman spectroscopy
17:00 – 17:20	<b>Armin Zankel</b>	The combination of electron microscopy, Raman microscopy and EDX. Examples from materials science
19:00		<i>Conference dinner &amp; Poster Award ceremony</i>

Wednesday, 25. September 2019		WITec Headquarters, Lise-Meitner-Str. 6, Ulm
08:30		<i>Departure of shuttle bus from Ulm city center to WITec headquarters</i>
09:15 – 09:30	<b>A very short overview</b>	Confocal Raman imaging system configurations
09:30 - 12:30	<b>Equipment Demonstration</b>	<ul style="list-style-type: none"> <li>• Confocal Raman imaging &amp; automation</li> <li>• The inverted confocal Raman microscope alpha300 Ri</li> <li>• TrueSurface™ for topographic imaging</li> <li>• Correlative AFM - Raman microscopy</li> <li>• WITec Project <i>FIVE</i> data evaluation software</li> <li>• RISE™ Microscopy</li> <li>• Find, classify and identify microparticles with ParticleScout</li> </ul>
12:30 - 13:30		<i>Lunch</i>
13:30 – 14:45	<b>Equipment Demonstration</b>	<i>Continued</i>
14:45 – 15:00		<i>Wrap-up &amp; coffee</i>
15:30		<i>Shuttle bus from WITec headquarters to Ulm city center</i>



## Please note our policy regarding photography and recording of symposium presentation images

1. Attendees are not permitted to take photos or videos of speakers' slides, posters or demonstration instruments unless the speakers/poster presenters give their explicit permission.
2. We will take pictures during talks and the poster sessions and also will take a group photo of all participants that we will use for press activities. We will not ask for written consent. Please inform us (i.e. during registration) if you do not want appear in our photos.

# Invited Speakers

## **Sebastian Schlücker**

As Professor of Physical Chemistry at the University of Duisburg-Essen (Germany), his research interests include the design, synthesis and bioanalytical applications of SERS nanoparticle probes as well as the development and application of laser spectroscopic techniques in biophysical chemistry.

## **Olaf Hollricher**

Olaf Hollricher is Managing Director of WITec (Ulm, Germany) and head of Research & Development.

## **José F. Fernández**

Professor at CSIC, José Fernández is also head of the Ceramics For Smart Systems Group. His research interests include functional nanoparticles and nanostructures with unusual optical, magnetic, electric, dielectric and ferroelectric properties. He is also actively involved in knowledge transfer and scale-up activities.

## **Charles Lyman**

Charles Lyman is Professor Emeritus of Materials Science and Engineering at Lehigh University in Bethlehem, Pennsylvania (USA). He is a past president of both the Microscopy Society of America and the Microanalysis Society. He was Editor-in-Chief of the journal Microscopy and Microanalysis and he currently holds the same title at Microscopy Today.

## **Yuan Huang**

As Associate Professor at the Institute of Physics at the Chinese Academy of Sciences (IOP, CAS), in Beijing, China, Yuan Huang's research interests include photoelectric properties of 2D materials.

## **Holger Schmalz**

Holger Schmalz works in the Department of Macromolecular Chemistry at the University of Bayreuth (Germany). He is also member of the Bavarian Polymer Institute (BPI). His research focuses on the synthesis and self-assembly of block copolymers and the preparation of functional mesostructured materials employing electrospinning. He uses Raman imaging and co-localized Raman/AFM measurements as key techniques for the characterization of polymer-based mesostructured materials.

## **Simon Thiele**

Simon Thiele is head of the Electrocatalytic Interface Engineering Research Department (IEK-11) in Erlangen (Germany) and Professor in the Department of Chemical and Biological Engineering, Friedrich-Alexander University Erlangen-Nürnberg. His research focuses on electrocatalytic power to value approaches such as fuel cells and electrolyzers.

## **Maria Alexandrovna Sitnikova and Khulan Berkh**

Both scientists work at the Federal Institute for Geosciences and Natural Resources in Hannover (Germany) in the field of geophysical exploration and technical mineralogy. Maria Sitnikova is in charge of the SEM-RAMAN Laboratory where her main research interests include petrography and heavy mineral and ore analyses including the quantitative determination of mineral components by means of SEM and Raman imaging. Khulan Berkh is a Research Associate and investigates mineralogy and geochemistry of mine tailings using Raman microscopy in combination with SEM and X-ray spectroscopy.

## **Linda Prinsloo**

Linda Prinsloo is a Research Associate at the Evolutionary Studies Institute at the University of the Witwatersrand in Johannesburg (South Africa), specializing in applying Raman spectroscopy to all aspects of Stone Age archaeology.

## **Katja Schenke-Layland**

Professor of Medical Technologies and Regenerative Medicine in the Department for Women's Health at the University Women's Hospital Tübingen (Germany), Katja Schenke Layland is also Director of The Natural and Medical Sciences Institute (NM) at the University of Tübingen in Reutlingen.

**Peter Vikesland,**

At Virginia Tech in Blacksburg, Virginia (USA) Peter Vikesland is Director of the ICTAS Center for Sustainable Nanotechnology and of the Sustainable Nanotechnology Graduate Education Program. His research interests include the environmental implications of nanotechnology and the development of sensor technologies for the detection of environmental contaminants. A focus of his work in this area is the use of Raman spectroscopy to detect biological as well as organic contaminants.

**Lars Meyer**

Lars Meyer is a Research Scientist at BASF SE in Ludwigshafen (Germany) where he is heading a laboratory for analytical chemistry with special emphasis on vibrational spectroscopy and microscopy.

**Erik Emmons and Ashish Tripathi**

Both scientists work at the U.S. Army CCDC Chemical Biological Center of the Army Research Laboratory in Aberdeen, Maryland (USA). Ashish Tripathi is a Research Scientist with over 20 years of experience with various types of chemical analyses including Raman spectroscopy, chromatography and mass spectrometry. He has applied these technologies to a wide variety of applications in chemical, biological and explosives defense.

Erik Emmons is a Research Physicist. He has 15 years of experience using a variety of spectroscopic techniques including Raman and infrared microscopy, electron spectroscopy and synchrotron-based techniques. He is currently using Raman spectroscopy and other related techniques for applications in chemical, biological and explosives defense.

# Invited Talks



# Correlative Raman Microscopy: Techniques and Applications

*J. F. Fernández.*

*Electroceramic Department, Instituto de Cerámica y Vidrio, CSIC, Kelsen 5, 28049, Madrid, SPAIN. e-mail: [jfernandez@icv.csic.es](mailto:jfernandez@icv.csic.es)*

Raman spectroscopy has benefited extraordinarily from its combination with optical microscopy techniques generating Raman Microscopy. The strong development of Raman Microscopy (RM) has been associated with the incorporation of correlated techniques. The combination of different techniques to enhance the use of Raman Microscopy has been marked by the increase in both spectra and spatial resolution. In this sense, the introduction of Confocal Optical Microscopy together with piezoelectric positioners has led to the generation of high-quality Raman images by Confocal Raman Microscopy (CRM) in which each pixel in the image collects a Raman spectrum. In search of improvements in spatial resolution, other co-related techniques have been incorporated into Raman Microscopy, such as Atomic Force Microscopy (AFM) and Scanning Electron Microscopy (SEM). In both cases, dimensional information of objects that are bound below the optical resolution limit can be obtained in situ. Moreover, the versatility of optical microscopes to incorporate the correlative techniques associated with the material functionalities open new avenues of research in which in situ CRM can be done by applying external stimuli as tensile or compression forces, thermal stress, or electric, magnetic or optical fields.

The correlative Raman Microscopy has become a unique technique to provide combined information that covers the structure, the micro-nanostructure and the functional properties. In summary, correlative Raman Microscopy meets the requirements of modern materials science in a multidisciplinary environment. In particular, it has been revealed as one of the most efficient techniques to address the study of nanomaterials in real operating conditions.

This presentation covers different aspects that have allowed correlative Raman Microscopy to be used to address the complex study of a growing number of materials. In the first place, some aspects to be taken into account in the performance of experiments on samples of different dimensions and morphology as single crystals, dense ceramics, composite materials, thin films, powder materials and nanomaterials will be exposed. Secondly, different techniques used to obtain structural information on the materials will be presented. These techniques are based on the development of Raman images in signal intensity, phase analysis and Raman shift. The methodologies will be shown on real examples of application in different materials. Finally, examples of in situ materials studies under different external fields are shown.

# Confocal Raman Microscopy: Instrumentation, Resolution, Configurations and Correlative Techniques

Olaf Hollricher  
WITec GmbH, Ulm, Germany, [www.witec.de](http://www.witec.de)

Confocal Raman microscopy is an indispensable tool for the analysis of chemical species and their spatial distribution either on surfaces or in small 3D volumes.

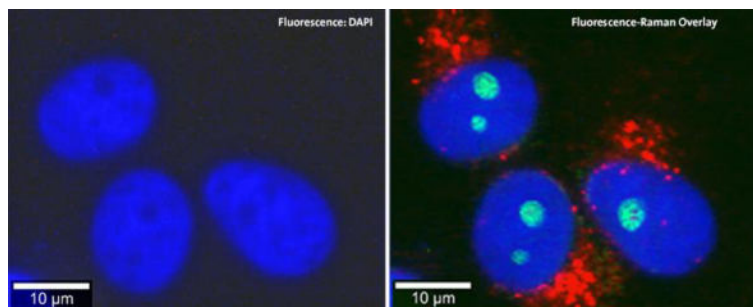
As the name states, two techniques are combined in one instrument. The confocal microscope provides diffraction limited spatial information, while Raman spectroscopy reveals the chemical composition of the sample. By acquiring a complete Raman spectrum at every image pixel, the chemical information can be linked to the spatial distribution in the sample volume, resulting in nondestructive imaging of chemical properties without specialized sample preparation. Differences in chemical composition appear in the Raman image, although they are completely invisible in the optical image.

Aim of this contribution is to highlight the instrumental requirements for a high throughput, high resolution confocal Raman microscope. Several new developments and their field of application will be presented.



Top: Confocal Raman microscopy - alpha300 Ri for inverted Raman microscopy

Bottom: Correlative fluorescence (DAPI) – Raman microscopy of cells. Left: fluorescence of DAPI, marking the nuclei. Right: fluorescence-Raman overlay. Red = endoplasmic reticula, green = nucleoli



# Raman and Photoluminescence Studies of 2D Materials Under Strain

Yuan Huang

*Institute of Physics, Chinese Academy of Sciences, Beijing, China*

The past decade has witnessed an extraordinary increase in research progress on two-dimensional (2D) nanomaterials in the fields of condensed matter physics, materials science after the exfoliation of graphene from graphite in 2004. 2D materials are sensitive for electrical field, magnetic field and also strain field, which provide a unique playground for exploring novel physics. In this presentation, I will mainly focus on strain-induced Raman and photoluminescence (PL) behaviors in 2D materials. Firstly, an overview of the research progress in this field will be presented. Based on our recent studies, I will introduce some strain related Raman and PL properties in graphene and other 2D semiconductors. By optimizing exfoliation procedures, we developed some methods to prepare bubble and wrinkle structures, which can be used as ideal models to study strain related optical properties. Thanks to the WITec Confocal Raman Microscopy, we found standing wave induced Raman oscillation on the exfoliated graphene bubbles, and also observed PL enhancement and oscillation in multilayer MoS<sub>2</sub> bubbles. From Raman and PL spectra measured on graphene and MoS<sub>2</sub> wrinkles, we found the interlayer coupling has been weakened under strain. In the near future, Raman spectroscopy will show great potential for exploring new properties in 2D materials.

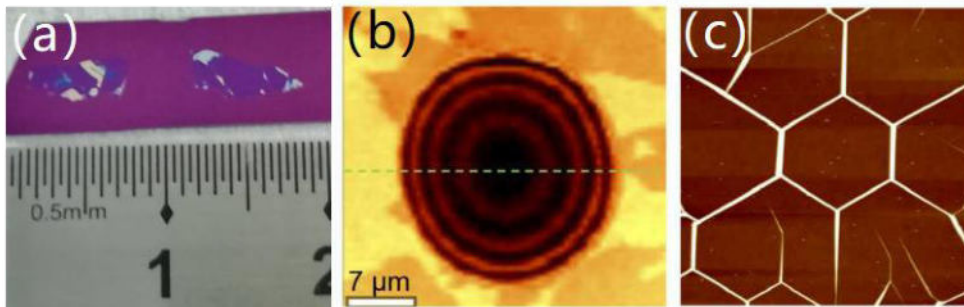


*Fig. 1: (a) Optical image of exfoliated large area 2D material (MoS<sub>2</sub>). (b) Raman oscillation image on graphene bubble. (c) AFM image of graphene wrinkle.*

# Raman microspectroscopy in industrial research: A medley of analytical applications

Lars Meyer<sup>1</sup>, Michael Liebel<sup>1</sup>, Matthias Kellermeier<sup>1</sup>

<sup>1</sup>BASF SE, Competence Center Analytics & Material Physics, Ludwigshafen, Germany

At BASF SE chemistry is created for a sustainable future by combining economic success with environmental protection and social responsibility. Research and innovation have always been of paramount importance for the company with the Competence Centers Analytics and Material Physics as an integrated facility dedicated to state-of-the-art chemical analytics. Alongside a fleet of analytical devices, the corresponding spectroscopy unit runs a WITec alpha300 R microscope. The instrument is frequently used for, e.g., supporting product-related research projects and marketing campaigns as well as product trouble-shooting in daily business.

The talk aims at giving a glimpse on the variety of analytical tasks that a confocal Raman microscope is facing in an industrial environment. Rather than focusing on one specific topic, an overview of applications will be given spanning from research efforts to follow the effect of additives on the crystallization of gypsum (see Fig. 1 below) or incrustation processes (inorganic scaling) on surfaces, to more routine tasks such as characterizing polymeric multilayer foils.

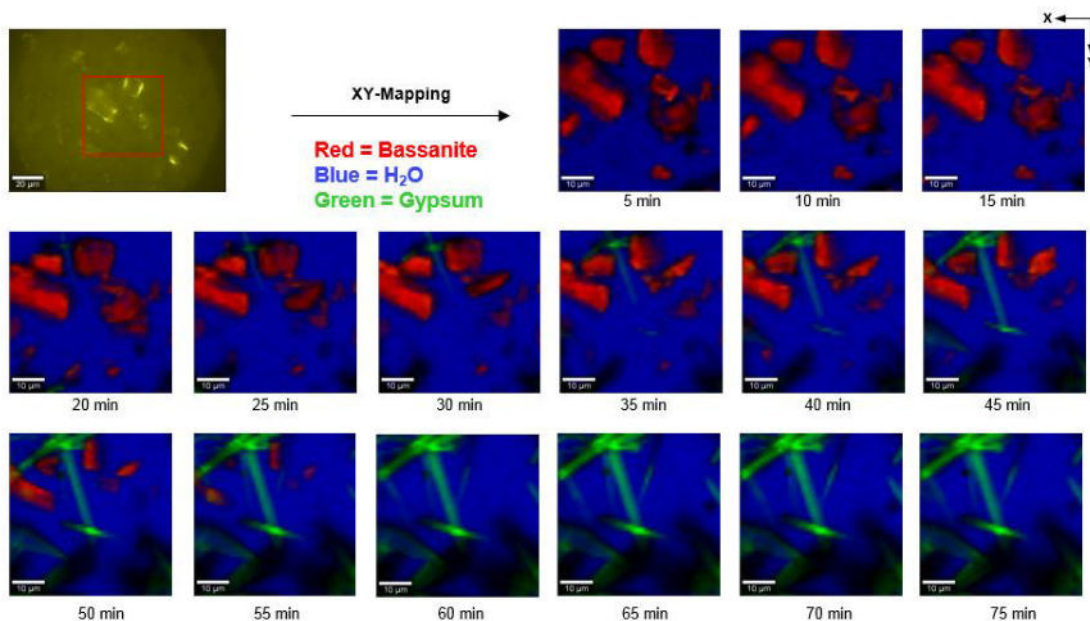


*Fig. 1: The reaction of Bassanite ( $\text{CaSO}_4 \cdot 0.5 \text{H}_2\text{O}$ ) to Gypsum ( $\text{CaSO}_4 \cdot 2 \text{H}_2\text{O}$ ) is fundamental for hydraulic binders used in construction technology. Confocal Raman microscopy proved to be a suitable analytical tool to follow this hydration process thus enabling investigations on the effect of different chemical additives on the rate and mechanisms of recrystallization.*

## The role of Raman microscopy in pre-historic stone tool research

Linda Prinsloo<sup>1</sup>, Luc Bordes<sup>2</sup>, Lyn Wadley<sup>1</sup>

<sup>1</sup>*Evolutionary Studies Institute, University of the Witwatersrand, Johannesburg, South Africa*

<sup>2</sup>*Plateforme d'imagerie, Pôle de Biotechnologie Végétale Castanet Tolosan, France*

Stone tools are the most common artefacts excavated at archaeological sites dating from the Stone Age and they are, in many instances, the only remaining evidence of how people lived in the distant past. Studying the morphology of a tool provides information on its original use and a study of the technology used to produce the tool (including heat treatment) can be linked to cognitive development. Investigating traces of use, such as plant and animal material trapped in crevices and adhering to tool surfaces, can provide detailed information on the activities undertaken with such implements (remnants of hafting, food processing, the use of poison etc.) and forms a useful tool to reconstruct past human behaviours.

Raman microscopy, which simultaneously provides optical and chemical information, is ideally suited to contribute to all of these aspects of stone tool research and it complements traditional usewear studies undertaken by optical microscopy. We illustrate with examples from a variety of archaeological sites namely Liang Bua (Flores island, Indonesia), Denisova cave (Altai mountains, Siberia) and Sibudu (KwaZulu-Natal, South Africa). We highlight the importance of in-depth characterization of the minerals that the tools are made off, including responses to heat treatment, and as not all residues identified on tools are related to the original use of a stone tool we present a key to assist in classifying residues identified by Raman spectroscopy as related to tool use, contamination or geological in origin.

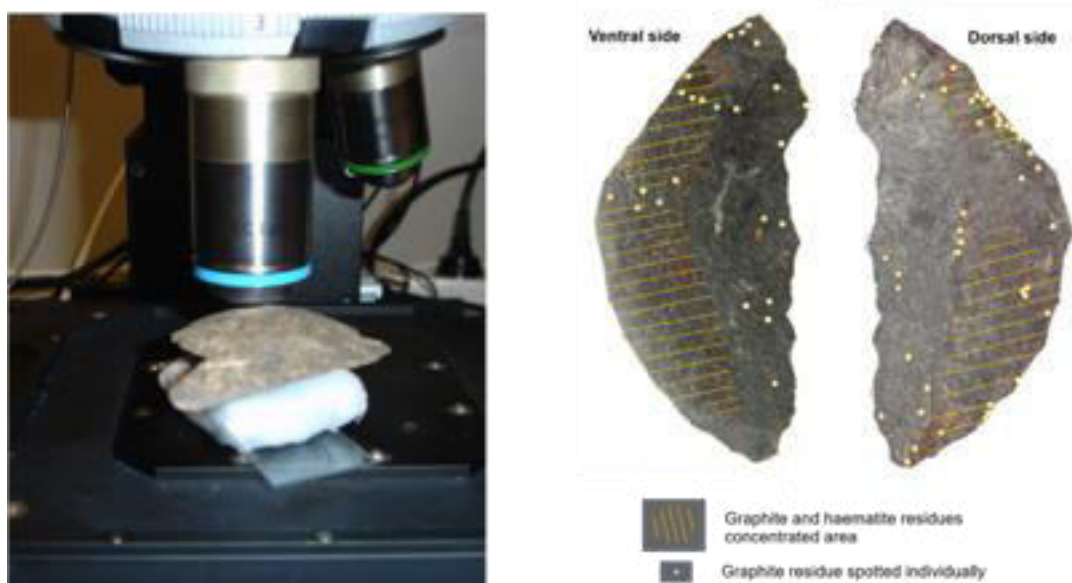


*Fig. 1: Stone tool positioned under Raman microscope (left) and distribution of graphite on stone tool from Sibudu, KwaZulu-Natal, South Africa. (right.)*

# **Application of Raman microspectroscopy and imaging in personalized medicine approaches**

Katja Schenke-Layland<sup>1,2,3</sup>

<sup>1</sup> Department of Women's Health, Research Institute for Women's Health, Eberhard Karls University Tübingen, Tübingen, Germany

<sup>2</sup> The Natural and Medical Sciences Institute (NMI) at the University of Tübingen, Reutlingen, Germany

<sup>3</sup> Department of Medicine/Cardiology, Cardiovascular Research Laboratories (CVRL), University of California (UCLA), Los Angeles, CA, USA

As the field of regenerative and personalized medicine matures, the need for novel enabling technologies to characterize cells and tissue-engineered constructs (i.e. cells/tissue combined with scaffolds and/or growth factors) as well as their individual components in a more insightful, quantitative and preferably non-invasive manner becomes imperative. Raman microspectroscopy and Raman imaging are emerging techniques based on light scattering that allow assessing molecular interactions and the biochemical structure of a sample in a non-invasive, marker-independent manner. Specifically for tissue engineering applications, it has been proven to allow determining biochemical information on cells, tissues and/or material-cell tissue constructs without the need to use labels.

The aim of this talk is to show the applicability of Raman microspectroscopy and Raman imaging for regenerative and personalized medicine applications, and to discuss the added value of the generated data for cell and tissue engineering construct design optimization and preclinical as well as clinical applications.

# **The Principles of Raman Spectroscopy and its Application in Microscopy**

Sebastian Schlücker  
*University of Duisburg-Essen, Germany*

This lecture gives an introduction into the principles of Raman spectroscopy and its applications in microscopy.

First, both classical and quantum mechanical descriptions of the Raman effect are discussed. The latter (perturbation theory, Kramers-Heisenberg-Dirac dispersion formula) then serves as a starting point for introducing the concept of resonance Raman scattering (RRS). Several examples of RR (from diatomics to proteins) highlight the advantages of this Raman technique.

In addition to the Raman effect, also fundamentals of molecular vibrations and their symmetry (basic group theory) are covered by using the water molecule as an example.

We then make the transition to Raman microscopy, starting with the invention of the first Raman "microprobe" in the 1970s. Also other specialized Raman techniques such as surface-enhanced Raman scattering (SERS) and coherent-anti-Stokes Raman scattering (CARS) microscopy are briefly introduced and their specific advantages over conventional Raman spectroscopy are highlighted.

Finally, quiz questions allow the participants to test their knowledge anonymously in an interactive format (feedback and discussion).

# Raman imaging as versatile tool for the characterization of multicomponent polymer particles/fibers and mesostructured systems

H. Schmalz

*Macromolecular Chemistry II and Bavarian Polymer Institute, University of Bayreuth, Universitätsstraße 30, 95447 Bayreuth*

Raman imaging is an excellent tool for the characterization of multicomponent polymer fibers and microparticles, as well as complex mesostructured materials. The inherent lack of a sufficient electron density contrast between different polymers limits the use of scanning (SEM) and transmission (TEM) electron microscopy for the characterization of multicomponent polymer structures in the  $\mu\text{m}$ -range, as usually a selective staining of one of the polymer phases with heavy elements is necessary. However, selective staining methods are only available for specific polymer combinations and a time-consuming sample preparation, like the preparation of ultra-thin sections for TEM, is often required. Here, confocal Raman imaging with a lateral resolution of about 300 nm allows to directly determine the spatial distribution of the polymeric components without the need of a preceding sample preparation, as the chemically different polymers can be easily identified *via* specific Raman bands.

As an example, Fig. 1A, B depicts the morphology of bicomponent fibers produced by side-by-side electrospinning (the two different polymers are colored in red and blue).<sup>[1]</sup> Depending on the employed solvent a Janus-type (Fig. 1A) or bead-like (Fig. 1B) structure, where the beads exhibit a core-shell morphology, is formed. Fig. 1C shows the successful encapsulation of bacteria (colored in red) within a poly(vinyl alcohol) microparticle (colored in blue), produced by a facile emulsion process. These biohybrid microparticles can be incorporated into a pH-responsive fiber mat, which was utilized for phenol degradation under acidic conditions, where neat bacteria will not survive.<sup>[2]</sup>

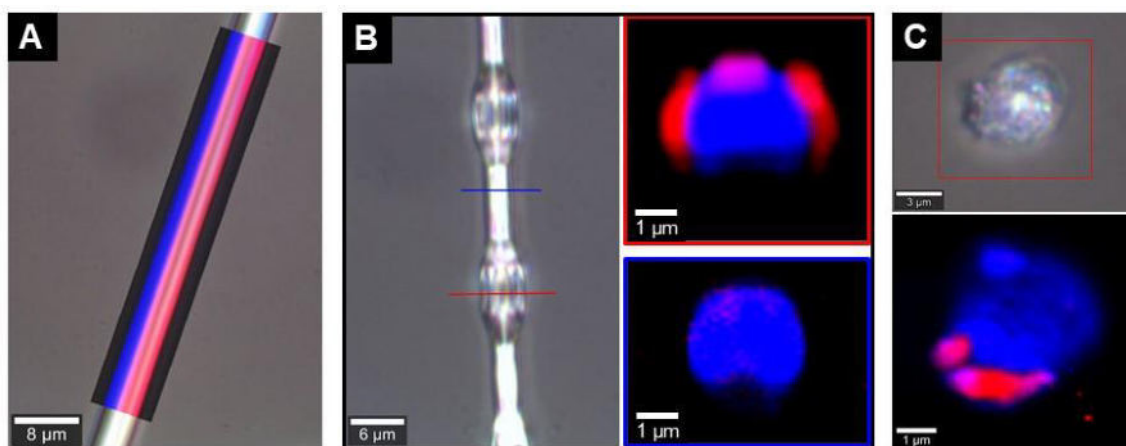


*Fig. 1: Raman imaging of bicomponent polymer fibers with A) Janus and B) bead-like structure (blue and red lines in B) show the positions for the Raman cross-sections), as well as C) poly(vinyl alcohol) microparticles (blue) with encapsulated bacteria (red).*

[1] Gernhardt, M.; Peng, L.; Burgard, M.; Jiang, S.; Förster, B.; Schmalz, H.; Agarwal, S. *Macromol. Mater. Eng.* **2018**, *303*, 1700248.

[2] Pretscher, M.; Pineda-Contreras, B. A.; Kaiser, P.; Reich, S.; Schöbel, J.; Kuttner, C.; Freitag, R.; Fery, A.; Schmalz, H.; Agarwal, S. *Biomacromolecules* **2018**, *19*, 3224.

## Correlative Raman imaging and scanning electron microscopy (RISE): Mineralogical case studies

Maria A. Sitnikova<sup>1</sup>, Khulan Berkh<sup>1</sup>  
<sup>1</sup>BGR, Hannover, Germany

In the mineral world there are several issues with the identification of some mineral groups, which can only be solved by applying a combination of methods. Since we have the unique system of combined Raman and scanning electron microscopes (SEM), we can semi-simultaneously perform a mineralogical as well as a chemical investigation on a single spot.

We will present a few case studies of accurate mineral identification with the Raman instrument. For instance, chemically identical polymorphs like kyanite, andalusite and sillimanite or chemically similar Fe-oxides and -hydroxides such as magnetite, hematite, and goethite can be clearly distinguished with the instrument. Moreover, recognition of minerals bearing light elements (Li, B, Be etc.) has become a routine procedure, which is not possible with SEM.

Internal structure and zoning within crystals are well visualized by the Raman imaging technique. For example, a trace amount of Co substitution in pyrite can be indirectly visualized by a certain change in Raman signature of the mineral. Crystallographically oriented zoning, structural defects and mineral inclusions in fluorite become more visible. 3D mapping method allows investigation of melt inclusions below mineral surface.

Additionally, W-bearing mine tailings were investigated with the Raman technique. Grain distribution of the main W-carrier mineral scheelite was analyzed and compared with SEM. Fine intergrowth of scheelite with other minerals in unpolished rockslides was characterized and compared with a  $\mu$ -energy dispersive X-ray fluorescence mapping.

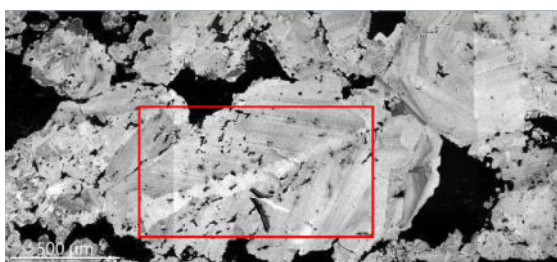


Fig.1a CL image of zoned fluorite crystal

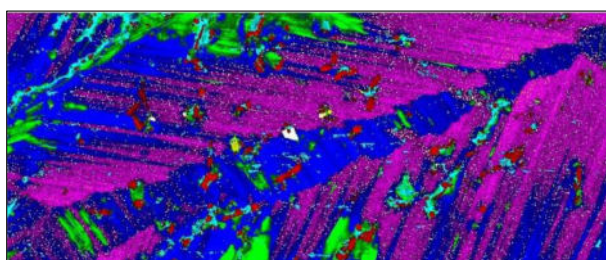


Fig.1b Raman mapping of the fluorite crystal: blue, pink and green – different fluorite varieties, red – apatite inclusions.

# Serial section-based Raman tomography

Thomas Böhm<sup>1,2</sup>, Simon Thiele<sup>1,2</sup>

<sup>1</sup>Forschungszentrum Jülich GmbH, Helmholtz-Institute Erlangen-Nürnberg for Renewable Energy (IEK-11), Egerlandstr. 3, 91058 Erlangen, Germany

<sup>2</sup>Department of Chemical and Biological Engineering, Friedrich-Alexander-Universität Erlangen-Nürnberg, Egerlandstr. 3, 91058 Erlangen, Germany

Confocal Raman imaging in polymers typically comes along with a loss of information along the through-plane coordinate of a sample due to refraction. To overcome this limitation, we combined a serial sectioning ultramicrotomy-based approach with 2D Raman imaging for the first time (Fig. 1A). Consequently, a 3D image can be formed by stacking 2D images of sections to a 3D image (Fig. 1B).

The resolution of the novel approach is defined by the thickness of the sections. We show that Raman images of sections with a thickness down to 100 nm can still produce high-quality Raman images, which results in an about 10 times higher resolution compared to confocal through-plane Raman imaging under perfect conditions. We present first results of a 3D reconstruction of a polymer blend of polystyrene and poly-l-lactide. The results show that serial section Raman tomography enables high quality 3D imaging and a successive quantitative analysis of the sample in terms of e.g. size-distributions and phase fractions.

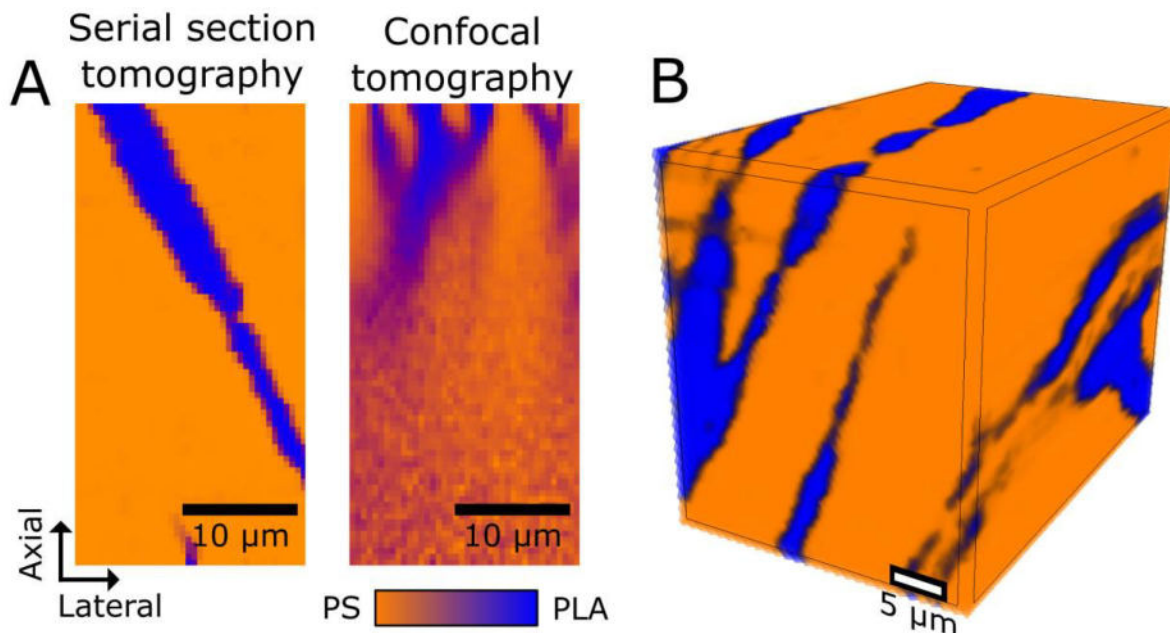


*Fig. 1: Volume imaging with Raman microscopy. A) Comparison of through-plane images of a polystyrene (PS) and poly-l-lactide (PLA) blend, obtained by serial section tomography (left) and confocal tomography (right). Confocal through-plane imaging suffers from severe resolution and data quality losses with increasing focus depth, whereas serial section tomography is not affected by increasing the imaging volume. B) 3D reconstruction of the polymer blend after imaging with serial section Raman tomography.*

# Raman Chemical Imaging Microscopy for Rapid Analysis of Samples in Chemical, Biological, and Explosives Defense

Ashish Tripathi and Erik D. Emmons

US Army CCDC Chemical Biological Center, Aberdeen Proving Ground, MD, USA

Raman chemical imaging microscopy is a powerful tool for analysis of samples of interest for chemical, biological, and explosives defense. At the U.S. Army CCDC Chemical Biological Center we are using this technique for a diverse range of applications. These include forensic applications such as detection of explosive and narcotic contaminants in fingerprints and determination of the viability of biological spores. Physical and chemical changes have also been studied including observation of phase transitions in explosives and tracking of chemical decontamination reactions in space and time. Finally, vapor phase sensing is being pursued with waveguide-enhanced Raman spectroscopy, where vapor phase molecules captured by a sorbent material are excited over a long path length by the evanescent wave of a laser confined to an optical waveguide. Advances in the Raman chemical imaging technique over the past two decades has led to the ability to examine these samples rapidly and with unprecedented spatial and spectral resolution, providing new insights into both fundamental science and technological aspects necessary for developing more advanced fieldable detection equipment. A variety of examples will be discussed as well as their relation to applications such as surface detection, trace vapor sensing, and forensics.

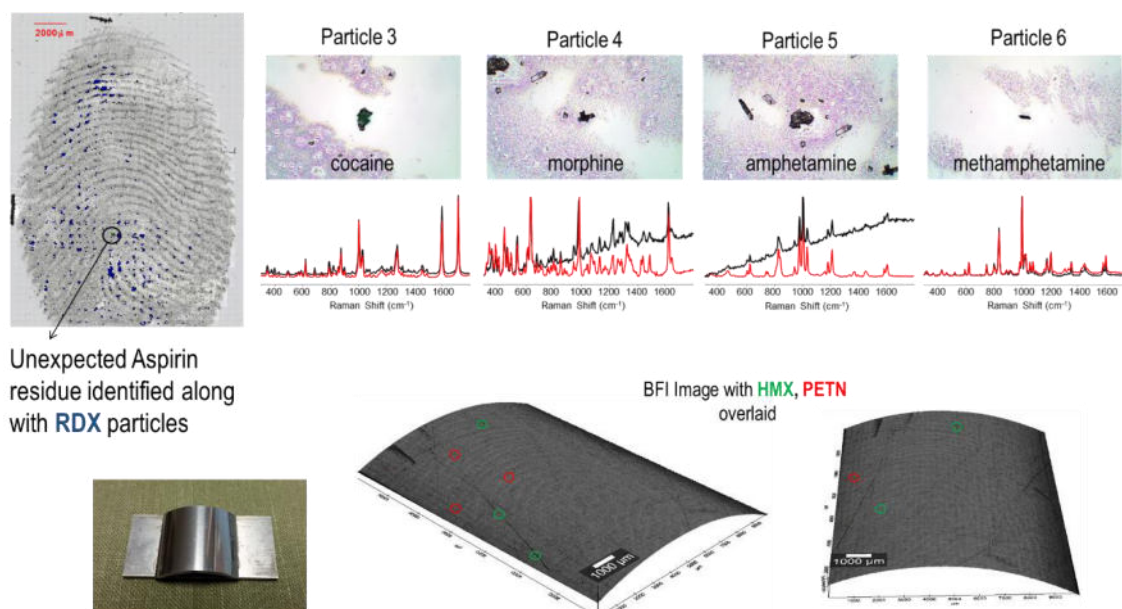


*Fig. 1: Raman chemical imaging analysis of fingerprints contaminated with explosives and narcotics. Combining brightfield image processing with Raman imaging of down selected targets can enable rapid detection of threat materials, including on curved surfaces.*

## Surface-Enhanced Rayleigh Scattering: A Novel Means to Improve SERS Quantitation?

P. Vikesland<sup>1</sup>, H. Wei<sup>1</sup>, W. Leng<sup>1</sup>, J. Song<sup>2</sup>, and W. Zhou<sup>2</sup>

<sup>1</sup>*Department of Civil and Environmental Engineering, Virginia Tech, Blacksburg, USA*

<sup>2</sup>*Department of Industrial and Computer Engineering, Virginia Tech, Blacksburg, USA*

Surface-enhanced Raman spectroscopy (SERS) has long been proposed as an ultrasensitive analytical technique. However, it remains a challenge to make SERS quantitative due to the heterogeneity of “hot spots” across SERS substrates. While uniform SERS substrates have been developed, they are generally difficult to make at large scale and at reasonable cost. Recently, internal standards have been incorporated into SERS substrates to reduce point-to-point SERS signal variability; however, the use of guest molecules as internal standards not only adds to the complexity of material synthesis, but also reduces “hot spot” volume and produces potentially interfering Raman bands. In this presentation, we will discuss a new approach towards quantitative SERS that exploits surface plasmon enhanced elastic scattering signals as internal standards for SERS signal normalization. Our measurements show that the intensity of the surface plasmon enhanced elastic scattering signal of a low-wavenumber band ( $\nu_e$ ) linearly scales with SERS “hot-spot” density, and can be used as an internal standard to minimize the inherent signal heterogeneity of SERS substrates. We have found that weak spontaneous emission light in the off-lasing low wavenumber range ( $\nu_e < 150 \text{ cm}^{-1}$ ) from the diode laser couples with localized surface plasmons in hot spots and induces plasmon enhanced elastic scattering signals that can be used as internal standards for quantitative SERS normalization and calibration.

Applying  $\nu_e$  as an internal standard (i.e., “hot spot” normalization) reduces signal variation resulting from 1) changes in hot spot density, 2) hot spot intensity, 3) laser intensity, and 4) laser focus, thus leaving the concentration of analyte within the “hot spot” as the defining variable. We will show the application of “hot spot” normalization for quantification of pH in droplets as well as its application towards quantitative detection of pollutants in contaminated water.

# Contributed Talks



## Enabling cryogenic Raman Spectroscopy

C. Dal Savio<sup>1</sup>, P. Altmann<sup>1</sup>, M. Bacani<sup>1</sup>, Y. Chen<sup>1</sup>, M. Zech<sup>1</sup>, C. Faugeras<sup>2</sup>, P. Kossacki<sup>2</sup>, M. Potemski<sup>2</sup>, K. Karrai<sup>1</sup>  
<sup>1</sup>attocube systems AG, Haar, Germany  
<sup>2</sup>LNCMI-Grenoble, CNRS-UJF-UPS-INSA, Grenoble, France

Variable-temperature Raman spectroscopy in high magnetic fields is becoming indispensable in studying novel materials, in particular for the researchers focused on phase-transitions or emergent properties of low-dimensional materials like graphene and transition-metal dichalcogenides. Our attoRAMAN platform combines state-of-the-art WITec's Raman instrumentation with attocube's cutting-edge cryogenic instrumentation which allows for variable-temperature (1.8 K to 300 K) and high-magnetic-fields of up to 15 T. The platform has proven to be perfectly suited also for studying the dependence of photoluminescence on temperature and/or magnetic field.

With attoRAMAN you remain using WITec's Raman technology (controller, software, laser and spectrometer), while attocube provides you with a cryostat, a magnet, cryogenic positioners and a microscope system based on a patented low-temperature apochromatic objectives especially developed for Raman confocal microscopy. Attocube's technology allows you to position the sample precisely. With a specially designed piezoelectric scanner, the Raman image is obtained by raster scanning the sample directly via WITec's alphaControl suite.

This is illustrated by Figs. 1a) and 1b), which show high-resolution images of the substrate and a single graphene flake, respectively. Fig. 1c) shows the change of the Raman spectra of a single graphene flake with magnetic field. Anti-crossings are a signature of the resonant hybridization of the  $E_{2g}$  phonon and a magnetoexciton of the Dirac cone. Furthermore, we will highlight some excellent publications that our customers have achieved with the attoRAMAN system.

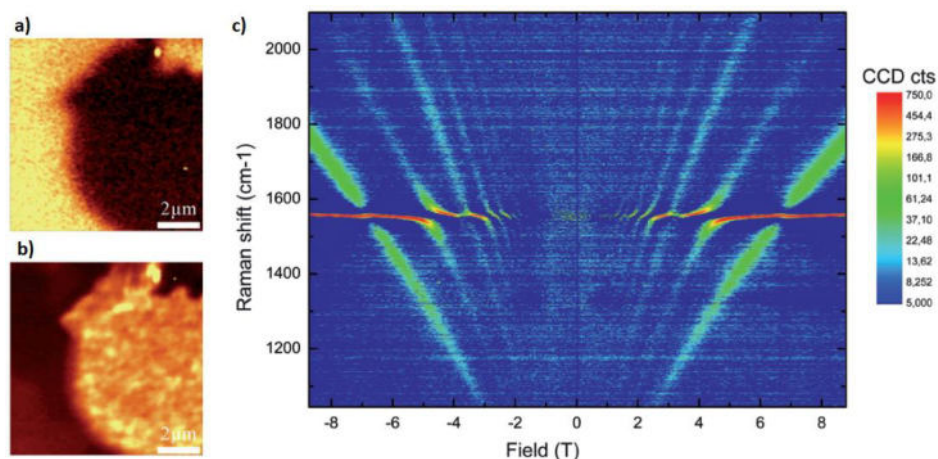


Figure 1: Raman images of the substrate (a) and a single graphene flake (b) at 4 K taken by attoRAMAN. c) Dependence of the Raman spectra on the magnetic field with the zero-field response subtracted.

# Raman Imaging of Additives in Polymers: Multivariate Decomposition of 3D Maps and Super-resolution Imaging

Bastian Barton, Mingyi Zou, Guru Geertz, Elke Metsch-Zillingen, and Robert Brüll  
*Fraunhofer Institute for Structural Durability and System Reliability LBF, Darmstadt, Germany*

Micro- and nanoscale additives are of growing importance for the functionalization of industrial polymer materials. They may act as flame retardants, UV absorbers, structural reinforcement, or electrical conductors. There is an urgent need for analytical tools providing insight to concentration, dispersion, size and structural integrity of additive particles embedded in the polymer matrix after compounding, with minimal effort of preparation.

We have developed dedicated numerical tools enabling high-resolution confocal Raman microscopy of complex, multi-component polymer materials with true chemical contrast. These can be combined with computational super-resolution algorithms, and extended to 3D. Results can be directly interpreted, and the technique gives access to sample scales that typically require time-consuming methods such as (T)EM.

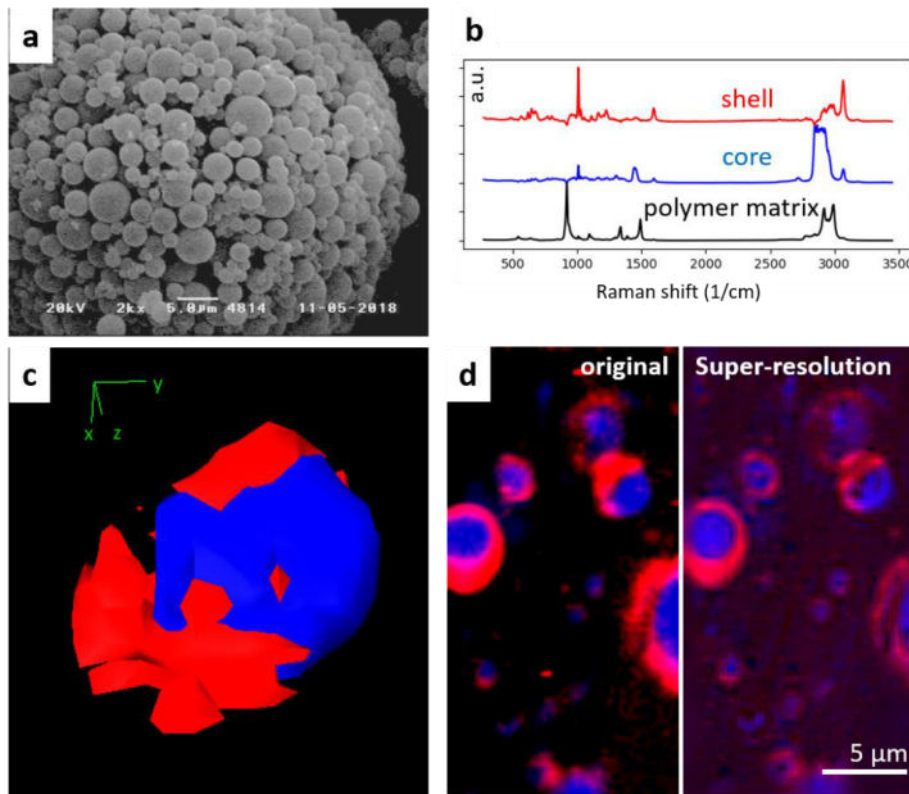


*Fig. 1: (a) SEM image of a cluster of commercial lubricant-containing core-shell microcapsules (MC) at 20 kV with Au coating. (b) Multivariate decomposition of Raman image (d) of a cross-section of MCs embedded in a Polyoxy-methylene (POM) matrix (100x100 spectra,  $\lambda = 532$  nm, 10 mW, 1s/pixel). (b) shows the pure component spectra and (d) the spatial concentration of each component. (c) Isosurface view of a  $6 \times 6 \times 2$   $\mu\text{m}$  ( $30 \times 30 \times 10$  px) 3D map of a single MC. Components are shown with the same color coding as in (b) and (d). (d) Comparison of raw 2D map and corresponding multi-frame super-resolution map.*

# Detecting document fraud with Raman spectroscopy

Emil Tveden Bjerglund, Morten Bormann Nielsen and Simon Frølich  
*Section for Resources and Materials Chemistry  
Danish Technological Institute, Aarhus, Denmark*

Falsification of documents is a societal problem – we depend on being able to trust that ID papers, receipts, contracts are real and valid. Despite technological advances, many documents are still signed physically using ink. In case there is doubt about the authenticity of a document, there are very limited options for verifying the validity using scientific methods. Handwriting experts can provide some insights on *who* signed a document, but a validated method for *dating* of pen-ink would provide a reliable control method of *when* a document was signed. This information is useful for public and private agencies such as the police, insurance companies, lawyers etc.

We have developed new methods and have shown that Raman spectroscopy is a valuable method for analysis of pen-ink. The method is fast, non-destructive, and can be used for identification of ink types and for absolute and relative dating of documents. This means, that the method can be used on sensitive, important documents without damaging them.

In this presentation, we will use examples to show that the method is useful for identification of document fraud by checking the date on documents, as illustrated in Figure 1. The figure shows an analysis of a document which appears to be younger than the printed date shows (arabic date, March 3, 2017). It can also be used to check documents for alterations, as illustrated in Figure 2, where a “1” on a receipt had been changed to a “7”, in attempt to increase the compensation from an insurance company.

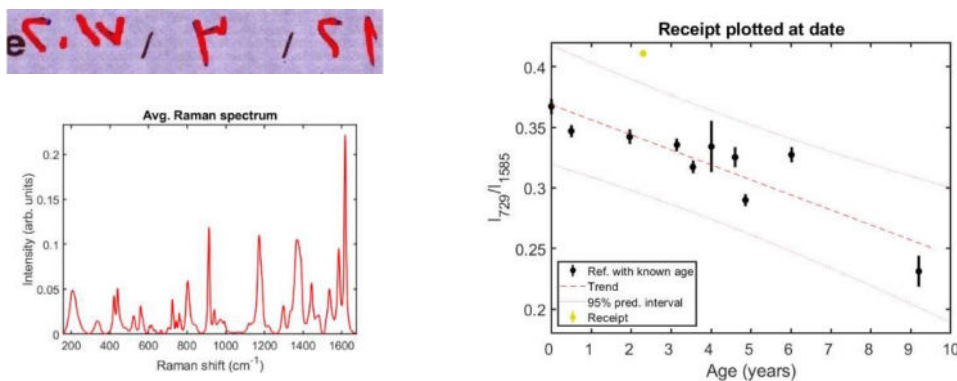


Fig. 1: Analysis of specific peaks in the spectrum of blue ink reveals that the document is younger than stated.

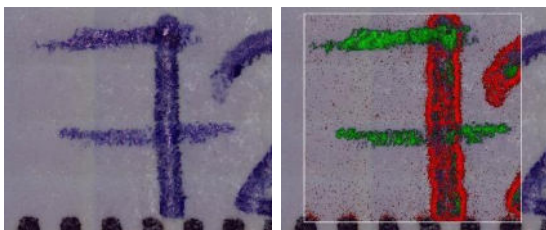


Fig. 2: Raman imaging used to detect alteration of a receipt.

# The Combination of Electron Microscopy, Raman Microscopy and Energy Dispersive X-Ray Spectroscopy. Examples from Materials Science

A. Zankel<sup>1,2</sup>, R. Schmidt<sup>1,2</sup>, M. Nachtnebel<sup>2</sup>, H. Fitzek<sup>2</sup>, C. Mayrhofer<sup>2</sup>,  
H. Schrottner<sup>1,2</sup>

<sup>1</sup>*Institute of Electron Microscopy and Nanoanalysis, NAWI Graz, Graz University of Technology, Steyrergasse 17, Graz, Austria.*

<sup>2</sup>*Graz Centre for Electron Microscopy, Steyrergasse 17, Graz, Austria*

At the FELMI-ZFE (Institute of Electron Microscopy and Nanoanalysis Graz together with Graz Centre for Electron Microscopy) the system RISE was recently established. This was enabled by “HRSM-Projekt ELMINet Graz” (i.e. a cooperation within “BioTechMed-Graz”, a research alliance of the University of Graz, the Medical University of Graz, and Graz University of Technology), which was financed by the Austrian Federal Ministry of Education, Science and Research.

RISE stands for Raman Imaging and Scanning Electron microscopy. The seamless combination of two techniques offers the possibility of high resolution imaging by the scanning electron microscope Sigma 300 VP (Zeiss, Oberkochen, Germany) and chemical analysis with the attached Raman microscope from Witec (Ulm, Germany). Additionally the setup is equipped with a modern silicon drift detector from Oxford (UK) for energy dispersive X-ray spectroscopy (EDXS). It enables spectra and mappings in a comparatively short time (realised by the project “Innovative Materialcharakterisierung”, SP2016-002-006, which is part of “ACR Strategisches Projektprogramm 2016” of the Austrian Cooperative Research, ACR).

In this work, the investigation of a broad range of samples including metal-oxides, inclusions in metals, polymers [1], organic-inorganic compounds, diverse particles and mineral samples, are presented (see Fig. 1). Using some of these examples synergies from correlative Raman-SEM and EDXS, potential pitfalls during both sample preparation and measurements, as well as best practices rules are presented and discussed.

Reference: [1] Ruth Schmidt *et al.*, Macrom. Symp., Vol. 384, 1, 2019

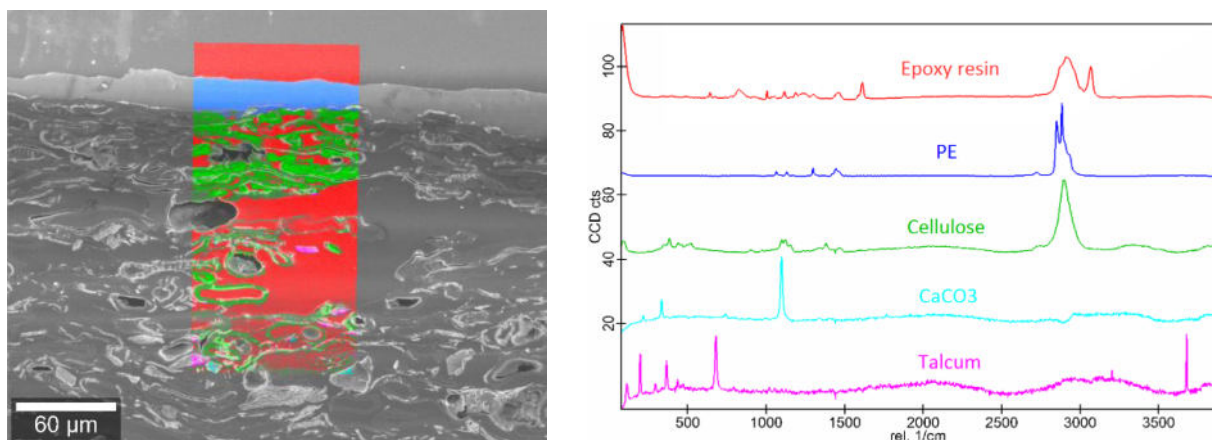


Fig. 1: Left: Correlative Raman map - SEM image of a paper coffee cup. Right: Raman spectra and component identification.

# Poster Abstracts



# Ionomer membrane characterization with confocal Raman microscopy

Thomas Böhm<sup>1,2</sup>, Riko Moroni<sup>3</sup>, Muhammad Solihul Mu'min<sup>3</sup>, Matthias Breitwieser<sup>3,4</sup>, Severin Vierrath<sup>3,4</sup>, Roland Zengerle<sup>3,4</sup>, and Simon Thiele<sup>1,2</sup>

<sup>1</sup>Forschungszentrum Jülich GmbH, Helmholtz-Institute Erlangen-Nürnberg for Renewable Energy (IEK-11), Erlangen, Germany

<sup>2</sup>Department of Chemical and Biological Engineering, Friedrich-Alexander-Universität Erlangen-Nürnberg, Erlangen, Germany

<sup>3</sup>Laboratory for MEMS Applications, IMTEK Department of Microsystems Engineering, University of Freiburg, Freiburg, Germany

<sup>4</sup>Hahn-Schickard, Freiburg, Germany

Ionomer membranes are crucial components of many electrochemical devices, like proton exchange membrane (PEM) fuel cells and PEM water electrolyzers. The membranes act as separators between the electrodes and have to provide high ion conductivity while maintaining their structural integrity during long term operation at harsh electrochemical and physical conditions. Perfluorosulfonated acids (PFSA) are widely employed as ionomer membranes due to their beneficial properties of excellent mechanical and chemical stability combined with high proton conductivity. Nonetheless, research is focusing on gaining higher performance from fuel cells and electrolyzers without sacrificing longevity: the requirements for membranes are constantly increasing, and an in-depth investigation of ionomers is mandatory for targeted material optimization.

We employ confocal Raman imaging as a tool to characterize PFSA-based ionomer membranes. In a study on a commercial PFSA membrane (Nafion) in a PEM fuel cell, we showed that chemical membrane degradation can be quantified with Raman microscopy (Fig. 1A). Also, we investigated electrospun polymer blend nanofibers as mechanical membrane reinforcements. Using non-destructive confocal Raman imaging, we are e.g. able to analyze the influence of the fiber blend composition on local membrane hydration (Fig. 1B).

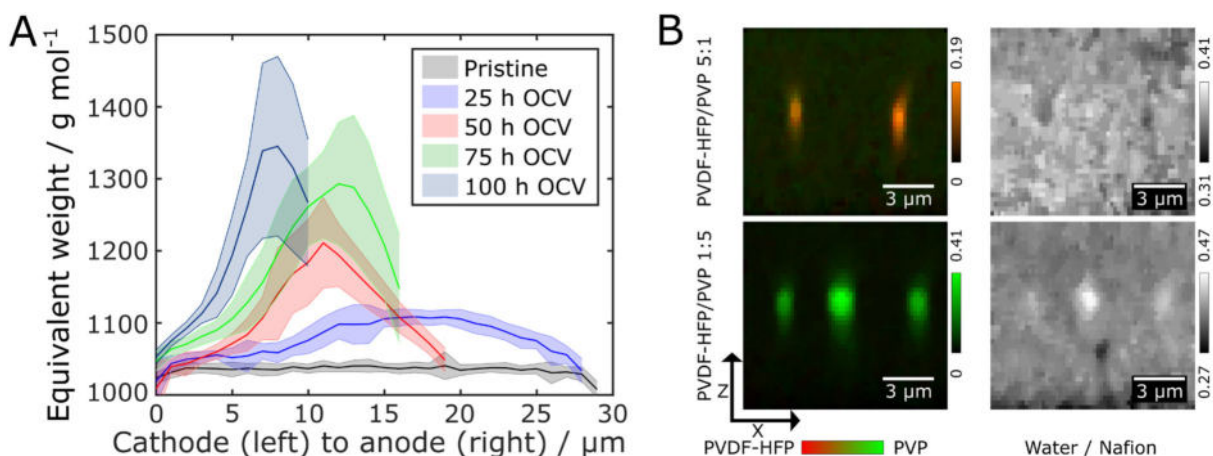


*Fig. 1: Data on ionomer membranes from Raman microscopy. A) Nafion NR-211 was aged in a PEMFC with an accelerated stress test (open circuit voltage (OCV) hold). Membrane thinning as well as loss of sulfonate groups, which leads to increased equivalent weight, are quantified with Raman microscopy. B) Electrospun nanofibers from poly(vinylidene fluoride-co-hexafluoropropylene) (PVDF-HFP) and polyvinylpyrrolidone (PVP) were embedded in Nafion and analyzed by confocal through-plane Raman imaging. Evaluation of hyperspectral images reveals fiber composition as well as local membrane hydration.*

# Characterization of normal endometrium and endometriosis using Raman microspectroscopy and imaging

Eva M. Brauchle<sup>1,2,3</sup>, Tara Beyer<sup>1</sup>, Daniel A. Carvajal Berrio<sup>1,2</sup>, Andrea Hornberger<sup>1</sup>, Hans Bösmüller<sup>4</sup>, Katharina K. Rall<sup>1</sup>, Sara Y. Brucker<sup>1</sup>, Martin Weiss<sup>1,3</sup> and Katja Schenke-Layland<sup>1,2,3,5</sup>

<sup>1</sup>Department of Women's Health, Research Institute for Women's Health, Eberhard-Karls-University Tübingen, Tübingen, Germany

<sup>2</sup>Cluster of Excellence iFIT (EXC 2180) "Image-Guided and Functionally Instructed Tumor Therapies", University of Tübingen, Germany

<sup>3</sup>The Natural and Medical Sciences Institute (NMI) at the University of Tübingen, Reutlingen, Germany

<sup>4</sup>Department of Pathology, Eberhard-Karls-University Tübingen, Tübingen, Germany

<sup>5</sup>Department of Medicine / Cardiology, Cardiovascular Research Laboratories, David Geffen School of Medicine at UCLA, Los Angeles, CA, USA

Endometriosis is one of the most common gynecological diseases affecting millions of women worldwide and causing chronic pelvic pain and infertility. It is defined by the presence of endometrial epithelium and extracellular matrix-composed stroma outside the uterine cavity. The current gold standard for treatment is solely symptomatic and includes surgical removal of the affected tissue. Endometriosis is considered as a benign disease; however, it shares features with cancer, such as neovascularization and metastatic cell behavior. In this study, we aimed to gain new insight into the molecular composition of healthy endometrium, endometriosis and endometrial cancer by employing Raman microspectroscopy and Raman imaging.

Tissue sections of normal endometrium, as well as endometriosis and endometrial cancer tissues were investigated. Raman spectra were collected from epithelial glands and their surrounding stroma and were compared using principal component analysis (PCA). Raman images were generated using true component analysis (TCA).

Our results show that Raman microspectroscopy and Raman imaging are suitable methods to characterize and image normal endometrium and endometriosis. Raman images revealed differences in the molecular composition of epithelial gland cells and the surrounding extracellular matrix in normal endometrium compared to endometriosis. We further identified similarities in Raman spectra from epithelial cells in endometriosis and endometrial cancer tissues. This study demonstrates the potential of Raman microspectroscopy as a new tool for the marker-independent identification and characterization of pathological tissues.

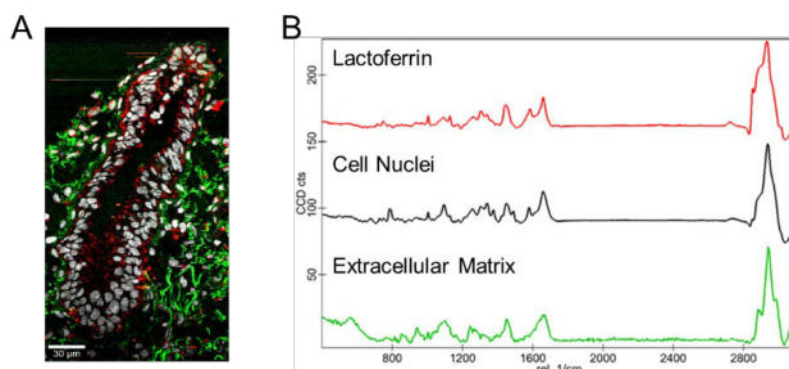


*Fig. 1: (A) Raman image of an endometrial gland in control tissue and (B) identified spectral components (left).*

# Surface Characterization of *Escherichia coli* -imprinted Polymers using Confocal Raman Microscopy

B. Bräuer<sup>1</sup>, F. Thier<sup>1</sup>, M. Bittermann<sup>1</sup>, D. Baurecht<sup>1</sup>, P. Lieberzeit<sup>1</sup>

<sup>1</sup> University of Vienna, Faculty for Chemistry, Department of Physical Chemistry, Währinger Straße 42, 1090 Vienna, Austria

The Gram-negative bacterium *Escherichia coli* (*E. coli*) is considered an indicator of hygiene in food and water. Therefore, a variety of methods has been established for the detection, identification and quantification of this microorganism, most of which require growing the bacteria. In addition, available techniques such as flow cytometry require trained staff with substantial expertise (1). However, it is possible to generate *E.coli*-sensitive sensors based on *E.coli*-selective molecularly imprinted polymers (MIPs) as receptors on Quartz Crystal Microbalances (QCMs) for direct detection of the microorganism in water (2). In order to render the synthesis of the MIPs reproducible and to assess success of the imprinting, different techniques have been established to characterize MIPs, including Atomic Force and Optical Microscopy. Both provide topological information but no information about chemical composition of the surface.

To combine chemical and optical information, we employed Confocal Raman Microscopy for the characterization of *E.coli*-imprinted polystyrene. Overlaying Raman Image Scans of *E.coli*-imprinted polystyrene with the corresponding white light images allowed for straightforward differentiation between imprints and polymer (Figure 1A) as well as imprints and bacteria (Figure 1B) based on discrepancies in signal intensity at 2908 cm<sup>-1</sup>. The accuracy of this distinction could be confirmed by Atomic Force Microscopy (AFM). Furthermore, different bacteria species such as *E.coli* and *L.lactis* could be distinguished on *E.coli*-imprinted polystyrene on the basis of their Raman spectra when combining Raman microscopy with chemometrics (Partial Least Squares Discriminant Analysis (PLS-DA)). This is essential for further experiments concerning the selectivity of the sensor and cannot be achieved by AFM. Distinction of *E.coli* and *L.lactis* on *E.coli*-imprinted polystyrene is possible due to spectral differences that cannot be seen visually but can be extracted by PLS-DA.

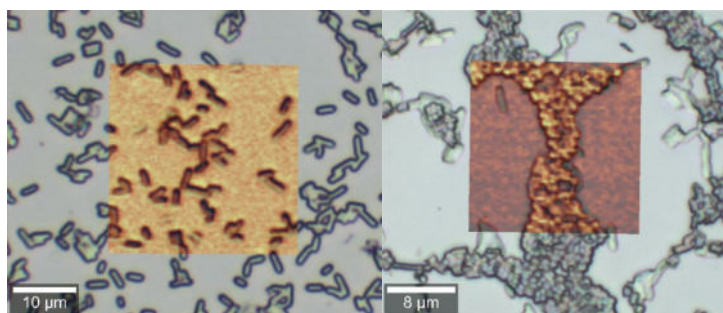


Fig. 1: Overlays of Raman TV and white light images of A: *E.coli*-imprinted polystyrene and B: *E.coli*-imprinted polystyrene treated with *E.coli*

1. Davey, Hazel M. and Kell, Douglas B. Flow Cytometry and Cell Sorting of Heterogeneous Microbial Populations: The Importance of Single-Cell Analyses. *Microbiological Reviews*. 1996, Vol. 60, pp. 641-696.
2. Poller, Anna-Maria, et al. Surface Imprints: Advantageous Application of Ready2use Materials. *ACS Applied Materials and Interfaces*. 2017, Vol. 9, pp. 1129-1135.

# Raman microscopic chemical image analysis to understand consolidation of fibres in cultural materials conservation

Samanali Garagoda Arachchige<sup>1</sup>, Kia Paasi<sup>1</sup>, Bronwyn Lowe<sup>2</sup>, Catherine Smith<sup>3</sup>, Sara Miller<sup>1</sup>, Keith Gordon<sup>1</sup>

<sup>1</sup> Department of Chemistry, University of Otago, Dunedin, New Zealand

<sup>2</sup> Centre for Materials Science and Technology /Te Tari Pū taiao Whakahā ngai, University of Otago/Te Whare Wānanga o Otāgo, Dunedin/ Ōtepoti, New Zealand/Aotearoa

<sup>3</sup> Archaeology, School of Social Sciences, University of Otago, New Zealand

Customary Māori textiles are often made using harakeke fibres (muka) which are extracted from New Zealand flax (*Phormium tenax*) and some of them are dyed with natural Paru (black) iron-tannate dyes. These dyed textiles are liable to degrade via acid-catalyzed hydrolysis and iron-catalyzed oxidation. Conservators use both natural and synthetic consolidants to alleviate this degradation for preservation purposes. But there are few systematic studies relating to the interaction between consolidants and harakeke fibres. In this study, Raman microscopy combined with chemometrics was applied to understand the distribution of consolidants into fibres and how the concentration of the consolidant effected distribution. Muka samples were treated with six consolidants; sodium alginate, zinc alginate, Paraloid B-72™ (ethyl methyl methacrylate), TRI-Funori™ (polysaccharide), Klucel G™ (hydroxypropyl cellulose), and methyl cellulose with three different concentrations per consolidant (0.5, 1.0 and 2.0 % w/v). Consolidated fibres were sectioned and then the cross section of the fibre analyzed using Raman microscopy mapping configuration with 532 nm. The relative intensity of consolidant and fibre signals were used to analyze and generate chemical images of the distribution of the consolidant within the fibre. Data were analysed using both univariate analysis of unique single band integrals for each component and true component analysis (pattern recognition algorithm). According to these analyses, the interaction of Paraloid B-72™, TRI-Funori™, and Klucel G™ with muka could be identified. This study illustrates the potential of applying Raman microscopy (as a non-destructive vibrational spectroscopic technique) to guide conservators to select consolidants and their concentration in conservation of valued Māori textiles.

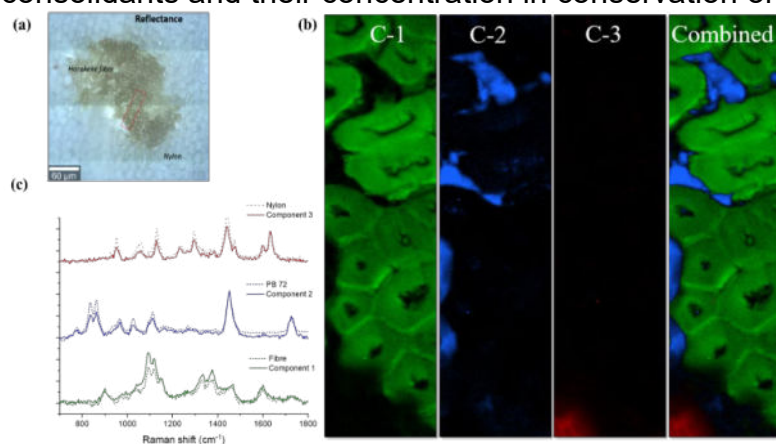


Fig. 1: (a) A bright field image of the fibre cross section mounted in nylon, (b) Image of mapped regions of 2 % w/v Paraloid B-72 fibre sample based on true component analysis (component1= green = fibre signal, component 2= blue = consolidant signal, and component 3= red= nylon signal), and (c) Reference spectra with component spectra

# Characterization of food gels through confocal Raman imaging

Laura G. Gómez-Mascaraque<sup>1</sup>, Samantha C. Pinho<sup>1,2</sup>, Sean A. Hogan<sup>1</sup>

<sup>1</sup>Teagasc Food Research Centre, Fermoy, Co. Cork, Ireland

<sup>2</sup>University of Sao Paulo, Pirassununga, SP, Brazil

Confocal Raman imaging is a powerful technique to provide microstructural and chemical information of materials. Our work explores its potential to study the structure and composition of food gels. For this purpose, two different systems were studied, i.e. hydrogels and oleogels. Protein hydrogels were produced using either a whey protein isolate (WPI), a soy protein isolate (SPI) or a mixture of both, by gelation of the proteins in aqueous solutions at 95 °C for 30 min. Oleogels were prepared by mixing anhydrous milk fat (AMF) and ethyl cellulose at 180 °C and 300 rpm, until the ethyl cellulose became solubilized, followed by cooling to room temperature.

Sections of the gels were cut with a blade, placed on glass microscopy slides, and imaged at room temperature using an Alpha300 R confocal Raman microscope (WITec, Germany) equipped with a 532 nm laser and an ultra-fast Raman imaging CCD camera. A 50x microscope objective (0.55 numerical aperture) was used and the laser power and integration time was optimized for each type of sample in order to maximize the signal while avoiding sample damage. Images were processed using Project Five software v5.0 (WITec, Germany). Different image processing protocols were applied and the microstructural information provided was compared.

Confocal Raman imaging provided valuable information on the microstructure and composition of the food gels studied, which complemented that obtained with other microscopy techniques. The selected image processing protocol had a critical impact on the quality of the information obtained.

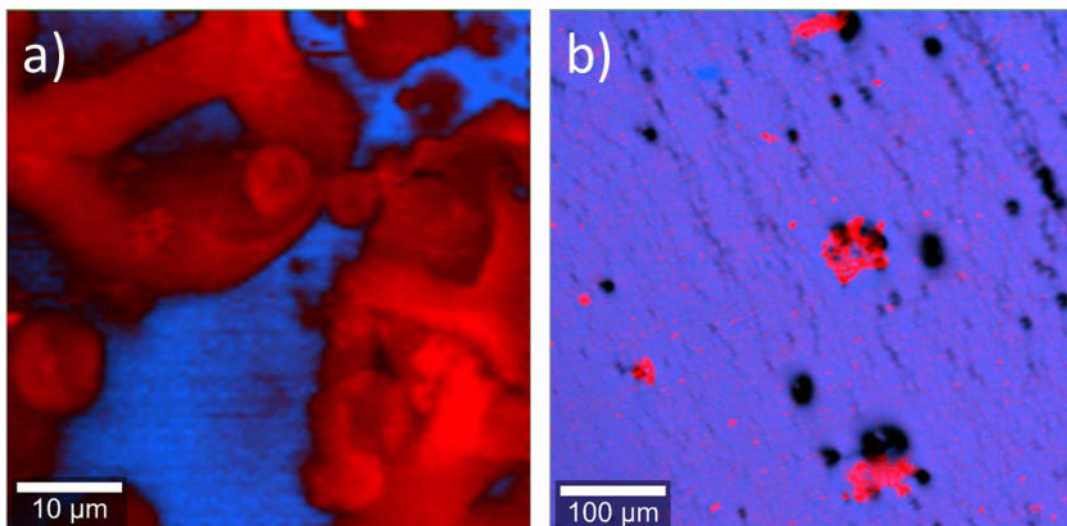


*Fig. 1: a) Proposed distribution of WPI (red) and SPI (blue) in a mixed protein hydrogel. b) Microstructure of an oleogel showing polysaccharide clusters (red)*

# Biospectroscopy and Multivariate Statistical Analysis based on Dilated Cardiomyopathy Mouse Model

M. Grahovac<sup>1</sup>, P. Ebersbach<sup>1</sup>, T. Saeidi<sup>1</sup>, P. Lampen<sup>1</sup>, J. Schmitt<sup>2</sup>, E. Freier<sup>1</sup>,  
E. Tolstik<sup>1</sup> and K. Lorenz<sup>1,3,4</sup>

<sup>1</sup>Leibniz-Institut für Analytische Wissenschaften – ISAS – e.V., Dortmund, Germany

<sup>2</sup>Institute of Pharmacology and Clinical Pharmacology, Düsseldorf University Hospital, Düsseldorf, Germany

<sup>3</sup>Institute of Pharmacology and Toxicology, University of Würzburg, Würzburg, Germany

<sup>4</sup>Comprehensive Heart Failure Center, University of Würzburg, 97078 Würzburg, Germany

A tool for differentiation between healthy mouse cardiomyocytes and cardiomyocytes affected by dilated cardiomyopathy (DCM) was aimed to be established using Coherent anti-Stokes Raman Scattering (CARS) and Second Harmonic Generation (SHG) imaging on e.g. isolated mouse cardiomyocytes. This combination of nonlinear spectroscopic techniques provided fast, non-invasive and label-free investigations of biological samples. The study was conducted on a DCM mouse model, which is characterized by a reduced myocardial function and pathological remodelling with premature death. One point mutation in a calcium cycling protein reduces calcium reuptake into the intracellular calcium store, which leads to impairment of cardiac contraction and relaxation. We further compared the DCM model to a model with cardio protective features due to an overexpression of Raf-kinase inhibitor protein (RKIP), which regulates cellular signalling and improves calcium cycling.

Three-dimensional images of wild-type, DCM affected and RKIP transgenic cardiomyocytes ( $n > 30$  cells of  $> 5$  mice each) showed slight cell volume differences, but no significant changes in sarcomere lengths. Two-dimensional, hyperspectral scans collected in the C-H stretching vibrations range were analyzed using multivariate analysis techniques, such as principal component analysis (PCA), k-means clustering (KMC) and hierarchical cluster analysis (HCA). The workflow, as illustrated in Fig.1, provided characteristic signals at  $2850 \text{ cm}^{-1}$  and  $2930 \text{ cm}^{-1}$  showing variations of protein/lipid content and their morphological localization between different cells. In sum, this multimodal approach of spectroscopic, biochemical and computational methods can improve the characterization of cardiac pathologies such as DCM.

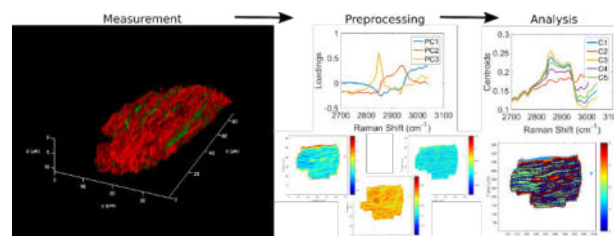


Fig. 1: Workflow from combined CARS and SHG measurements in the C-H stretching vibrations range to preprocessing using principal component analysis followed by KMC applied to first three principle components.

# Studying the mineralogical and textural evolution of a kaolinite-calcite mixture with time at temperatures between 800 and 1100°C with hyperspectral Raman imaging

K. Hauke<sup>1</sup>, S. Zimmer<sup>2</sup>, J. Kehren<sup>2</sup>, N. Böhme<sup>1</sup>, T. Geisler<sup>1</sup>

<sup>1</sup> Institute of Geosciences, Rheinische Friedrich-Wilhelms Universität, Bonn, Germany

<sup>2</sup> University of Applied Science Koblenz, Höhr-Grenzhausen, Germany

Here, we present a novel method to study the sintering process in silicate ceramics by in situ hyperspectral Raman imaging. Solid-solid reactions and phase transitions can be studied in situ at high temperature and thereby spatially resolved. Thermodynamic and kinetic phenomena can be investigated without the need to quench the sample to room temperature before analyzing the run products. In the present study, hyperspectral Raman spectroscopic imaging has been applied to *in situ* study the isothermal sintering process of a calcite-kaolinite mixture at different temperatures. Confocal micro-Raman spectra were recorded with a 2W Nd:YAG laser (532.09 nm) and an electron-multiplier CCD detector. Six samples were fired with a heating rate of 10°C/min to temperatures between about 800°C and 1100°C. For each experiment 24 hyperspectral Raman images (100 x 100 μm, 1 μm step size) were recorded within a dwell time of about 48 hours. With a counting time of 0.6 s per pixel, the total exposure time was about 2 hours per image. The classical least squares (CLS) fitting procedure with house-internal reference spectra was used to obtain the relative phase proportions from each Raman spectrum (i.e., pixel of the image). The hyperspectral Raman images were then created by false-colouring each pixel of the image relative to the fraction of each component in the spectrum. From the data, the fraction of each phase (e.g., gehlenite, wollastonite, and anorthite) in an imaged area can semi quantitatively be determined as a function of time from which kinetic information can be gained.

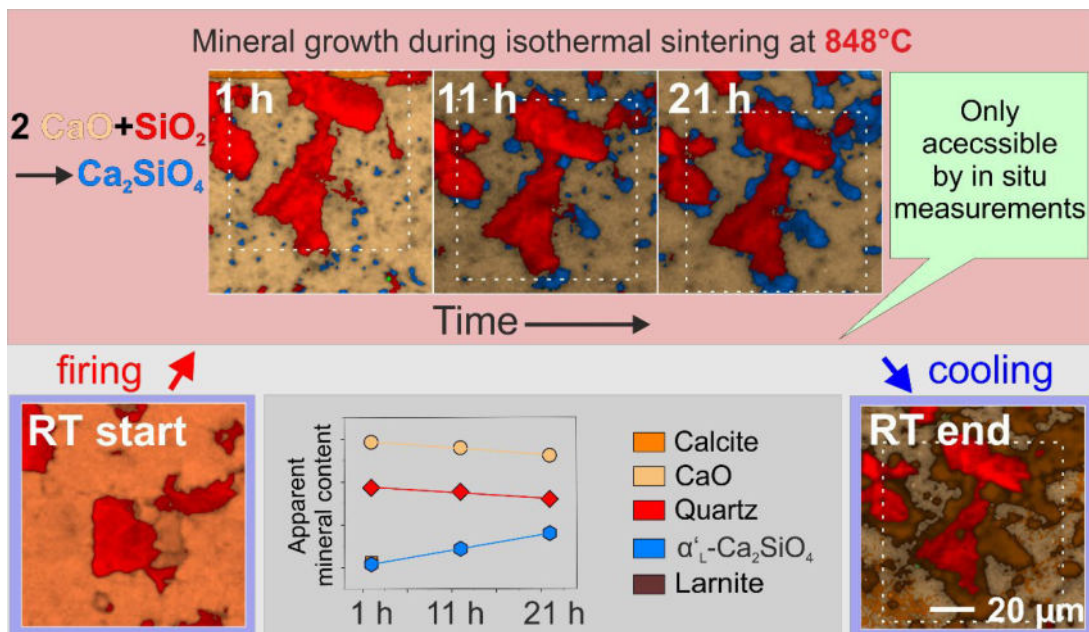


Fig. 1: *In situ* hyperspectral Raman imaging enables the investigation of the firing process of silicate ceramics temperature-, time-, and spatially resolved (adapted from Hauke et al. 2019).

# Fast detection of malign human cells by confocal Raman microscopy

Daniel Hermann<sup>1</sup>, David Lilek<sup>1</sup>, Katerina Prohaska<sup>1</sup>, Birgit Herbringer<sup>1</sup>  
<sup>1</sup>Austrian Biotech University of Applied Sciences, Campus Tulln, Austria

When dealing with cancer treatments, a timely detection is crucial. If the cancer is discovered early enough, a simple surgical procedure is often sufficient to eradicate the illness completely, as opposed to a costly and strenuous chemotherapy with dramatically lowered survival rates. However, common detection systems often require long incubation periods and specifically labelled bio-probes.

Raman spectroscopy, coupled with a microscope, constitutes a promising alternative to these methods. This approach is label- and destruction-free and this particular setup makes the analysis of samples on a cellular level possible.

To show the potential of these procedures, we applied them to differentiate between cells treated with a cytostatic drug and a control group. Metastatic melanoma cells (MCM1-DLN) treated with Epigallocatechin gallate and their untreated counterparts were investigated. To increase the signal intensity of the signals and shorten the analysis time, the cells were coated with 80 nm nanoparticles, providing a plasmon based enhancement of the Raman signals. Spectra of the fingerprint area ( $400\text{-}1800\text{ cm}^{-1}$ ) were gathered 5 times per analyzed cell. For the statistical processing, these spectra were restricted to the area with the greatest signal intensity variation ( $950\text{-}1080\text{ cm}^{-1}$ ), baseline corrected and a first order derivate was applied.

A clustering analysis of the cell spectra based on the first two principal components (PC) was possible, separating the control cell group from the treated cells on the first component (Fig.1b, black/red), proving the ability of Raman microscopy to detect minimal differences in cells. This method can therefore be used to quickly and easily characterize cell samples according to their Raman spectra.

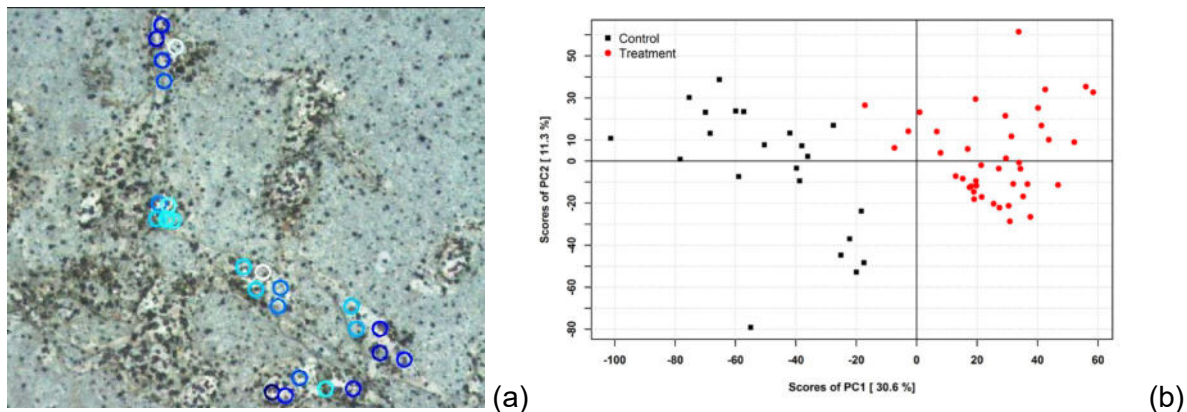


*Fig. 1: Enhancing the Raman signal with controlled Ag-NPs application, focusing five spots on five cells (a), and calculating the PC scores, explaining 43 % of the total data variance (b)*

# Influence of sulfate carriers on the hydration of $C_3S$ and the formation of C-S-H

D. Hinder, M. Lindén

*Ulm University, Institute of Inorganic Chemistry II, Albert-Einstein-Allee 11, Ulm, Germany*

Raman spectroscopy and microscopy have proven to be applicable in a wide area of mineral studies. Therefore they provide interesting tools for the construction industry as well. Since Raman measurements do not require an extensive sample preparation, and because water is not interfering with the measurement, *in situ* measurements of the hydration behavior of Portland cement and other cementitious materials are feasible.

Portland cement, which is the most commonly used type of cement, is a heterogeneous mixture of different clinker phases, such as tricalcium silicate (cement notation:  $C_3S$ ) or tricalcium aluminate ( $C_3A$ ) as well as other admixtures like sulfate carriers. As sulfate carriers anhydrite or gypsum can be used, which are added to prevent premature hardening of the paste due to the reaction of  $C_3A$  to tetracalcium aluminate hydrate. Instead a passivating layer of ettringite is formed around the  $C_3A$  grains.

The heterogeneous nature of Portland cement makes following the exact mechanism of the cement hydration very challenging, since the different clinker phases all show a distinct behavior during the hydration and can be influenced by each other as well as by admixtures. Therefore simplified systems are used to gain insight.

In this study, the hydration behavior of systems consisting of only the silicate based clinker phases ( $C_3S$  and  $C_2S$ ) and different sulfate carriers were analyzed. By means of Raman spectroscopy sulfate carriers were found to accelerate the hydration of  $C_3S$ . In addition Raman microscopy was able to deliver insights about the possible influence of sulfate ions on product formation. As shown in Fig. 1, which displays a sample of  $C_3S$  (red) and gypsum after 3 days of hydration, the sulfate ions (green) could only be found in the same region as the reaction product calcium silicate hydrate (C-S-H, yellow). Sulfate uptake into the product or onto its surface even delivered a qualitatively improved image, because of the sulfate peak being more pronounced than the peaks of C-S-H, and provided a verification of the image showing the C-S-H distribution.

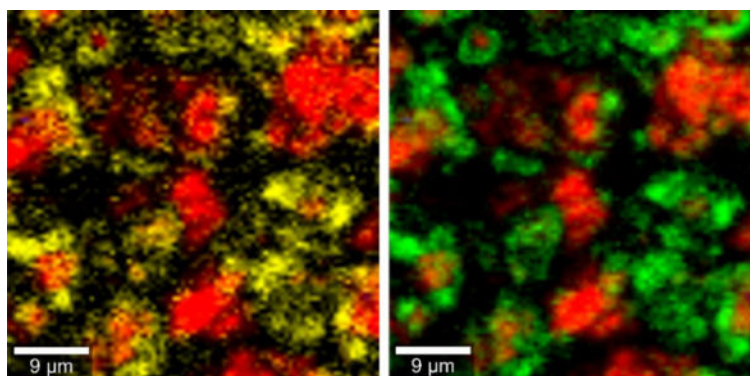


*Fig. 1:  $C_3S$  (red) sample with 2% gypsum after 3 days of hydration. Product C-S-H (yellow, left) and sulfate (green, right) distribution on the same sample area.*

# Hyperspectral Raman Imaging: A new method to in-situ study solid-solid reactions at high temperatures

J. Kehren<sup>1</sup>, K. Hauke<sup>2</sup>, S. Zimmer<sup>1</sup>, T. Geisler<sup>2</sup>

<sup>1</sup> Hochschule Koblenz, Höhr-Grenzhausen, Germany

<sup>2</sup> Institute of Geosciences, Rheinische Friedrich-Wilhelms-Universität, Bonn, Germany

High-temperature solid-solid reactions are commonly studied by firing a sample to high temperature and, after a given time, quenching the samples to room temperature before they are further analysed by various means. For each temperature or time step new samples have to be used. With such an approach it is (i) difficult to detect the presence of intermediate or metastable phases, (ii) to directly study the reaction path of a solid-solid replacement reaction, or (iii) to determine whether a particular phase formed during heating or cooling. Hyperspectral Raman imaging is a powerful method that overcomes these shortcomings (Stange et al. 2018; Hauke et al. 2019). In this study, mixtures of calcite and quartz grains were fired to temperatures of up to ~1100 °C with a firing rate of 10°C/min. At multiple temperature steps, hyperspectral Raman images of a 100x100 µm<sup>2</sup> large area were recorded with a step size of 1 µm in x and y direction (= 10,000 spectra). A 2W Nd:YAG laser (532.09 nm) was used as excitation source and an electron-multiplier CCD detector to detect the scattered light. A counting time of 0.6 s for each Raman spectrum (pixel of an image) was chosen, which lead to a total exposure time of around 2 h for a single image. In order to be able to ambiguously identify each phase involved in the reaction even at higher temperatures heating studies of pure phases were additionally conducted. These reference spectra from all phases involved in the reaction were also needed to quantify the phase proportions by the classical least-squares method. The hyperspectral Raman images of the high-temperature reaction between lime (CaO) and quartz showed, for instance, the formation and disappearance of metastable phases and the movement of a solid-solid reaction front (Fig. 1).

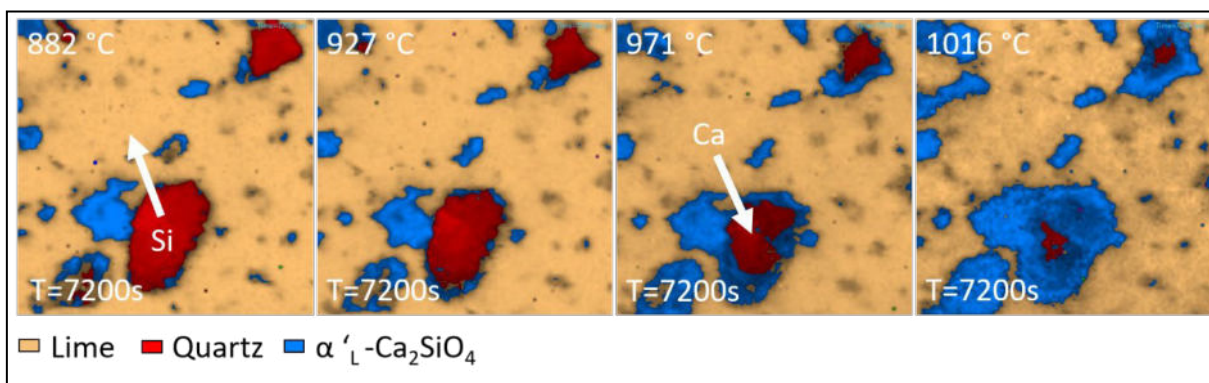


*Fig. 1:* Hyperspectral Raman images from a sintering experiment with quartz and lime (CaO), showing grain boundary migration during the solid-state reaction between both reactants. At the beginning of the reaction, dicalcium silicate ( $\alpha'_L\text{-Ca}_2\text{SiO}_4$ ) rims seem to have grown around the quartz grains, whereas with increasing temperature (and time) the reaction direction turned over and the dicalcium silicate has replaced the quartz grains.

# Raman microscopy as a tool to study mineralization of Cretaceous dinosaur bones

A. Królikowska<sup>2</sup>, B. Wrzosek<sup>1</sup>, K. Owocki<sup>2</sup>, B. Kremer<sup>2</sup>, J. Kaźmierczak<sup>2</sup>

<sup>1</sup>Faculty of Chemistry, University of Warsaw, Warsaw, Poland

<sup>2</sup>Institute of Paleobiology, Polish Academy of Sciences, Warsaw

Use of Raman spectroscopy in paleobiology is advantageous as a non-destructive, label-free technique, allowing molecular identification of both organic and inorganic components, including characterization of polymorphs. Coupling of Raman spectrometer with a confocal microscope offers detection of compositional and crystallographic differences at the microscale, providing both chemical and spatial information. Combining Raman data with the other results of geochemical analysis enables assessment of potential diagenetic alteration of microscopic fossils.

Two various types of specimen of Cretaceous dinosaur bones from the Gobi Desert (Nemegt Valley, Mongolia) were examined, including Raman point mapping technique [1,2]. Iron-rich mineral microspheres of possibly microbial origin were identified in the tibia of *Saurolophus angustirostris* [1] and petrographic thin section containing such objects (for optical image see Fig. 1a) were analyzed by Raman mapping. Organic material was identified in the center (see Fig. 1b), surrounded by the iron oxide concretions (see Fig. 1c and d for respectively goethite and hematite). We assign this organic core to the remnants of the bacteria, responsible for the early diagenetic microbial mineralization of the bone. Presence of calcite and gypsum precipitates filling the bone cavities indicates the second stage of bone mineralization. The risk of confusing the fossil related organic matter with hematite Raman band and signal due to resin used as a conservation material was also discussed.

Raman spectroscopy was also used to support the conclusions derived by means of other techniques (optical and electron microscopy, cathodoluminescence analyses), which demonstrated occurrence of fungi-like structures preserved in dinosaur bones, accompanied by presence of calcite, barite and ferromanganese oxides [2]. Although the Raman mapping showed no signature of barite, it confirmed two stages of mycelium mineralization: early post-mortem one proceeding with a formation of Fe/Mn oxides and the much later second one, resulting in a precipitation of calcite. Raman microscopy proved to a valuable tool, relating chemical composition with its spatial distribution within the fossil sample and clarifying its diagenetic changes. Hierarchical cluster analysis (HCA) confirmed the spectral differentiation in the dataset.

1. Kremer *et al.*, *Palaeogeogr. Palaeoclimatol. Palaeoecol.* 358–360, 51 (2012).
2. K. Owocki *et al.*, *PLoS ONE* 11, e0146293 (2016).

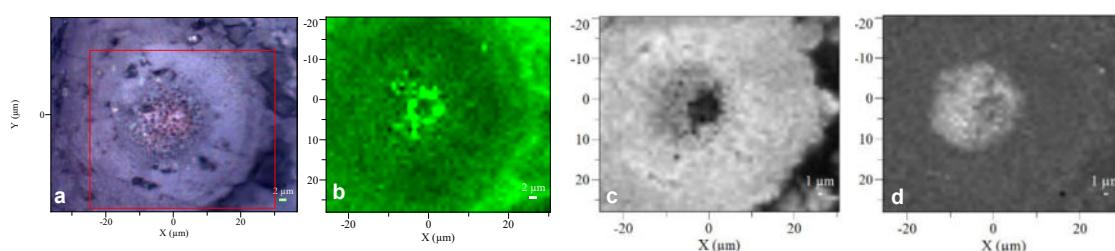


**Fig. 1:** a) Optical image of the analyzed microsphere in fossil bone. Raman maps showing the distribution of b) organic matter, c) goethite and d) hematite [1].

## Bioimaging of tessellated scaffold with SERS Tags

E. Lenzi<sup>1</sup>, D. Jiménez de Aberasturi<sup>1,2</sup>, M. Henriksen-Lacey<sup>1,2</sup>, J. Langer<sup>1</sup>, L. Liz-Marzán<sup>1,2,3</sup>

<sup>1</sup> CIC biomaGUNE, Paseo de Miramón 182, 20009 Donostia-San Sebastián, Spain;<sup>2</sup> Ciber-BBN, 20014 Donostia-San Sebastián, Spain; <sup>3</sup> Ikerbasque, Basque Foundation for Science, 48013 Bilbao, Spain

Surface Enhanced Raman Scattering (SERS) imaging is an interesting bio-imaging technique to study cells in real-time. Developments in SERS probe fabrication related to Nano Particle properties and the discovery of new Raman encoding molecules have opened up their use as tools to monitor complex 3D cellular systems. By coupling these technologies with confocal Raman microscopy, a more detailed overview of cells in 4D can be achieved.

The aim of this project is monitoring the evolution of cancer cells over time inside a structure able to mimic a real environment, by SERS imaging technique. In fact, differently from the most used techniques, SERS present a strong and stable signal, which grants narrow peaks and can be exploited for multiplexing. We used a scaffold (Figure 1A) composed of Poly(lactic-co-glycolic) Acid (PLGA) and printed using electrohydrodynamic co-jetting technology<sup>1</sup> as structure. The scaffold and the cells (Figure 1B) are labelled with two different SERS probes: gold-nanostars (AuNSs) (Figure 1C) encoded with two different Raman Reporter (RaRs) molecules, 2-naphthalenethiol (2NAT) and 4-biphenylthiol (BPT). Gold nanoparticles enhance the Raman scattering effect of the molecules that are close to their surface. Furthermore, AuNSs sharp edges and tips provide high sensitivity to local changes in the dielectric environment, as well as larger enhancements of the electric field around the nanoparticles<sup>2</sup>.

In order to monitor the growth and progression of cells and the scaffold, 3D SERS imaging was conducted using a NIR laser (785nm) over various days.

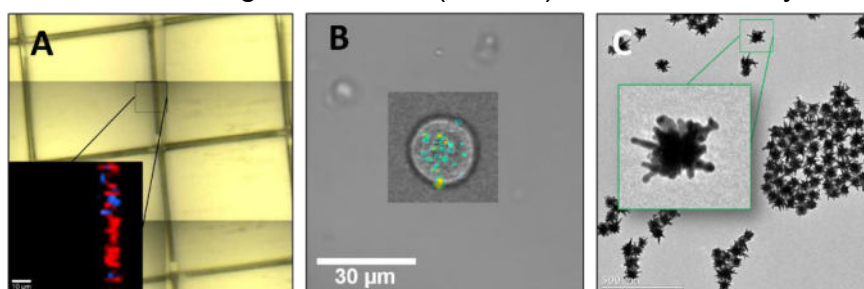


**Fig. 1:** A) Optical image of the scaffold and in the zoom a fiber SERS map filtered with True Components Analysis (TCA) tool; B) Optical images of a cell overlapped with the SERS map analyzed with the TCA tool C) TEM images of the AuNSs.

### References:

- (1) Jordahl, J. H.; Solorio, L.; Sun, H.; Ramcharan, S.; Teeple, C. B.; Haley, H. R.; Lee, K. J.; Eyster, T. W.; Luker, G. D.; Krebsbach, P. H. *Adv. Mat.* **2018**, 1707196, 1–9
- (2) Reguera, J.; Langer, J.; Jiménez De Aberasturi, D.; Liz-Marzán, L. M. *Chem. Soc. Rev.* **2017**, 46 (13), 3866–3885

## The role of adions in the SERS switch-on of anionic analytes

Stefania D. Iancu<sup>1,2</sup>, Andrei Stefanu<sup>1,2</sup>, Nicolae Leopold<sup>2</sup> Loredana F. Leopold<sup>1</sup>

<sup>1</sup>Faculty of Food Science and Technology, University of Agricultural Sciences and Veterinary Medicine, Cluj-Napoca, Romania

<sup>2</sup>Faculty of Physics, Babeş-Bolyai University, Cluj-Napoca, Romania

Our recent experimental results support the adatom model of surface-enhanced Raman scattering (SERS), highlighting the necessity of an electronic contact between adsorbate and silver metal nanoparticle, which is mediated in a specific manner by adsorbed ions (adions) [1, 2].

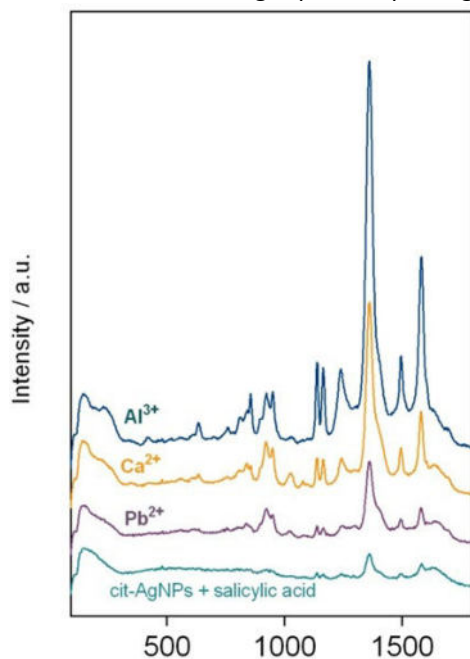


Fig.1. SERS spectra of salicylic acid after silver nanoparticles activation with  $Al^{3+}$ ,  $Ca^{2+}$ , or  $Pb^{2+}$ .

SERS spectra of anionic molecules are rarely reported, the main difficulty being the chemisorption of such species to the metal nanoparticle surface.

The here proposed methodology enabled the SERS spectra recording of anionic analytes such as citrate, uric acid, salicylic acid and fumaric acid at  $\mu M$  concentrations, by activating the silver surface with  $Ag^+$ ,  $Ca^{2+}$ ,  $Mg^{2+}$ ,  $Pb^{2+}$ ,  $Al^{3+}$  adions.

By adding such cations in form of their nitrate or sulphate salt to the silver colloid obtained by citrate reduction, the SERS spectrum of citrate capping agent is turned-on [1, 2]. The subsequent addition of one of the anionic test analytes (uric acid, salicylic acid, fumaric acid) leads to high intensity SERS spectra of the corresponding analyte, as these anionic species replace the citrate anions from the silver surface, due to their higher affinity for the silver surface. Accordingly, the chemisorption of anionic species occurs competitively in order of their affinity towards the

surface, determining thus their selective SERS detection.

### References

[1] Leopold, N., et al., Beilstein Journal of Nanotechnology, 2018, **9**, 2236.

[2] Stefanu, A., et al., Romanian Reports in Physics, 2018, **70**(4), 509.

## Probing the methylation landscape of genomic DNA by SERS

Nicolae Leopold<sup>1,2</sup>, Andrei Stefanu<sup>1,2</sup>, Vlad Moisoiu<sup>1</sup>, Stefania D. Iancu<sup>1</sup>,  
Florin Elec<sup>3</sup>, Ciprian Tomuleasa<sup>4</sup>

<sup>1</sup>*Faculty of Physics, Babeş-Bolyai University, Cluj-Napoca, Romania*

<sup>2</sup>*MEDFUTURE - Research Center for Advanced Medicine, Iuliu Hatieganu University of Medicine and Pharmacy, Cluj-Napoca, Romania*

<sup>3</sup>*Department of Urology, Iuliu Hatieganu University of Medicine and Pharmacy, Cluj-Napoca, Romania*

<sup>4</sup>*Department of Hematology, Iuliu Hatieganu University of Medicine and Pharmacy, Cluj-Napoca, Romania*

Cancer cells display an aberrant cytosine methylation pattern characterized by a decrease in the overall percentage of methylated cytosines.

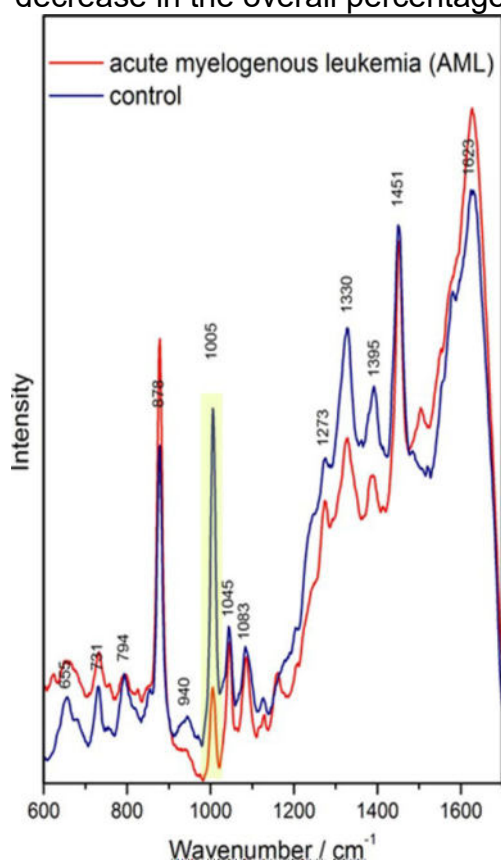


*Fig.1. Representative SERS spectra of genomic DNA, extracted from peripheral blood of AML patients and controls.*

The label-free SERS detection of cancer DNA from peripheral blood, without requiring any DNA amplification step, represents a promising strategy that could be translated in the clinical setting for the screening and follow-up of cancer patients.

Our experiments indicate that SERS spectra of DNA can be obtained in the presence of  $\text{Cl}^-$ , which forms DNA-specific SERS active sites on the surface of colloidal silver nanoparticles. On the other hand, cations such as  $\text{Ca}^{2+}$  or  $\text{Mg}^{2+}$  aid the acquisition of SERS spectra of DNA by facilitating the chemisorption of  $\text{Cl}^-$  [1,2]. The main spectral feature indicating the methylation level of genomic DNA, is represented by the  $1005\text{ cm}^{-1}$  band, assigned to the rocking vibration of  $-\text{CH}_3$ .

Furthermore, we assessed by SERS the methylation level of  $n=34$  samples of genomic DNA extracted from peripheral blood, of which  $n=17$  were from patients diagnosed with acute myelogenous leukemia (AML) and  $n=17$  samples from healthy controls. An overall accuracy of 82% for the classification of the AML and control samples was achieved, based only on the intensity of methylcytosine SERS band at  $1005\text{ cm}^{-1}$  [3].

### References

- [1] Leopold, N., et al., *Beilstein Journal of Nanotechnology*, **2018**, 9, 2236.
- [2] Stefanu, A., et al., *Romanian Reports in Physics*, **2018**, 70(4), 509.
- [3] Moisoiu, V., et al., *Analytical and Bioanalytical Chemistry*, *in review*.

# Raman-microscopy for the in-vivo identification of PHB producer in cyanobacterial cultures

David Lilek<sup>1</sup>, Daniel Hermann<sup>1</sup>, Katerina Prohaska<sup>1</sup>, Christina Daffert<sup>2</sup>, Birgit Herbinger<sup>1</sup>

<sup>1</sup>Austrian Biotech University of Applied Sciences, Campus Tulln, Austria

<sup>2</sup>University of Natural Resources and Life Sciences Vienna, IFA-Tulln

With increasing demand for plastic materials and a growing awareness for the limits of crude oil reservoirs, polymers based on biological raw materials have attracted much attention. Polymers composed of interlocked polyhydroxybutyrate (PHB) molecules are popular representatives of these, characterized by an easy manufacturing and good biodegradability.

Most research in this area focuses on the production of PHB by cyanobacteria, since their autotrophic nature and innate agglomeration of PHB constitutes a promising basis for an industrial application. Common techniques to optimize the PHB yields are media limited in essential nutrients or molecular biologically improved expression of relevant gene clusters.

The focus of this study was to verify the success of these optimizations. Raman-microscopy was combined with the application of 80 nm Ag-nanoparticles (SERS-Surface-enhanced Raman spectroscopy), providing a significant signal enhancement, to differentiate between cyanobacteria grown on adapted state of the art media. With the gathered spectral data, were pre-treated with the detrend-function in R. Then a principal component analysis (PCA) was conducted. Based on the loadings and comparison measurements of pure PHB, the spectral area between 920 and 1280  $\text{cm}^{-1}$  was selected to construct a differentiation. As can be seen in Fig. 1, the clustering between the low and high producer of PHB could be achieved. Some outliers can be explained by the different states of the cells, since the used setup works on a cellular level. Each data point represents a single cell, and depending on their state in the cell cycle, the PHB agglomeration varies. The culture, where a medium level of PHB was expected, also clustered between the two groups.

Therefore, Raman microscopy showed the potential for the use as an easy and fast identification system for PHB producing cyanobacteria. In its possible application as analytical tool in the optimization of cyanobacteria strains in terms of PHB production, Raman spectroscopy stands out due to its destruction free analysis, fast workflow and generation of multidimensional data.

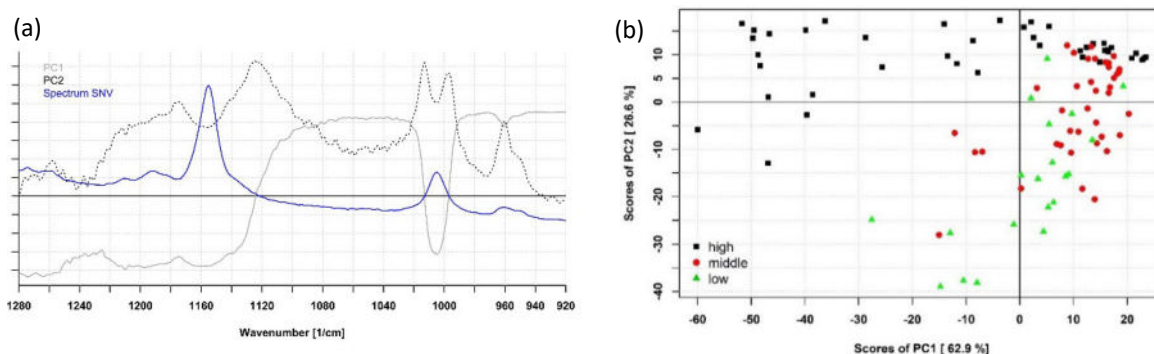


Fig. 1: Results of the conducted PCA, with the loadings of the first two principal components and a Spectrum – scaled for clarity (a) and the corresponding score values (b) enabling a differentiation of the differently cultivated cyanobacteria.

## **Raman spectrum analyses and microstructure characteristics of glass transition, crystallization and hydration of semi-crystalline lactose.**

Valentyn Maidannyk<sup>1</sup>, Laura Mascaraque<sup>1</sup>, Valeria Cenini<sup>2</sup>, Sharon Montgomery<sup>1</sup>,  
Barry O'Hagan<sup>2</sup>, Noel McCarthy<sup>1</sup>

<sup>1</sup> *Teagasc Food Research Centre, Moorepark, Fermoy, Co. Cork, Ireland.*

<sup>2</sup> *School of Biomedical Sciences, University of Ulster, Coleraine, UK.*

Generally solids may exist in crystalline, amorphous or partially (e.g. semi) crystalline phases. Crystalline and amorphous materials show significantly different physicochemical properties due to differences in microstructure. Phase transition, crystallization and hydration of non-equilibrium lactose is of practical importance for dairy and food industry as it may effect on sensitive processes during manufacturing and storage

Semi-crystalline lactose powders with various (100:0; 50:50; 0:100) amorphous to crystalline ratios were analysed. Amorphous components were prepared from water solution (20% of total solids) by freeze-drying. The Guggenheim-Anderson-de Boer (GAB) equation was used to model water sorption isotherms. The glass transition ( $T_g$ ) and  $\alpha$ -relaxation ( $T_\alpha$ ) temperatures were obtained by differential scanning calorimetry (DSC) and dynamic mechanical analysis (DMA) respectively and cover broad range for structural strength assessment. Polarised and confocal-Raman microscopies were applied for all anhydrous and humidified systems. Environmental Scanning Electron microscopy (ESEM) allowed direct real-time inspection of hydration.

The effect of water content inside semi-crystalline lactose powders was in a focus. GAB water sorption isotherm shows lactose crystallisation at high relative humidities ( $RH \geq 54.5\%$ ), which is in agreement with ESEM micrographs. The results indicated that water content significantly decreases glass transition,  $\alpha$ -relaxation temperatures and structural strength parameter, while the effect of crystalline component is less pronounced. The Gordon-Taylor (GT) equation was fitted to experimental  $T_g$  data and allow prediction of  $T_g$  at all water content range.

Raman spectrometer investigates changes in molecular interaction and clearly shows difference between amorphous and crystalline form of lactose. The intra-molecular interaction responses sensitive to changes of water content in a system. Also Raman technique proved increasing water content inside amorphous lactose powders with increasing relative humidities until crystallization point at 54.5% RH.

The changes in molecular interactions play a significant role for plasticizer-induced phase transition of amorphous carbohydrate. The data obtained in this study provide new information about molecular interaction during phase transition of lactose and can be used in processing and characterization of amorphous sugar containing products.

# Comparison of Spectral Resolution of Three Raman microscopes

Ashutosh Mukherjee<sup>1,2</sup>, Anita Lorenz<sup>1</sup>, Claus Burkhardt<sup>3</sup>, Dai Zhang<sup>2</sup>, Alfred Meixner<sup>2</sup>  
and Marc Brecht<sup>1,2</sup>

<sup>1</sup> *Process Analysis and Technology (PA&T), Reutlingen Research Institute, Reutlingen University, Alteburgstr. 150, 72762 Reutlingen, Germany*

<sup>2</sup> *Institute of Physical and Theoretical Chemistry, University of Tübingen, Auf der Morgenstelle 18, 72076 Tübingen, Germany*

<sup>3</sup> *Natural and Medical Science Institute (NMI) at University of Tübingen, Markwiesenstr. 55, 72770 Reutlingen*

Raman microscopy (spectroscopy) is a powerful technique to determine the chemical composition, crystallinity, effects of strain/doping/temperature of various classes of materials. However, to have reliable and comparable analysis of the critical experimental data it is of utmost importance to determine the spectral resolution (SR) of the setup. SR depends on various parameters. Some are instrument specific, such as the gratings, slit widths, pinhole diameters, focal length, system magnification and excitation source. Others are sample specific, such as *the* Raman shift, and true Raman bandwidth. Different manufacturers design their setups differently according to the needs of specific applications; thus, resulting in different SRs for instruments of different producers. In this work, we compare the SRs of two commercial Raman setups, Renishaw inVia Raman microscope and WITec alpha300RAS Raman microscope with a home-built parabolic mirror assisted Raman setup<sup>1,2</sup>.

To compare the three setups, SR is calculated using a basic equation derived by Liu *et al.*<sup>3</sup> by measuring the bandwidth of characteristic Raman signatures of diamond and the aberration-diffraction correction factor (ADCF) as a function of slit width or pinhole diameter, grating groove densities and excitation sources. We compare these results by measuring the bandwidth of a narrow band light source (in this case a neon lamp) as a function of slit width or pinhole size and grating groove. A detailed correlation of SR between theoretical bandwidths expected from a particular setup (using basic formula) and measured bandwidth from experimental results is illustrated in this article. We provide useful insights into the technical aspects of these setups and their potential inter-transferability of results using a common platform. Additionally, we also discuss the dependence of spectral resolution on Raman shift axis as a function of grating. This work opens to novel dimension of transferability and comparability of results within setups of different spectrometer designs.

## References

1. Lieb, M.; Meixner, A. *Optics express* **2001**, *8* (7), 458–474, DOI:10.1364/OE.8.000458.
2. Zhang, D.; Wang, X.; Braun, K.; Egelhaaf, H.-J.; Fleischer, M.; Hennemann, L.; Hintz, H.; Stanciu, C.; Brabec, C. J.; Kern, D. P.; Meixner, A. *J. Raman Spectrosc.* **2009**, *40* (10), 1371–1376, DOI:10.1002/jrs.2411.
3. Liu, C.; Berg, R. W. *Appl Spectrosc* **2012**, *66* (9), 1034–1043, DOI:10.1366/11-06508.

# Lysozyme stabilized Silver-Gold Nanoclusters with Graphene as a Turn-Off Fluorescence System

Nurul Farhana Abd Razak<sup>1</sup>, Shadreen Fairuz<sup>1</sup>, Xin Yi Wong<sup>2</sup>, Siu Yee New<sup>1</sup>, Kasturi Muthoosamy<sup>2</sup>

<sup>1</sup>*School of Pharmacy, University of Nottingham Malaysia, Malaysia*

<sup>2</sup>*Nanotechnology Research Center, University of Nottingham Malaysia*

The growing popularity of nanocluster (2 – 10 nm in size) in sensing and imaging applications has been acknowledged in the past decade. It is believed that synergistic effect of two types of transition metals which is gold (Au) and silver (Ag) can produce higher fluorescence intensity under UV light compared to single metal nanoclusters.

Herein, bimetallic silver-gold nanocluster was synthesized in aqueous solution using lysozyme that acts as a stabilizing and reducing agent. The prepared lysozyme-silver-gold nanocluster (Lys-AgAu NCs) show higher emission intensity at 574 nm compared to the single metals: lysozyme-silver nanocluster (Lys-Ag NCs) and lysozyme-gold nanocluster (Lys-Au NCs). Lys-AgAu NCs emitted intense orange fluorescence under UV light ( $\lambda_{\text{ex}}$  365 nm) and are of approximately 2 nm in size with quantum yield of 5%.

Optimization of the reaction parameters were conducted and followed by characterizations such as circular dichroism, FESEM (Field emission scanning electron microscopy), EDX (Energy dispersive X-Ray spectroscopy), XPS (X-Ray photoelectron spectroscopy) and HRTEM (High resolution transmission electron microscopy). As a preliminary investigation on possible application of Lys-AgAu NCs in imaging and sensing, Graphene oxide (GO) was added to the Lys-AgAu NCs, to demonstrate its interaction and function as a potent quencher in turning off the fluorescence of the nanoclusters. Hence, a fluorescence turn 'on' and 'off' system can be realized.

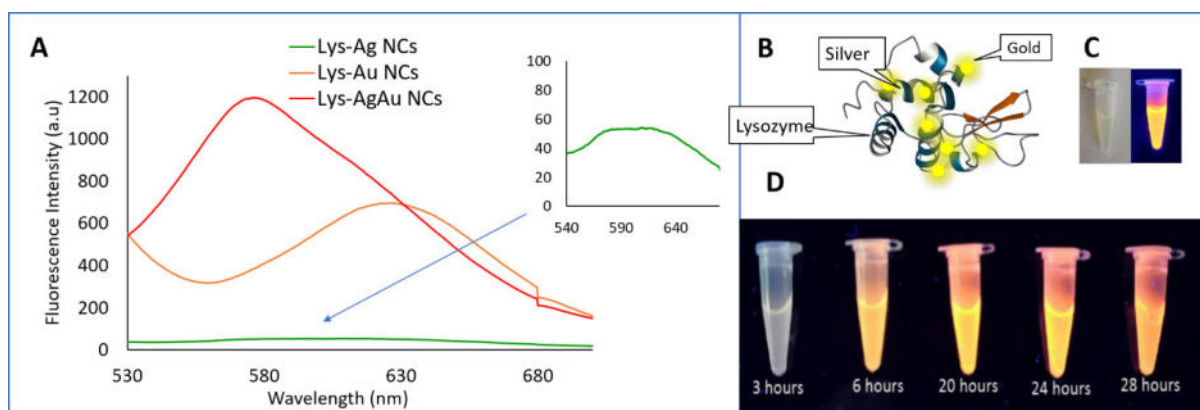


Figure 1: (A) Comparison of emission intensity of Lysozyme (Lys) bimetallic (AgAu NCs) to single metal (Ag and Au NCs) with excitation at 365 nm. (B) Schematic diagram of Lys-AgAu NCs. (C) Lys-AgAuNCs under visible (left) and UV light (right). (D) Fluorescent images of Lys-AgAu NCs taken under UV light, at different incubation time (3, 6, 20, 24 and 28 hours).

# Hidden smart templates for blue bioeconomy: complex functional structures of marine invertebrates revealed by confocal Raman imaging

Fran Nekvapil<sup>1,2</sup>, Simona Cintă Pinzaru<sup>1</sup>, Branko Glamuzina<sup>3</sup>

<sup>1</sup>Biomolecular Physics Department, Babeş-Bolyai University, Cluj-Napoca, Romania

<sup>2</sup>Physics of Nanostructured Systems, INCDTIM Cluj-Napoca, Romania

<sup>3</sup>Department for Aquaculture, University of Dubrovnik, Dubrovnik, Croatia

Blue bioeconomy concept prompted for added-value by-products from aquaculture and seafood sector, while current knowledge on broaden diversity of species and their by-products is quite scant in terms of high resolution morphological and chemical composition. Biomaterials of marine origin, especially hard tissue of marine invertebrates consisting usually of an organic scaffold mineralized with calcium carbonate and/or various phosphates, are attracting an increased interest to blue bioeconomy. Here we investigate structure-function relationship in the exoskeleton of a spearer mantis shrimp *Squilla mantis*, namely the raptorial claw (Fig. 1 left), which is used for striking its prey, and the abdominal cuticle (Fig. 1 right), which protects against predators and conspecific fighters. Confocal Raman imaging analysis of the claw cross-section revealed a radial gradient structural organization, with poorly crystallized calcite forming the core (main band at  $1082\text{ cm}^{-1}$ ), and highly crystallized phosphate salts ( $963\text{ cm}^{-1}$ ) forming the coating layer. Moreover, point-analysis revealed that claw teeth are notably reinforced with phosphate salts. The abdominal cuticle is much more elastic, showing a strong Raman signal of chitin ( $1108\text{ cm}^{-1}$ , bands in  $1200\text{-}1400\text{ cm}^{-1}$  range), which forms an organic fibre network. The network appears to be denser towards the cuticle interior face, while the intensity of chitin signal gradually decreases towards the outer face with concomitant increase of biomineral signal (broad band around  $1080\text{ cm}^{-1}$ ). Hence two templates are revealed which have been tested throughout thousands of years of evolution: one for sharp and wear-resistant spearing structure, and the other for an impact resistant and lightweight shield. The blue bioeconomy sector is discovering and exploiting biomaterials hidden in marine environment as biomimetic inspirations, and confocal Raman imaging plays an important role in detailed and reliable chemical characterization of these materials.

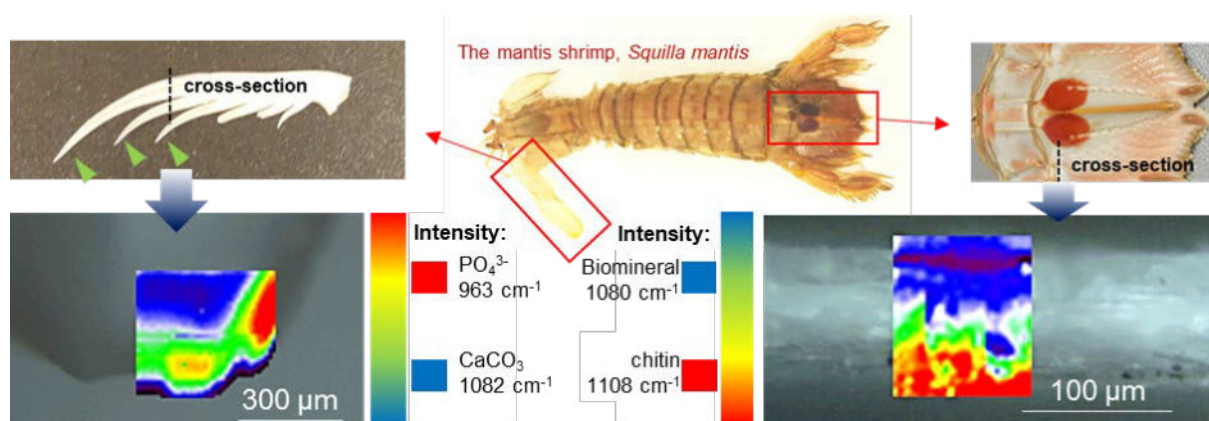


Fig. 1. Confocal Raman imaging results obtained on mantis shrimp *Squilla mantis* raptorial claw (left) and the abdominal cuticle (right). Green arrows indicate phosphate-reinforced claw teeth.

# Surface enhanced Raman Spectroscopy of stable - isotope labelled biological samples

Katerina Prohaska<sup>1</sup>, Theresa Stelzer<sup>1</sup>, David Lilek<sup>1</sup>, Birgit Herbinger<sup>1</sup>  
<sup>1</sup>Austrian Biotech University of Applied Sciences, Campus Tulln, Austria

The potential was evaluated of the stable – isotope Raman Microspectroscopy (SIRM) in combination with surface enhanced Raman signals (SERS) to investigate metabolic pathways in biological samples.

Untargeted isotope labelling by cultivation of *E. coli* (DSM 498) in M9 mineral medium with a <sup>13</sup>C carbon source and a <sup>15</sup>N nitrogen source was successful. The expected typical red shift of Raman signals towards lower wavenumbers caused by <sup>13</sup>C, and <sup>15</sup>N respectively, could be verified. While compared to the label-free signals the isotope labelled *E.coli* cells show the red shift, the CaF<sub>2</sub> substrate signal, which was used as reference, remained unaltered and reproducible in all spectra at 325 cm<sup>-1</sup>. The red shifted signals enabled a differentiation between label-free and labelled *E.coli* cultivated.

Of each *E. coli* 2D cell layer, 75 spectra were collected with which a principle component analysis (PCA) was carried out. All spectra were baseline corrected and normalized and in order to minimize the impact of the noise, the first derivative was calculated. The spectral range was reduced to 700-775 cm<sup>-1</sup>, in which the strongly shifted adenine and cytosine/uracil signals were located (see figure 1).

In the following SERS set up the Raman signals of the *E.coli* 2D cell layer could be enhanced by factor of 10<sup>4</sup> by drying the *E.coli* culture on CaF<sub>2</sub> substrate and covering the sample drop with colloidal solution of 40 nm Ag-nanoparticles. Albeit a significant enhancement effect was observed, the reproducibility of these measurement requires further optimization.

In an advancement of these experiments, targeted substitution of <sup>12</sup>C atoms in molecules of interest can be achieved by using defined <sup>13</sup>C cultivation protocols. Two major application fields are in focus of future studies: on one hand the physiology of fungi as pathogenic agents for crops, and on the other hand the chemical substances secreted by insects to study their communication.

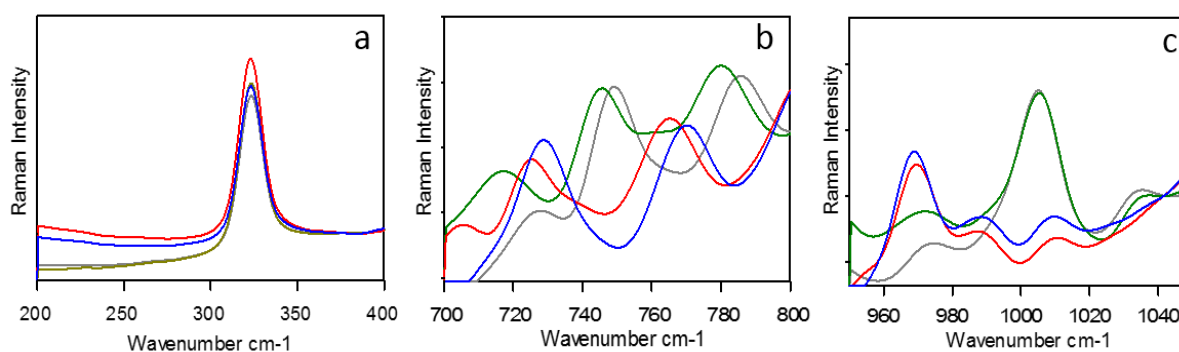


**Fig. 1:** SIRM-relevant spectral ranges: a) CaF<sub>2</sub> signal (325 cm<sup>-1</sup>); b) shift of adenine (749 cm<sup>-1</sup>) and cytosine/uracil (786 cm<sup>-1</sup>); c) shift of phenylalanine (1003 cm<sup>-1</sup>); label-free grey: <sup>12</sup>C/<sup>14</sup>N; labelled blue: <sup>13</sup>C, green: <sup>15</sup>N, red: <sup>13</sup>C/<sup>15</sup>N. Spectra were recorded with laser 532 nm, laser power 20 mW, exposure time 2x10 sec and a resolution of 9-15 cm<sup>-1</sup>.

# Evaluation of differences in normal and treated carbon fibre surfaces using Raman microscopy and chemometrics

Chima Robert<sup>1</sup>, Sara J. Fraser-Miller<sup>1</sup>, Aaron Marshall<sup>2</sup> and Keith C. Gordon<sup>1</sup>

<sup>1</sup>Department of Chemistry, University of Otago, Dunedin, New Zealand.

<sup>2</sup>Department of Chemical and Process Engineering, University of Canterbury, Christchurch, New Zealand.

Carbon fibre treatment is of immense importance in its ultimate performance for polymer reinforcement. In this work, Raman spectroscopy in combination with chemometrics was utilized to investigate differences in carbon fibre surfaces treated using different procedures. The Raman spectra data were collected from chemically treated, heat treated and untreated fibre samples. Preprocessed spectral data were analysed using principal component analysis (PCA) and support vector machine (SVM) classification. PCA highlighted the variation among the fibres and distinguished the control fibres from the treated samples as well as the heat treated from the chemically treated fibre samples. Results obtained using SVM classification yielded 62 % accuracy for classifying the four groups of treated fibres. Curve fitting analysis on the D and G-bands show little differences in the surface crystalline sizes which might be indicative of the variation in their graphitic structures post-treatment.

**Key words:** Carbon fibre, Raman spectroscopy, chemometrics, surface crystalline sizes.

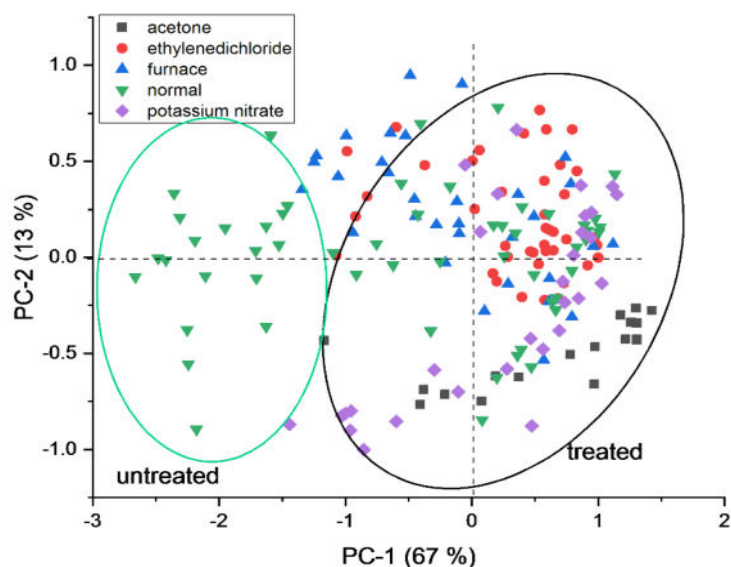


Fig. 1: PCA scores plot of spectral data from different carbon fibre

## References

1. Sadezky, A.; Muckenhuber, H.; Grothe, H.; Niessner, R.; Pöschl, U., Raman microspectroscopy of soot and related carbonaceous materials: Spectral analysis and structural information. *Carbon* **2005**, *43* (8), 1731-1742.

# A detailed Raman spectroscopy and correlative study of the electrochemical intercalation of sodium ions into highly crystalline birnessite in aqueous solution

Philipp Scheitenberger<sup>1</sup>, Mika Lindén<sup>1</sup>,

<sup>1</sup>Institute of Inorganic Chemistry II, Ulm University, 89081 Ulm, Germany<sup>2</sup>

Metal oxides with layered structure are, due to their large theoretical capacities attractive electrode materials for sodium-ion/potassium batteries and pseudocapacitors in consumer electronics, memory backup systems and electric vehicles. One promising material belonging to this compound class are birnessite-type manganese oxides with a theoretical capacitance of  $1370 \text{ F g}^{-1}$  for one-electron transfer over a potential range of  $1 \text{ V}^{[1]}$ /  $243 \text{ mAhg}^{-1}[2]$ . Their layered structure is comprised of edge-sharing  $\text{MnO}_6$  octahedra, with water molecules and charge-balancing metal cations such as  $\text{Li}^+$ ,  $\text{Na}^+$ ,  $\text{K}^+$  occupying the interlayer region. Different charge storage mechanisms have been proposed for birnessite-type  $\text{MnO}_2$ . Nevertheless, all mechanisms have in common that during charging, de-intercalation of charge balancing alkali ions leading to an increased interlayer charge repulsion and intercalation of water lead to an increase of the interlayer distance.<sup>[3]</sup> In addition, a phase transition from monoclinic to hexagonal was reported when the alkali-ion content decreases/falls below some threshold value<sup>[4]</sup>. However, since most birnessites reported in literature possess a rather low crystallinity, detailed structural analysis applying Rietveld method is difficult. Therefore electrochemical intercalation and de-intercalation of  $\text{Na}^+$  ions from aqueous solution into/from highly crystalline, layered manganese oxide in the form of birnessite has been studied using cyclic voltammetry, *ex situ* x-ray diffraction, and *in situ* and *ex situ* Raman spectroscopy. The calibration of *ex-situ* Raman against x-ray diffraction data allows detailed insight into processes taking place within the birnessite structure during  $\text{Na}^+$  intercalation and de-intercalation such as changes in the interlayer distance ( $d_{001}$ -spacing), phase transition from monoclinic to hexagonal and the occurrence of “electrochemical stress” at certain stages of the charging Process.

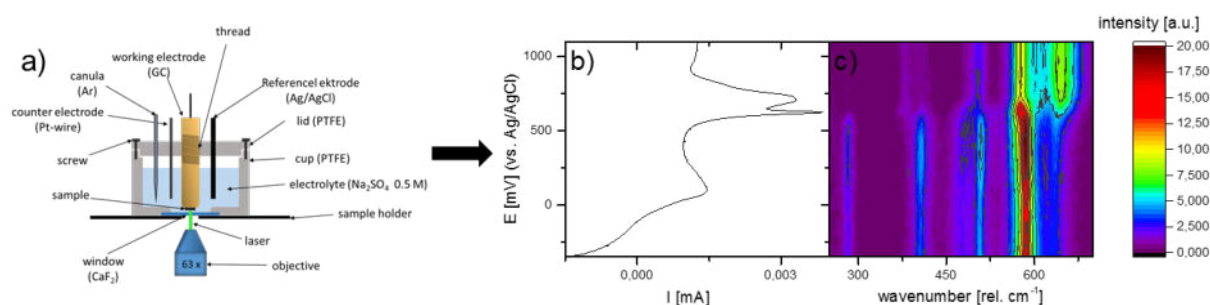


**Figure 1:** a) Sketch of the in-situ Raman-measuring cell. b) and c) cv-curve and corresponding Raman-spectra, respectively.

- [1] H. -a. Pan, O. Ghodbane, Y.-T. Weng, H.-S. Sheu, J.-F. Lee, F. Favier, N.-L. Wu, *J. Electrochem. Soc.* **2015**, *162*, A5106–A5114.
- [2] H. Xia, X. Zhu, T. Chen, L. Gu, J. Liu, Q. Liu, S. Lan, Y. S. Meng, *Nat. Commun.* **2018**, 1–10.
- [3] O. Ghodbane, J. L. Pascal, F. Favier, *ACS Appl. Mater. Interfaces* **2009**, *1*, 1130–1139.
- [4] S. Franger, S. Bach, J. Farcy, J. P. Pereira-Ramos, N. Baffier, *J. Power Sources* **2002**, *109*, 262–275.

# Raman spectroscopy of vanadium oxides

P. Shvets, K. Maksimova, A. Goikhman  
*REC "Functional Nanomaterials", Immanuel Kant Baltic Federal University,  
Kaliningrad, Russian Federation*

Vanadium oxides, particularly  $V_2O_5$ ,  $VO_2$  and  $V_2O_3$ , have attracted much attention because of their applications in catalysis, as cathode materials for batteries, electrochromic systems or supercapacitors, as smart windows, optical switching devices, and memory elements, including memristors. Vanadium is a multivalent transition metal that forms a large number of different stable oxides, and this number becomes even larger if we take into account metastable phases (for instance, there are at least 14  $VO_2$  polymorphs). Recent advances in thin film synthesis ensure precise control over the stoichiometry of growing films and allow the production of metastable phases in nonequilibrium conditions. Thus, there is a need for a simple technique for identifying the produced crystal phase. Raman spectroscopy is a well-established facility that promptly produces the desired result on a millimeter scale without sample degradation. However, this technique requires reference spectra, which are not always available.

Our work summarizes Raman scattering data for different stable and metastable phases of vanadium oxides available in literature. Further, we employ arc sputtering to produce vanadium oxide films, including  $\alpha$  and  $\beta$ -vanadium,  $V_{14}O_6$ ,  $VO$ ,  $V_2O_3$ ,  $V_3O_5$ , several phases of  $VO_2$ ,  $V_6O_{13}$ ,  $V_3O_7$ , and  $V_2O_5$ . All the films are studied using Raman spectroscopy. We demonstrate that a significant change in the  $V_3O_5$  spectrum takes place along the phase transition occurring at approximately 140 °C. Moreover, we describe differences between the spectra of  $VO_2$  polymorphs produced without doping impurities ( $VO_2$  (M1),  $VO_2$  (M2), and  $VO_2$  (T)). Finally, we analyze conflicting data on  $V_7O_{16}$  and  $V_3O_7$  and provide an explanation of the observed spectra. Our work is aimed at laying the groundwork for easy identification of vanadium oxide phases in thin films, using Raman spectroscopy.

This work was prepared in a framework of the project № 14.584.21.0028 (the unique number RFMEFI58417X0028) between Russian Ministry of Education and Science and Immanuel Kant Baltic Federal University.

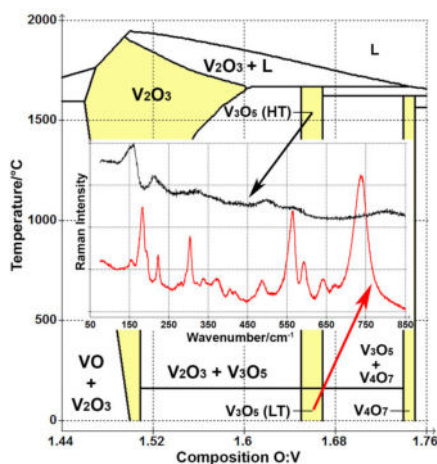


*Fig. 1: Vanadium-oxygen phase diagram and Raman spectra of  $V_3O_5$ .*

# Correlative Fluorescent and Raman Microscopy for Mitotic Phase Detection

Csaba Vörös<sup>1</sup>, Dávid Bauer<sup>1</sup>, Tivadar Danko<sup>1</sup>, Ede Migh<sup>1</sup>, Attila-Gergely Végh<sup>1</sup>,  
Balázs Szalontai<sup>1</sup>, Krisztian Koos<sup>1</sup>, Peter Horvath<sup>1,2</sup>

<sup>1</sup>Biological Research Centre, Hungarian Academy of Sciences, Szeged, Hungary

<sup>2</sup>Institute for Molecular Medicine Finland, University of Helsinki, Helsinki, Finland

Correlative microscopy techniques are widely used to complement their advantages. In this work we aim to profile the cell cycle, particularly the mitotic phases by combining fluorescent high content microscopy and Raman imaging.

First, the sample of HeLa cells is screened using a high content fluorescent microscope. The cells were stained using DAPI. The images are segmented using Mask-RCNN deep learning model (Hollandi *et al.*), and morphological and textural features are extracted using CellProfiler. The features are loaded into Advanced Cell Classifier (ACC) and classes are defined for the mitotic subphases and the interphase. A small number of cells are assigned to these classes for training a classical machine learning model. After predicting the rest of the dataset a given number of cells are selected from each defined phenotype. Their Raman spectra is measured in a fully automated manner. To reduce the duration of the measurement the optimal microscope stage route is calculated between the cells. The spectra is acquired over the bounding boxes of the selected nuclei.

We combine feature selection and dimensionality reduction methods to analyze the spectra. Using PCA and k-means clustering we could identify most of the previously defined classes. The preliminary results are promising. We aim to improve our methods to detect all the subphases of mitosis based only on the Raman signal.

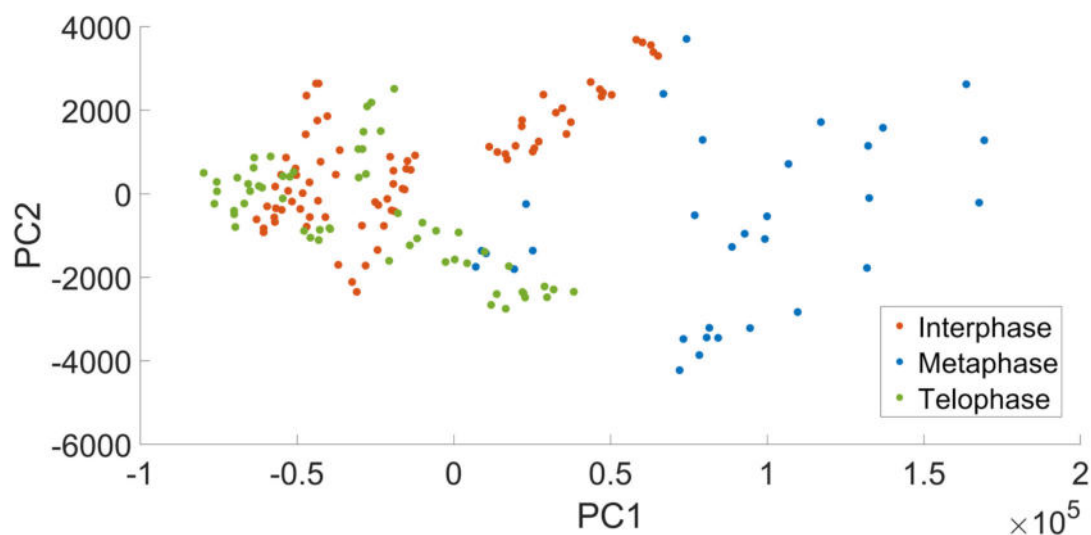


Fig. 1: Scatter plot of the dimensionality reduced spectra with PCA. The dataset includes five cells of each class.

# Bioinspired Polydopamine Based Surface-Enhanced Raman Spectroscopy (SERS) Platforms

Mehmet Yilmaz<sup>1,2</sup>, Asli Yilmaz<sup>2,3</sup>

<sup>1</sup>*Department of Chemical Engineering, Ataturk University, 25240 Erzurum, Turkey*

<sup>2</sup>*East Anatolia High Technology Application and Research Center (DAYTAM), Ataturk University, 25240 Erzurum, Turkey*

<sup>3</sup>*Department of Biology, Ataturk University, 25240 Erzurum, Turkey*

Since its discovery, surface-enhanced Raman spectroscopy (SERS) has attracted remarkable attention as a highly sensitive and powerful approach for the detection of chemical and biological substances in trace amount. Basically, the enhancement in Raman signals is due to the increase in electromagnetic field as a result of the close vicinity (in nm scale) of plasmonic (gold, silver or copper) nanostructures. Many novel strategies have been developed to fabricate a sensitive, selective, and reliable SERS platforms for the fingerprint SERS spectra of analyte molecules at ultralow concentrations.

The employment of the coinage metal colloidal nanoparticles is a simple, inexpensive, and facile method. However, the uncontrolled aggregation of nanoparticles leads to reproducibility problems in SERS spectra. This issue limits their employment as an ideal SERS platform for the practical applications. Alternative methods such as electron beam lithography, nanosphere lithography have been proposed to overcome the major drawbacks of colloidal nanoparticles. However, these complicated techniques require quite expensive and sophisticated devices as well as high experience of the user with long application time.

In this study, we aimed to decorate surface of the gold nanorod arrays (GNAs) with silver nanoparticles (AgNPs) through a thin layer of polydopamine (PDOP). Herein, PDOP, with its abundant functional groups, eliminates the aggregation of colloidal metal nanoparticles. Also, PDOP can be used as an interphase between GNAs and AgNPs which can provide additional enhancement in Raman signal. For this, PDOP via oxidative polymerization of dopamine was conformally coated onto the GNAs substrate (GNA@PDOP) and then this system was decorated with AgNPs (GNA@PDOP@AgNP). SERS measurement of the proposed system showed that the thickness of the PDOP layer was the dominant parameter in SERS activity. The distance between two nanostructures (GNAs and AgNPs) with controlled distance in nm scale via well-controlled PDOP layer lead to remarkable enhancement in electric field distribution which is required for an ideal SERS system.

# Insights into the mineral phase evolution of calcium aluminate cement (CAC) during hydration studied by *in situ* hyperspectral Raman imaging

S. Zimmer<sup>1</sup>, O. Krause<sup>1</sup>, K. Hauke<sup>2</sup>, T. Geisler<sup>2</sup>

<sup>1</sup> Hochschule Koblenz, Höhr-Grenzhausen, Germany

<sup>2</sup> Institute of Geosciences, Rheinische Friedrich-Wilhelms-Universität, Bonn, Germany

In this study, we used *in situ* hyperspectral Raman imaging to investigate the formation of calcium aluminate cement (CAC), which is an important inorganic binder for refractory monolithics and is broadly used in industrial thermal processes as lining material. In this area of use, CAC is used to obtain a green strength that is high enough to obtain a rigid structure after installation and demoulding. Beside the generic property of refractory materials, i.e., to withstand temperatures of up to 2000 °C, the setting process must be well understood, i.e., predictable in order to minimize service downtimes. Before use, the installations must be dehydrated by a monitored heating process. Therefore, it is indispensable to further deepen our understanding about the nature of the hydration and dehydration processes taking place in CAC bond refractory monolithics. Here, we focus on *in situ* Raman imaging of the hydration process of CAC clinker that consists predominantly of monocalcium aluminate (CA) and calcium dialuminate (CA<sub>2</sub>), but dodecacalcium heptaaluminate (C<sub>12</sub>A<sub>7</sub>) and calcium hexaaluminate (CA<sub>6</sub>) are also present in minor concentrations. After about 16 wt.-% of CAC to the dry castable mixture and after the addition of 7 wt.-% water, twelve point-by-point Raman images were subsequently recorded within a dwell time of 12 h from an area of 100x100 µm<sup>2</sup> with a step size of 5 µm. A 2 W Nd:YAG laser (532.09 nm) was used as excitation source and an electron-multiplier CCD detector to detect the scattered light. To interpret and visualize the time-resolved, 2-dimensional Raman measurements, the above mentioned CAC phases were synthesized by solid state reactions and Raman spectra were taken as references. Our preliminary *in situ* Raman images demonstrate the power of *in situ* Raman spectroscopy to determine the beginning of setting as well as the kinetics of the hydration process, i.e., of the formation of calcium aluminate hydrate phases.

# **Application Note / White Paper**



## Automated particle analysis with ParticleScout

High-resolution measurements of particles are of great interest in many fields of application. WITec's ParticleScout is an analysis tool for the alpha300 Raman microscope series that locates, categorizes, identifies and quantifies particles over even large sample areas. Automated routines sort particles and acquire their Raman spectra, generating reports that provide a detailed overview of the sample.

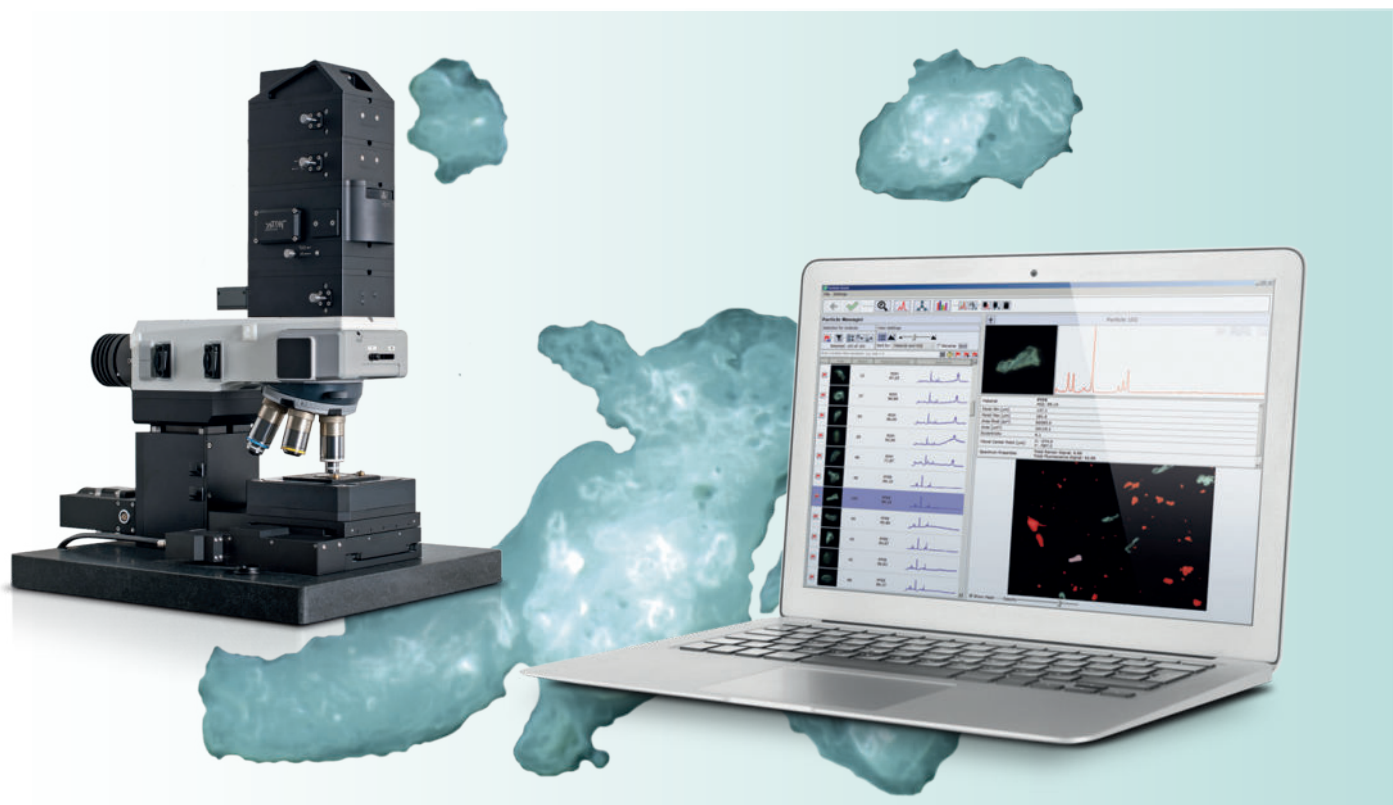
Pollen, dust, flour, metal flakes and pigments in paints, titanium dioxide in sunscreen and toothpaste, fat crystals in food emulsions – these and many more substances in our daily lives contain or consist of microparticles. Recently, the public and scientific communities have directed their attention towards microplastic particles in the environment.

Confocal Raman microscopy is ideally suited to finding, classifying and identifying microparticles because not only does it yield images with a resolution down to 200 nm, but with Raman vibrational

spectroscopy the chemical components of a sample can be identified. It is a nondestructive method that requires little, if any, sample preparation. A Raman microscope can generate high-resolution images that show both the structural features and distribution of molecules within a sample. However, Raman spectroscopic imaging is not yet widely applied to microparticle analysis.

The challenge in Raman microparticle analyses lies in automating the detection of individual particles and classifying those of interest by size or shape before

determining their chemical compositions. For such analyses, WITec has developed ParticleScout. In combination with a WITec Raman microscope, this tool enables measurements that proceed from a white light sample overview to particle detection, acquisition of Raman spectra, post-processing of spectra and chemical identification to creating a final report. During this procedure the user can define the criteria according to which the particles shall be investigated, such as area, perimeter, minimum/maximum Feret diameter, elongation or equivalent diameter and many more.



## How to identify and classify microplastic particles with ParticleScout

In order to illustrate the workflow of microparticle analysis, a mixture of microplastics was analyzed with an alpha300 Raman microscope equipped with ParticleScout. First, large-area bright-field (Fig. 1A) and dark-field (Fig. 1B) images were recorded by image stitching. This technique combines images from adjacent sample areas into one composite, so that high-resolution images of large areas can be acquired. Additionally, focus stacking yielded sharp outlines for all the differently sized particles by combining images from different focal planes (Fig. 1A, B).

A software algorithm detected particles in the overview image through a brightness threshold and represented their positions in the form of a two-color image (Fig. 1C). For each particle, structural characteristics were calculated automatically, such as area, perimeter, aspect ratio and many more. Conventional Raman imaging of large areas would include much of the empty space surrounding the sparsely distributed particles. In order to accelerate the measurement, ParticleScout automatically records spectra of selected particles only (see Fig. 1D for an example).

After processing the spectra (i.e. background subtraction) the particles were chemically identified using the seamlessly-integrated TrueMatch Raman database management software. TrueMatch automatically searches commercial or custom databases quickly and identifies particles reliably.

Finally, a report was generated (Table 1) that summarized the abundance and physical properties of the different materials in the sample. The relative abundance of the sample components is illustrated graphically (Figure 1E).

As particle classification, image processing and analysis of Raman spectra are executed within one platform, ParticleScout offers an effective solution for automated, comprehensive investigations of particles.

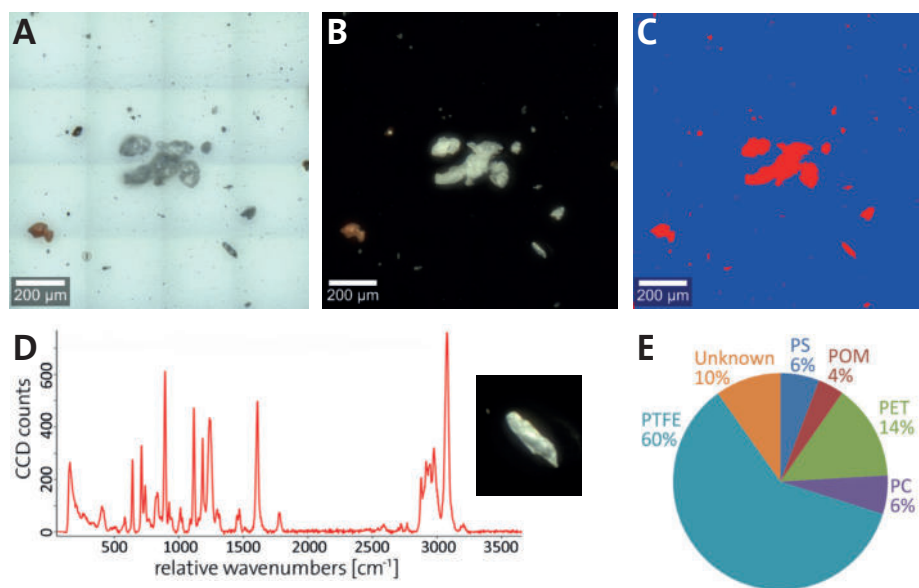


**Figure 1: Analysis of a mixed microplastic sample using ParticleScout.**

(A)-(B): Large-area (1 mm x 1 mm) bright-field (A) and dark-field (B) views of a mixture of microplastic particles were generated using image stitching and focus stacking.

(C): Particles are automatically detected through a brightness threshold and represented as a two-color mask.

(D): Background-corrected Raman spectrum of an example particle.

(E): Composition of the mixed plastic sample. After processing the spectra, the chemical compositions of the individual particles were identified using TrueMatch (see Table 1).

PS: polystyrene; POM: polyoxymethylene; PET: polyethylene terephthalate; PC: polycarbonate; PTFE: polytetrafluoroethylene; Unknown: unidentified particles.

**Table 1: Composition of a mixed microplastic sample.** Abundance and size distribution for the identified materials. See Figure 1 for abbreviations.

	Sum	5-10 µm	10-20 µm	20-50 µm	50-100 µm	> 100 µm
PS	89	47	12	8	17	5
POM	59	34	12	8	4	1
PET	217	106	70	20	17	4
PC	87	18	45	17	7	0
PTFE	913	417	297	103	77	19
Unknown	150	45	78	8	19	0
Sum	1515	667	514	164	141	29

## Microparticles in a cosmetic cream

In some pharmaceutical and cosmetic products, microparticles are responsible for the desired effects or consistency. Here, a cosmetic peeling cream was analyzed using an alpha300 R microscope equipped with ParticleScout. First, a large-area image was generated by image stitching (section shown in Fig. 2A). In the bright-field image, crystalline particles are clearly visible as bright blue structures, while the cream matrix appears as dark grey. A complete Raman image was acquired for a subsection of the image and overlaid, visualizing the spatial distribution of the sample components. The Raman image is color coded according to the recorded spectra of the identified components (Fig. 2B), showing that the cream consists mainly of anatase and boron nitride particles in an oil matrix. Anatase is a form of titanium dioxide and causes the peeling effect, while boron nitride is often used in cosmetics as a slip modifier.

In the next step, ParticleScout was used to analyze the cream's composition in more detail. Raman spectra were acquired automatically for 3941 particles. With the seamlessly-integrated TrueMatch software, the recorded Raman spectra were processed and the particles were identified by referencing the Raman database. Quantification of the sample components revealed 37% anatase and 31% boron nitride particles in the cream (Fig. 2C). The particles were further categorized according to their physical shape and size using Boolean filters. The size distribution of the different components was evaluated, revealing that anatase particles are statistically larger than boron nitride particles (Fig. 2D). For this histogram, the projection area was used as a measure for the particle size, but other parameters such as perimeter, bounding box, Feret diameter, aspect ratio or circular equivalent diameter could also be used for similar analyses.

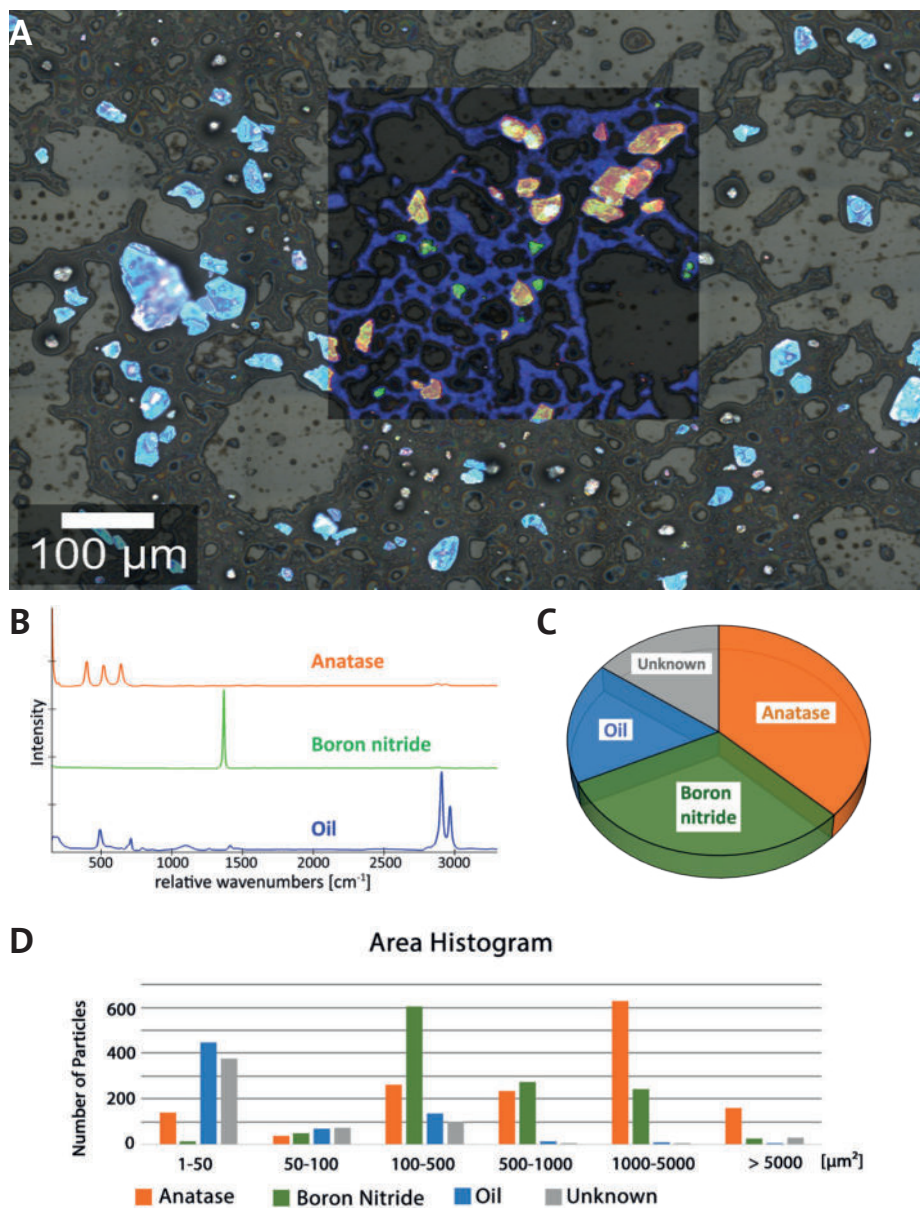


**Figure 2: Particles in a cosmetic peeling cream.**

(A): Optical bright-field image overlaid with the confocal Raman image (color coded according to the spectra in B).

(B): Raman spectra of the molecular components in the sample: anatase (orange), boron nitride (green) and oil (blue).

(C): Pie chart of the compound distribution in the sample: 37% anatase (orange), 31% boron nitride (green), 17% oil (blue), 15% not identified (grey).

(D): Area distribution of the chemical components (color coded as in C).

## Quantifying microplastics in environmental samples

Environmental pollution by microplastics is a growing concern because of their potentially harmful effects on human health and ecosystems. For assessing such effects, microplastics in environmental samples need to be quickly and reliably identified and their abundance and size distribution must be quantified. The aim of the following measurement was to quantify the amount of microplastic particles in a sludge sample from a wastewater

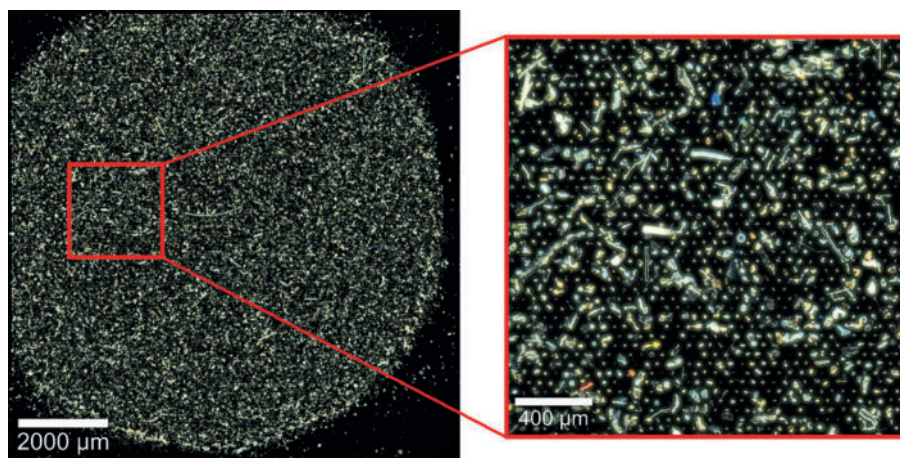
treatment plant (sample courtesy of Dieter Fischer, Leibniz Institute of Polymer Research, Dresden, Germany). The sludge sample (50 g) was pretreated, purified and filtered. Figure 3 shows the dark-field image of a filter (pore size 10 µm) on which tens of thousands of particles from the sludge sample were retained. ParticleScout automatically measured Raman spectra for about 18,000 particles. Out of these, 46 were unambiguously identified

as microplastics by the database software TrueMatch, corresponding to about 0.25% of all measured particles. The most abundant types of microplastics were polyethylene (25 particles) and polypropylene (12 particles). Their sizes ranged from 10 µm to 100 µm (circular equivalent diameter). Particles in this size range can be ingested by diverse marine organisms, but their potential consequences are still subject to investigation.

### Figure 3: Microplastics in a wastewater treatment plant sludge sample.

Dark-field image of a silicon filter with 10 µm pore size (left) and zoom-in image of the area marked in red (right). About 0.25% of all investigated particles were microplastics.

[Sample courtesy of Dieter Fischer, Leibniz Institute of Polymer Research, Dresden, Germany.]



### The five steps of microplastic analyses

A detailed microparticle analysis typically consists of the five following steps. A high level of automation is required because manually inspecting a large number of particles is time-consuming and error-prone.

- **Collecting and processing the sample:** Environmental samples have to be collected and purified for further analysis, for example by filtration or sieving.
- **Locating particles:** Particles are located in a large-area white-light image.
- **Categorizing particles:** Particles are grouped according to structural parameters such as size or shape.
- **Identifying particles:** Raman spectroscopy is well suited to investigating the chemical composition of microplastic particles.
- **Generating a report:** Tables and histograms summarize the sample composition and relate chemical to structural properties.

### Further reading

- Araujo et al. Identification of microplastics using Raman spectroscopy: Latest developments and future prospects. *Water Res.* 2018, **142**: p. 426-440.
- Hidalgo-Ruz et al. Microplastics in the marine environment: a review of the methods used for identification and quantification. *Environ. Sci. Technol.* 2012, **46**: p. 3060-3075.
- Ivleva et al. Microplastic in Aquatic Ecosystems. *Angew. Chem. Int. Ed.* 2017, **56**: p. 1720-1739.
- Käppler et al. Analysis of environmental microplastics by vibrational microspectroscopy: FTIR, Raman or both? *Anal. Bioanal. Chem.* 2016, **408**: p. 8377-8391.
- Van Cauwenberghe et al. Microplastics in sediments: A review of techniques, occurrence and effects. *Mar. Environ. Res.* 2015, **111**: p. 5-17.

## Detailed analysis of selected particle subsets

In many applications, only a fraction of the particles in a sample is of scientific interest. Particles in mixed samples must therefore be selected according to physical properties and further analysis will then be limited to those that meet the specified criteria. The following example shows how ParticleScout can be used to isolate particles of interest quickly and conveniently. The sample contained tungsten disulfide ( $WS_2$ ) nanowires, prepared by Reshef Tenne (Weizmann Institute, Israel) and kindly provided through Martin Konečný and

Tomáš Šíkola (CEITEC, Institute of Physical Engineering, Brno University of Technology, Czech Republic). Using an alpha300 R microscope equipped with ParticleScout, several thousand particles were located on the silicon dioxide substrate, but not all of them were the desired nanowires (Fig. 4A). These structures are several micrometers long, but only a few hundred nanometers thick. Manually inspecting all particles and selecting the nanowires would be tedious and time-consuming. Using ParticleScout, the desired nanowires were isolated

within seconds by their elongated shape: Specifying an aspect ratio of greater than 2.5 yielded 218 nanowires (Fig. 4B), which could be further investigated. For example, Raman spectra could be acquired from every particle to confirm that they consist of  $WS_2$ . Measurements with different laser polarizations demonstrated the anisotropic scattering behavior of the nanowires: The intensity of the Raman shift peak at  $421\text{ cm}^{-1}$  depends on the orientation of the nanowire with respect to the polarization of the excitation light (Fig. 4C).

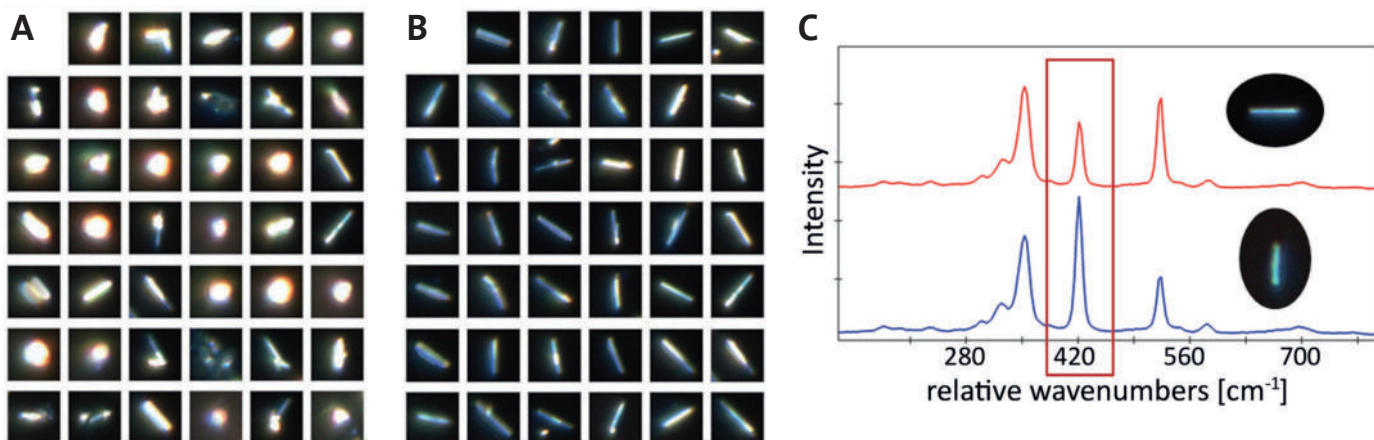


**Figure 4: ParticleScout distinguishes  $WS_2$  nanowires from globular particles within seconds.**

(A): Representative subset of the 3135 particles of less than  $5\text{ }\mu\text{m}$  in length detected in a sample of  $WS_2$  nanowires on silicon dioxide.

(B): Representative subset of the 218 nanowires isolated by additionally specifying an aspect ratio of greater than 2.5.

(C): Raman spectra for two orientations of nanowires with respect to the polarization of the laser light. The intensity at  $421\text{ cm}^{-1}$  depends on the angle between the nanowire and the laser polarization.

[Sample courtesy of Reshef Tenne (Weizmann Institute, Israel), Martin Konečný and Tomáš Šíkola (CEITEC, Institute of Physical Engineering, Brno University of Technology, Czech Republic).]

## Whitepaper

# Five criteria for high-quality Raman microscopes

## Introduction to correlative Raman techniques including application examples

Damon Strom, Sonja Breuninger, Eleni Kallis, Harald Fischer, Andrea Richter, Ute Schmidt, Olaf Hollricher  
WITec GmbH, Lise-Meitner-Str. 6, 89081 Ulm, Germany

90 years ago Chandrasekhara Venkata Raman and Kariamanickam Srinivasa Krishnan first documented "A New Type of Secondary Radiation", which then became known as the Raman Effect [1, 2]. Raman spectroscopy is based on this effect and is used for qualitative and quantitative analysis of the chemical components and molecules of a sample. It is a nondestructive method that requires little, if any, sample preparation.

Nevertheless, Raman spectroscopy long remained a technique that was only performed in special laboratories. In recent years, however, it has been increasingly losing its outsider status. The reason for this is the development of the confocal Raman microscope, with which not only individual Raman spectra, but also complete images generated from thousands of spectra can be acquired. Through continuous development, commercially-available Raman microscopes are also becoming more user-friendly. For example, modern software interfaces guide the user through the Raman measurement and the subsequent data analysis.

There are several key factors that can be used as criteria for determining the quality of confocal Raman microscopes (Fig. 1).

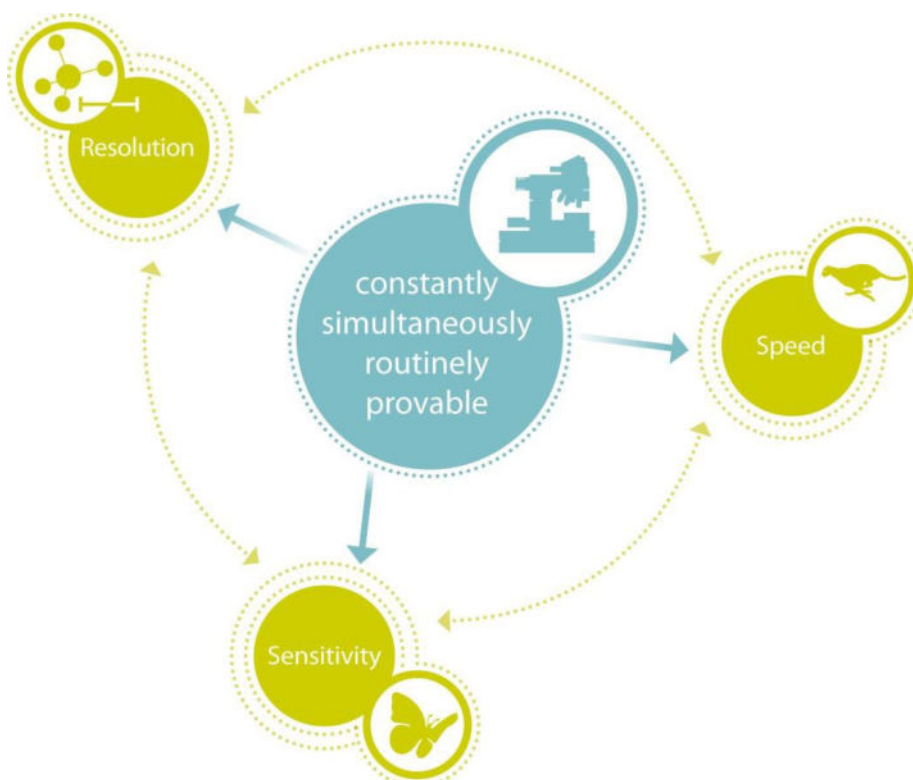


Fig. 1: Speed, sensitivity and resolution are some of the characteristics that can be used to identify a high-quality Raman microscope. These three characteristics should not be mutually exclusive. Ideally, the Raman imaging system should be configured in such a way that high-resolution images with a high signal-to-noise ratio can be acquired in a short period of time.

## 1) Speed

While in the past exposure times of minutes to hours were common for acquiring single Raman spectra, today these times are generally fractions of a second to less than one millisecond. In one second more than 1000 Raman spectra can be recorded. Thus a Raman image can be generated within a few minutes. To achieve this acquisition speed, the Raman imaging system should be equipped with optimized optics and an EMCCD camera.

High acquisition speeds are particularly important for measurements on sensitive and valuable samples in which the excitation energy must be as low as possible. Time-resolved investigations of dynamic processes can also benefit from rapid Raman spectral acquisition. Operating costs can also be reduced by shorter analysis times concurrent with increased data rates. Having a high system speed is also advantageous for time-critical work.

## 2) Sensitivity

The signal sensitivity of a system is critical for the quality of the results and is especially important when weak Raman signals are to be detected.

In order to achieve the best possible sensitivity, a confocal beam path, i.e. using a diaphragm aperture, must be employed to eliminate light from outside the focal plane to increase the signal-to-noise ratio. The entire Raman imaging system should also be optimized for high light throughput. This includes a spectrometer that ensures throughput of over 70% and is designed for measurements with low light and signal intensity. CCDs optimized for spectroscopy, which exhibit more than 90% quantum efficiency in the visible range, are most commonly used as detectors. Finally, the use of almost lossless photonic fibers ensures efficient light and signal transmission.

## 3) Resolution

The resolution of a Raman system is comprised of both spatial and spectral resolution.

The spatial resolution includes the lateral resolution (x- and y-directions) and the depth resolution (z-direction). The spatial resolution is determined by the numerical aperture of the objective used and the excitation wavelength. In addition, a confocal microscope produces images with a higher contrast because the background signal is reduced. The smaller the aperture of a confocal microscope, the higher its resolution is. In a confocal Raman microscope, the lateral resolution is about 200 - 300 nm and the depth resolution below 1  $\mu\text{m}$ . A confocal microscope can also create optical sections from different focal planes, which can be used with transparent samples for depth profiles and 3D images.

Spectral resolution defines the ability of a spectroscopic system to separate Raman lines near one another. Symmetric peaks in the spectrum are ensured by a spectrometer design that operates free of coma and astigmatism. The grating used, the focal length of the spectrometer, the pixel size of the CCD camera and the size of the aperture also affect the spectral resolution.

At room temperature, the width of the Raman lines is typically greater than  $3\text{ cm}^{-1}$ , but some applications (gases, low temperature or stress analysis) may require significantly higher resolution (Fig. 1).



Fig. 2: The confocal Raman Imaging microscope alpha300 R (WITec GmbH): modular and upgradable for adapting to new requirements.

#### 4) Modularity and Upgradeability

The introduction of Raman microscopy into laboratories places new demands on commercially-available systems. These requirements can sometimes appear contradictory: easy operation with diverse functionality, a wide range of applications with optimized sensitivity, low cost and high performance. In order to offer users a Raman system tailored to their individual requirements, it is particularly important that systems have a modular design that can be adapted to new conditions through being reconfigured or upgraded. A system can be optimized for specific requirements by individually combining suitable lasers, filters, lenses, spectrometers and detectors. With such a customized Raman imaging system (Fig. 2) the user is able to obtain meaningful Raman images, perform 3D volume scans and create depth profiles.

#### 5) Combinability

Confocal Raman microscopy can be combined with other microscopy techniques. By using different methods and correlating the data, the user attains a more comprehensive understanding of the sample. Common examples of correlative microscopy techniques are Raman-AFM (AFM = Atomic Force Microscopy), Raman-SNOM (SNOM = Scanning Nearfield Optical Microscopy) and Raman-SEM (SEM = Scanning Electron Microscopy). In order to correlate the data of these disparate technologies, the exact same sample location must be examined by each approach. If different instruments are to be used, finding this sample location can be very difficult and time-consuming. This is made much easier with a hybrid system that combines the different analysis methods in one instrument so that the sample can remain in place during all measurements. Some applications of correlative Raman microscopy are presented below.

#### Application examples for correlative Raman microscopy

##### Raman and Profilometry

For Raman microscopy, most samples do not need to be treated, stained or otherwise prepared prior to measurement. The combination of a confocal Raman microscope with a profilometer module for focus stabilization allows rough or inclined surfaces to be examined [3, 4]. During Raman analysis, the examination area is kept constantly in focus by the simultaneously-acquired profilometry data. This also compensates for thermal shifts and enables long-term measurements. The application example in Fig. 3 shows the analysis of a microstructured silicon sample. The chemical image of the Raman measurement was overlaid onto the topographic profile measurement.

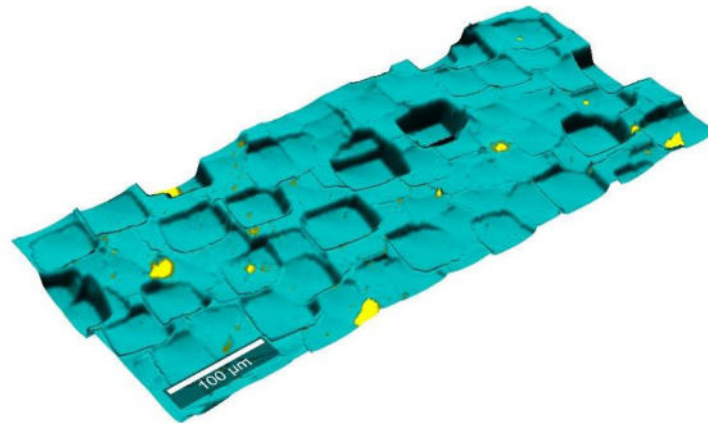


Fig. 3: Topographic Raman image of a silicon microstructure.

### Raman and Fluorescence

Fluorescence microscopy has been a widespread imaging method for the analysis of biological cells and organisms for decades. Samples are stained with fluorescent dyes or organisms are genetically engineered to express fluorescent proteins. The fluorescence signal is usually much stronger than the Raman signal. Nevertheless, correlative Raman fluorescence measurements are possible with an appropriate system. Fig. 4 shows a Raman fluorescence image of a live cell culture of eukaryotic cells. An inverted confocal Raman microscope was used to examine the cells in their aqueous cell culture medium in the Petri dish. The cell nuclei were stained with the fluorescent dye DAPI. An excitation wavelength of 532 nm was used for the Raman measurement. An image with  $50 \times 40 \mu\text{m}^2$  and  $150 \times 120$  pixels was acquired. A Raman spectrum was recorded at each pixel. The recording time was 0.2 s/spectrum. In the correlative Raman fluorescence image, the nuclei are shown in blue (recorded with fluorescence microscopy), the nucleoli in green and the endoplasmic reticula in red (recorded with Raman microscopy). The corresponding Raman spectra are shown in the same colors.

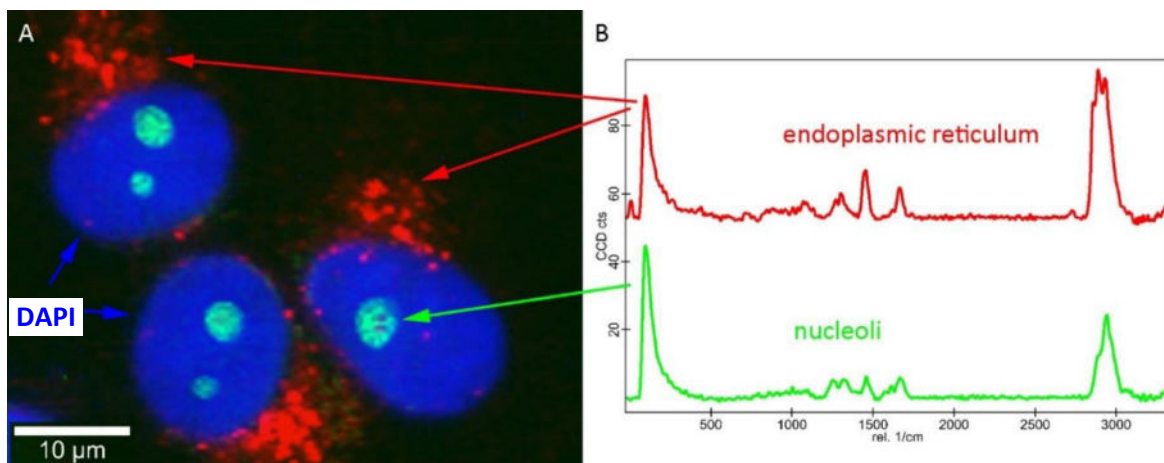


Fig. 4: A: Correlative Raman fluorescence image of primate cells in cell culture. Blue: Nuclei recorded by fluorescence microscopy; Red: Endoplasmic reticula, Green: Nucleoli recorded by Raman microscopy. B: Associated Raman spectra.

## Raman and AFM

The combination of Raman microscopy, which provides information about the type and distribution of molecules in a sample, and the high-resolution AFM technique, which determines the surface characteristics of a sample, enables the visualization of both chemical and morphological properties. Here the analysis of a 1:1:1 mixture of polystyrene (PS), 2-ethylhexyl acrylate (EHA) and styrene-butadiene rubber (SBR) is shown. For this, a correlative Raman-AFM microscope was used, in which Raman microscopy and AFM technologies are fully integrated. The measurement with AFM in intermittent AC mode documents the topography of the polymer mixture (Fig. 5A). The simultaneously-recorded phase image (Fig. 5B) provides information on the viscosity and elasticity of the individual components of the polymer mixture. The confocal Raman image (Fig. 5C) shows that PS (red) and EHA (green) are present separately. SBR (purple) partly mixes with EHA (mixture shown in blue). By correlating the Raman image with the AFM image, the chemical information can be linked to the structural information (Fig. 5D).

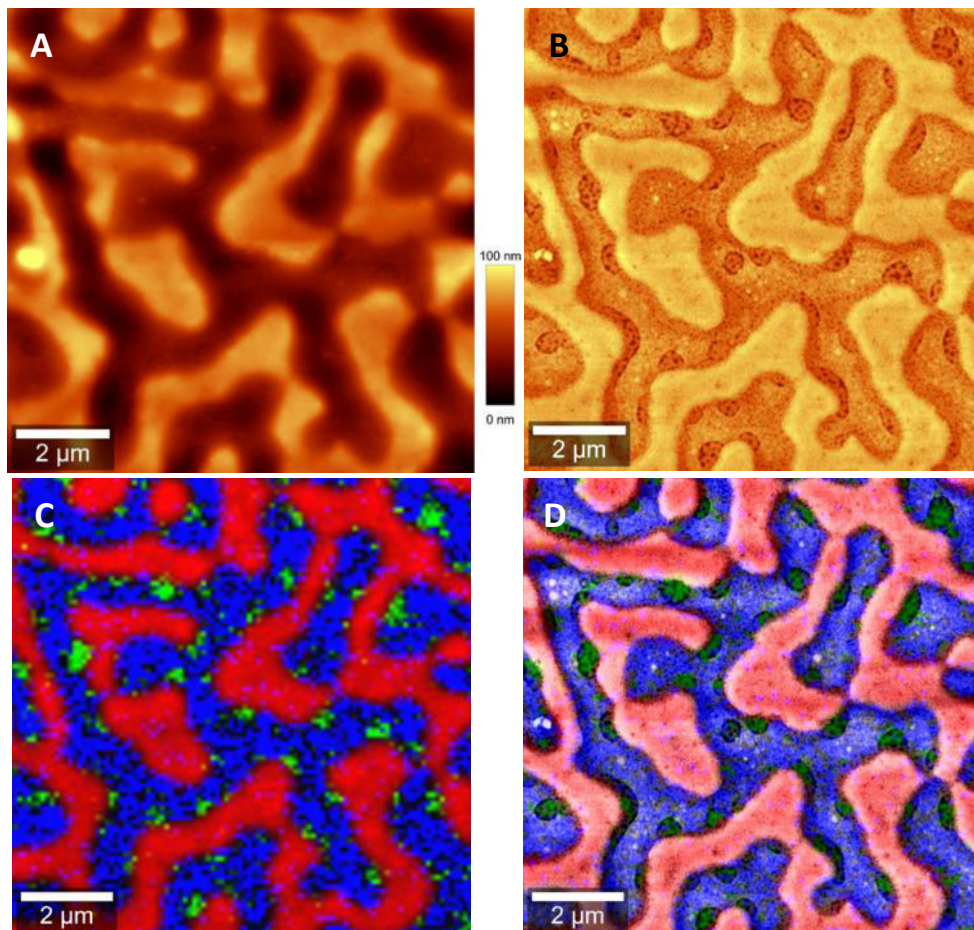


Fig. 5 : Correlative, high-resolution AFM-Raman microscopy of a 1:1:1 mixture of polystyrene (PS), 2-ethylhexyl acrylate (EHA) and styrene-butadiene rubber (SBR). Both measurement technologies are combined in the WITec alpha300 RA microscope. A: The topography of the polymer mixture was determined with AFM in AC mode. B: The phase of the AFM image shows the fine structure of the compound. C: A color-coded, confocal Raman image, generated from the Raman spectra, shows the distribution of the polymers. PS (red), EHA (green). SBR (purple), SBR-EHA mixture (blue). D: In the correlative Raman-AFM image the topography and distribution of the different polymers can be visualized.

## Raman and SEM

Scanning electron microscopy (SEM) is a well-established method for structural surface analysis. By combining Raman imaging with SEM in a correlative microscope, it is possible to combine results of SEM structural analysis with chemical and molecular information from confocal Raman microscopy [5]. The sample is placed in the vacuum chamber of the electron microscope. Both analysis methods are then carried out automatically at the same sample location. The obtained SEM and Raman images can then be superimposed.

In Fig. 6 a structure several atoms in thickness comprised of graphene layers was analyzed by correlative Raman-SEM microscopy. The Raman image consists of 22,500 spectra with 50 ms recording time per spectrum. While in the SEM image the contrast between the substrate and the graphene flake is visible, in the Raman image the number of graphene layers and their different orientations can be analyzed. This is not possible with SEM alone.

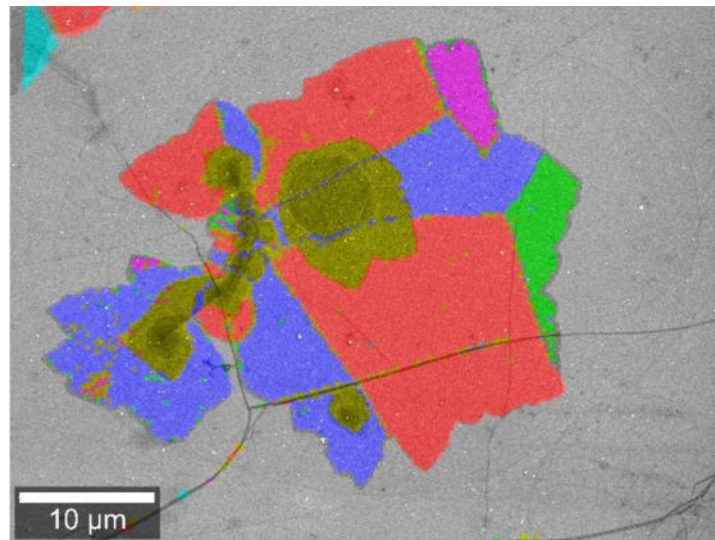


Fig. 6: Correlative RISE (Raman-SEM) microscopy image of a multilayer graphene flake. The different colors show folds and orientations in the graphene and could be identified by Raman analysis.

## Raman Particle Identification and Characterization

High-resolution investigations of particles are of great interest in many fields of application such as environmental science, pharmaceutical research and many others. Combining a particle analysis tool with the fast, label-free and nondestructive Raman imaging technique makes it possible to find, classify, and identify particles in a sample according to their size, shape and chemical characteristics. The physical and molecular attributes of the particles in a sample may be correlated and qualitatively and quantitatively evaluated. Fig. 7 shows the results of particle analysis carried out on a cosmetic peeling cream sample. Fig. 7A shows the overlay of an optical bright field microscope image with the corresponding confocal Raman image. Particles are identified according to their size and shape and further characterized by their molecular properties through confocal Raman imaging. The chemical analysis revealed anatase and boron nitride particles in an oil matrix (Raman spectra shown in Fig. 7B). Further evaluation of the results

determines the quantitative prevalence of the molecular sample components in the particles (Fig. 7C) and also the distribution of chemical compounds correlated to particle size (Fig. 7D). In extended analyses the chemical characteristics of particles could also be linked to parameters such as area, perimeter, bounding box, Feret diameter, aspect ratio, equivalent diameter and many others. This illustrates the potential for comprehensive investigations of particles in many fields of application.

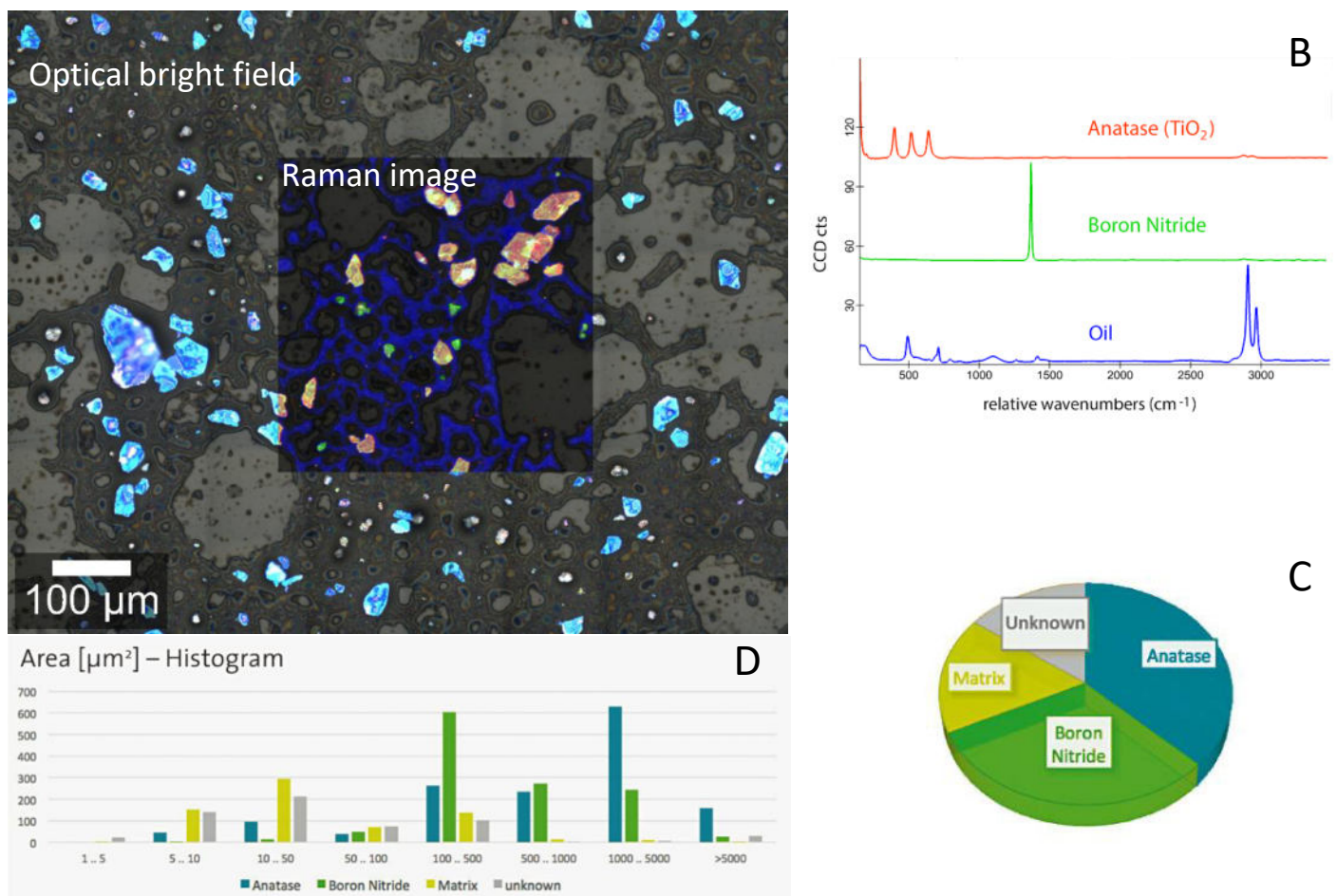
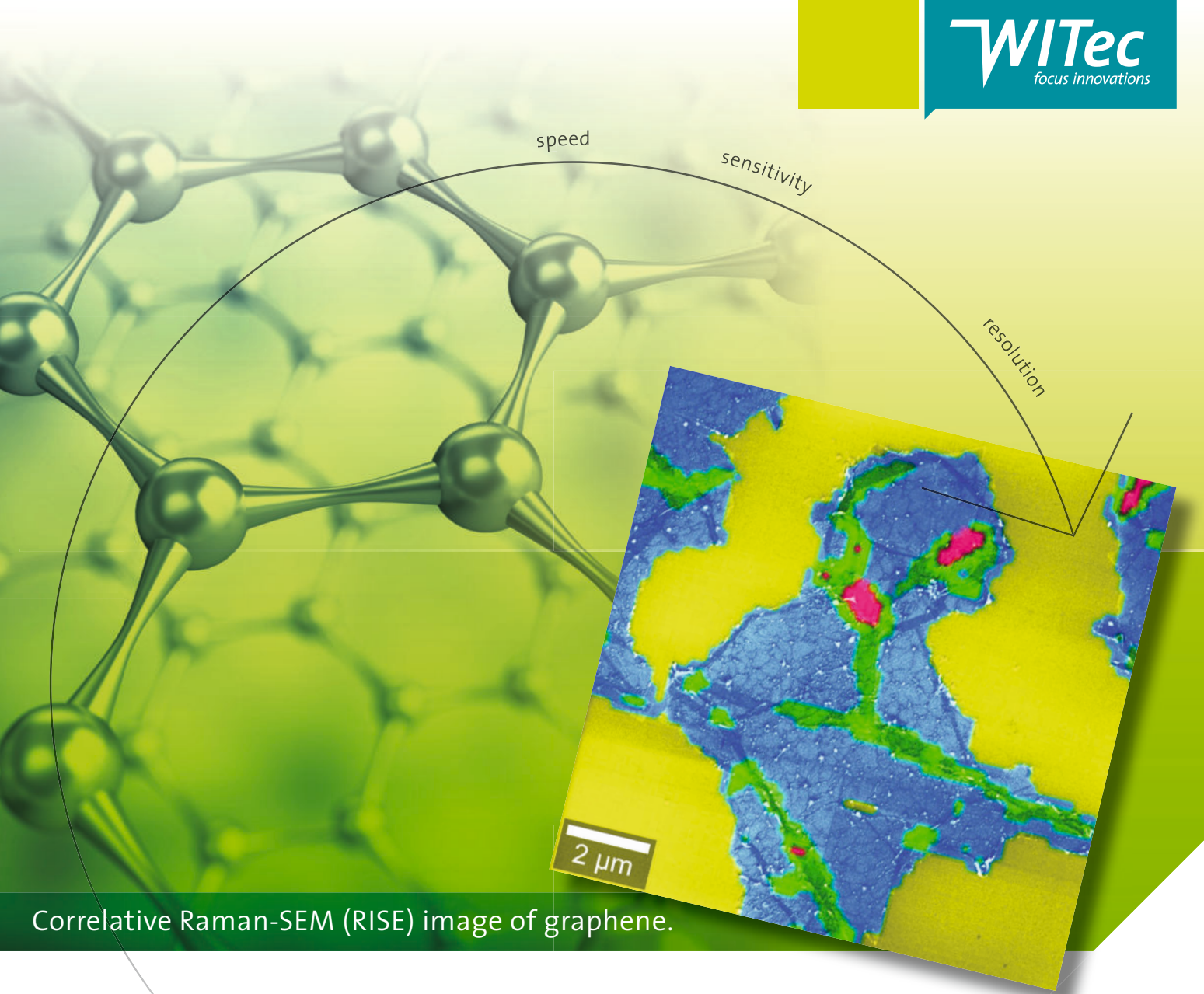


Fig. 7: Particles in a cosmetic peeling cream sample. A: Optical bright field image overlaid with the confocal Raman image. B: Corresponding Raman spectra of the molecular components in the sample. C: Pie chart of the quantitative compound distribution in the sample. D: Graphical representation of the correlation between chemical characteristics and particle size.

## Literature:

- [1] C.V. Raman, K.S. Krishnan, Nature 121, 501 (1928)
- [2] J. Toporski, T. Dieing and O. Hollricher (eds.), Confocal Raman Microscopy, 2<sup>nd</sup> Edition, Springer Series in Surface Sciences (66), Springer International Publishing (2018)
- [3] A. Masic, J. C. Weaver, Journal of Structural Biology 189, 269-275 (2015)
- [4] B. Kann, M. Windbergs, The AAPS Journal 15, 505-510 (2013)
- [5] G. Wille, C. Lerouge, U. Schmidt, Journal of Microscopy 270, 309-317 (2018)





Correlative Raman-SEM (RISE) image of graphene.

# 3D Raman Imaging

Turn ideas into **discoveries**

Let your discoveries lead the scientific future. Like no other system, WITec's confocal 3D Raman microscopes allow for cutting-edge chemical imaging and correlative microscopy with AFM, SNOM, SEM or Profilometry. Discuss your ideas with us at [info@witec.de](mailto:info@witec.de).



Raman · AFM · SNOM · RISE

[www.witec.de](http://www.witec.de)